The role of Ken&Barbie in JAK/STAT signalling during development of *Drosophila melanogaster*

Dissertation

Am Fachbereich Naturwissenschaften

der Universität Kassel

Natalia Arbouzova

2004

Dissertation

zur Erlangung des akademischen Grades

Doctor rerum naturalium

(Dr. rer. nat.)

im Fach Biologie

eingereicht am

Fachbereich Naturwissenschaften

der Kassel Universität

Erstgutachterin: Prof. Dr. Mireille A. Schäfer

Zweitgutachter: Prof. Dr. Herbert Jäckle

I dedicate this work to The Saint-Petersburg State University that taught me and fostered my interest in developmental biology without expecting me to apply this knowledge far away from home

Table of contents

Contents

Contents

Contents

1 Introduction

Embryonic induction is one of the first determined general principles of development. The first evidence that one tissue can induce other tissues to change their fates comes from the experiments of 1924 showing that the dorsal lip of the newt embryo blastopore, subsequently named Spemann's organiser, can induce surrounding tissues to differentiate and to undertake morphogenetic movements (Spemann & Mangold, 1924). However, not until 1990s when proteins secreted by the organiser and the first member of TGF-β signalling were isolated, was the nature of this induction uncovered (Hemmati-Brivanlou & Melton, 1994; Hemmati-Brivanlou & Melton, 1997).

Now signal transducing cascades are well known as key mechanisms that enable certain cells to respond to specific inducers. Cell-cell interactions during embryonic development are crucial for the co-ordination of growth, differentiation and maintenance of many different cell types. To achieve this co-ordination each cell must properly translate signals received from closely and distantly neighbouring cells, into spatially and temporally appropriate developmental responses. A variety of pathways are known to assist the cells transducing those signals. These pathways are especially important during embryonic development. Thus, Wnt signalling is essential for endoderm specification in early gastrulating mouse embryos (Lickert *et al.*, 2002), while later, the Hedgehog pathway is required for neural tube formation and limb patterning (Eggenschwiler *et al.*, 2001). Dpp/TGF-β is involved in pattern formation in *Drosophila* imaginal disc development (Pignoni & Zipursky, 1997; Affolter *et al.*, 2001).

Generally, these pathways are induced by a ligand binding to a transmembrane receptor, which in turns signals to intracellular transducers and activates transcription factors that alter the transcription profile of target genes. The resulting differential gene expression is another principle of development. It allows a zygote to give rise to the entire variety of cell types present in adult individuals. However, hundreds of different cell types are found in the animal kingdom, and only a few signalling pathways are involved to provoke their differentiation. As a result, the same pathways

are repeatedly used in development, with a cross-talk between them reinforcing and modifying cell responses.

Signal transduction is a growing field in modern developmental biology, as it sheds light on how adjacent cellular environment and distant interactions can specify cell fate. However, the importance of signalling cascades is not restricted to embryogenesis, but also essential for biological processes such as physiological control, neural system activity and immune response. One example of such pathways, the JAK/STAT signalling cascade, which is the main topic of this study, was first discovered as playing a key role in transducing signals from cytokines in lympho-hematopoietic system. Only later was its activity characterised and found relevant for embryogenesis. So far, many intriguing aspects of JAK/STAT signalling were uncovered, but every new fact brings about new questions. To answer those questions is the biggest aspiration for scientists. This study is dedicated to the JAK/STAT pathway as one of the mechanisms, which a single cell utilises to develop into a complex organism.

1.1 The JAK/STAT pathway

In 1991 the first transcription factors, now known as STAT (<u>s</u>ignal <u>t</u>ransducers and <u>a</u>ctivators of <u>t</u>ranscription), were purified from interferon-α induced DNA-protein complex (Fu *et al.*, 1992; Schindler *et al.*, 1992). In 1993 the first use of the term "STAT" was made in scientific literature, and by 1995 the first reviews summarised the data about the JAK/STAT pathway (Ihle *et al.*, 1995; Schindler & Darnell, 1995).

In its most simple form the JAK/STAT pathway represents a short cascade consisting of a ligand, a ligand-recognising transmembrane receptor, a receptor-associated kinase and a transcription factor. The principal families of proteins involved in the pathway, as implied by its name, are the receptor-associated kinases JAK (<u>Ja</u>nus <u>k</u>inase) and the transcription factors STAT. In the canonical model, signal transduction is triggered by the ligand binding to the receptor, which results in cross-phosphorylation of the associated with the receptor JAK molecules. Once activated, JAK mediates phosphorylation of the receptor and the STAT factors. Activated STATs dimerise, translocate to the nucleus and activate transcription of target genes (Fig 1.1).
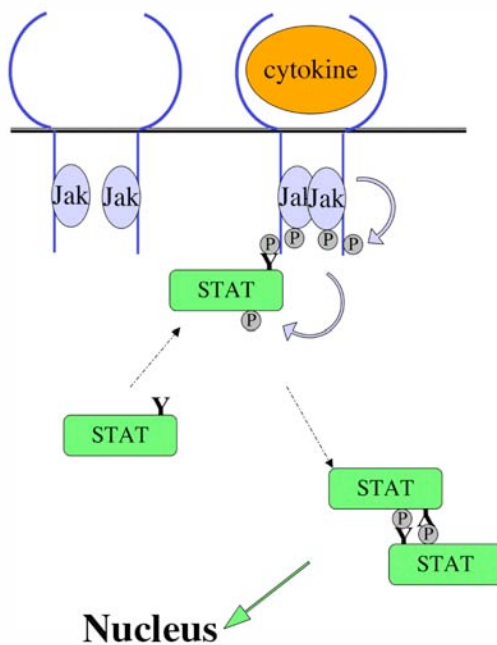
Figure 1.1. Scheme of JAK/STAT signalling.

Ligand-receptor binding triggers the activatation of JAKs that, in turns, phosphorylate the receptor. Phospho-tyrosine residues in the intracellular region of the receptor provide docking sites for SH2 domains in STATs. Bound to the receptor STATs undergo phosphorylation by JAKs, dimerise and are translocated to the nucleus.

1.2 Core components of the JAK/STAT pathway cascade

As the pathway was first discovered and extensively characterised in mammals, the best way to illustrate this cascade is to give an introduction how it functions in humans and mice.

1.2.1 Ligands

Ligands for the JAK/STAT pathway can be represented by various cytokines, a large group of low molecular weight glycoproteins, comprising big families of ligands like interleukins, interferons and growth factors (reviewed in Leonard & O'Shea, 1998; Hanlon *et al.*, 2002; Boulay *et al.*, 2003). Hormones such as prolactin, erythropoietin, trombopoietin, growth hormone, as well as some chemokines, also serve as ligands (Soriano *et al.*, 2003).

In *Drosophila* the only characterised ligand capable of activating JAK is encoded by *unpaired* (*upd*). Upd is a 45kDa (or larger when glycosilated) protein containing a functional N-terminal signal sequence that targets Upd for secretion, and sites for glycosylation, a modification essential for extracellular proteins. In tissue culture Upd

is mainly attached to the extracellular matrix. Though showing no similarity to the human or mouse cytokines, Upd has been demonstrated to activate *Drosophila* JAK, named Hopscotch (Hop) (Harrison *et al.*, 1998). Searches of *Drosophila* databases detected *upd*-like genes (*upd2* and *upd3*) clustered on the X chromosome. Since *upd* mutants show weaker phenotypes than the deletion *Df(1)os^{1A}*, that encompasses the entire region of *upd* and *upd*-like genes, it is likely that Upd-like proteins are mutually semi-redundant and supplement Upd functions (Castelli-Gair Hombria & Brown, 2002).

1.2.2 Receptors

All cytokines bind to either Class I or Class II cytokine receptors, large families of polypeptides with a single-pass transmembrane domain (reviewed in Langer *et al.*, 2004). In the N-terminal extracellular region, proximal to the membrane are fibronectin type III (FNIII)-like repeats forming two domains, one of which is known as the cytokine-binding module (CBM), a characteristic of cytokine receptor family members (Fig 1.2; reviewed in Heinrich *et al.*, 2003). The number and spacing of cysteine and proline residues within the FNIII-like domains underlies the classification of cytokine receptors into two classes (Langer *et al.*, 2004). In the intracellular domain, the terminal region contains several tyrosine residues (Tyr, or Y), which provide docking sites either for STATs or negative regulators such as SHP-2 and SOCS3 (De Souza *et al.*, 2002, see below). Proximal to the membrane are conserved box1 and box2 motifs, which are important for non-covalent association with JAK (reviewed in Yeh & Pellegrini, 1999).

Only one gene coding for a JAK/STAT pathway receptor has been identified in the *Drosophila* genome (Brown *et al.*, 2001). This gene, named *domeless* (*dome*), encodes a 1282 amino acid protein with a single transmembrane domain. The extracellular region contains five FNIII-like domains, of which two are similar to the CBM found in the mammalian cytokine receptor class I family (Fig 1.2). Its intracellular domain has a consensus site for STAT binding, and a physical interaction between Dome and STAT has been confirmed *in vitro* (Chen *et al.*, 2002). Searches through *Drosophila* databases have identified a *dome* homologous gene *CG14225*, that has yet to be characterised (Castelli-Gair Hombria & Brown, 2002).
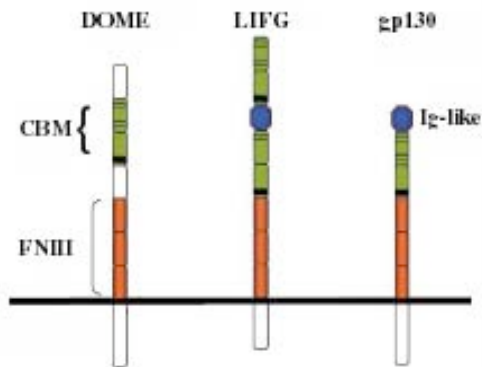
Figure 1.2. *Drosophila* **Dome compared to vertebrate interleukin-receptors (after Brown *et al.*, 2001).**

The cytokine binding module is marked in green. Other fibronectin-type-III repeats are represented in red boxes. The vertebrate receptors contain Ig-like motif, labelled by blue hexagon, absent in Dome.

1.2.3 JAKs

Four JAKs (JAK1-3 and Tyk2) are found in humans and mice. The family is characterised by presence of two critical domains: a catalytically active kinase domain, and adjacent to it an inactive pseudo-kinase domain (Fig 1.3A). These two structurally similar, though functionally distinct, domains resemble the two faces of the Roman god Janus (Fig 1.3B) and gave the kinase its name. Though no crystal structure of JAK is available, seven regions of homology were recognised among JAKs and initially named JH (JAK homology) domains. To date, functions of some of them are uncovered.

The kinase domain JH1 is essentially similar to that of other tyrosine kinases. It includes conserved residues, i.e. lysine involved in ATP binding and YY motif essential for catalytic activity (Vihinen *et al.*, 2000). Ligand-induced conformational changes of pre-existing receptor dimers bring JAK molecules, associated with the receptor, to the close proximity of each other, which enables auto- or cross-phosphorylation on YY in JH1 (reviewed in Frank, 2002).

The pseudo-kinase domain JH2 also contains sequences conserved in kinase domains. However, several residues required for phosphotransferase activity are altered, which makes the domain catalytically inactive. Recent studies in JAK2 have established that JH2 is required to maintain inactive state of JAK2 in the absence of IL stimulation, and to trigger the activation upon stimulation (Saharinen *et al.*, 2000; Saharinen & Silvennoinen, 2002). This characteristic is an intrinsic property of JAK2 and does not depend on additional regulatory proteins (Saharinen *et al.*, 2003).
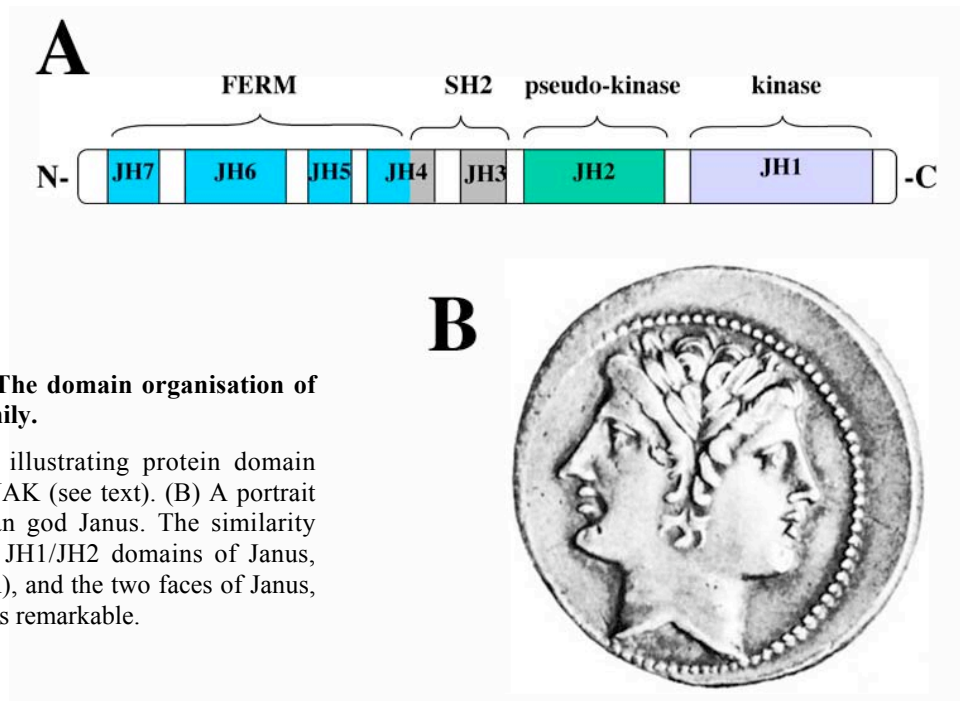
Figure 1.3. The domain organisation of the JAK family.

(A) Scheme illustrating protein domain structure of JAK (see text). (B) A portrait of the Roman god Janus. The similarity between the JH1/JH2 domains of Janus, the kinase (A), and the two faces of Janus, the god (B), is remarkable.

Binding of JAK to the cytokine receptors is mediated by a FERM domain (4.1, ezrin, radixin, moesin) encompassing JH7-JH4 regions of the initial nomenclature (Girault *et al.*, 1999; Usacheva *et al.*, 2002). In JAK2 this region also promotes the cell surface accumulation of the associated receptor, suggesting a strong synergy between the receptor and the kinase (Huang *et al.*, 2001).

Though the regions JH3-JH4 resemble an SH2 domain that mediates phospho-tyrosine (pY) binding in other proteins (see below), the precise function of this domain in JAK remains unclear, especially in Tyk2, whose SH2 lacks the conserved arginine residue absolutely required for binding to pY (Al-Lazikani *et al.*, 2001).

Among vertebrates, JAKs are also found in the chicken (Sofer *et al.*, 1998; Bartunek *et al.*, 1999), though no functional studies have yet been reported. JAK homologues are cloned in the zebrafish *Danio rerio*, the carp *Cyprinus carpio* and the pufferfish *Tetraodon floviatilis* (Oates *et al.*, 1999a; Leu *et al.*, 2000). No JAKs have been discovered in the nematode *Caenorhabditis elegans* or the mixameba *Dictyostelium discoideum*, although these organisms have STAT molecules (Liu *et al.*, 1999; Fukuzawa *et al.*, 2001, see below).

In *Drosophila,* a single JAK is encoded by the *hop* gene. Hop is most similar to the mammalian JAK1 and JAK2 and contains all domains present in other JAKs, with its

JH1 and JH2 domains sharing 39% and 27% identity with the corresponding domains of JAK1 (Binari & Perrimon, 1994).

1.2.4 STATs

Seven STAT proteins (STATs 1-6 including two forms of STAT5) have been identified in mammals. STAT molecule can be divided into five structurally and functionally conserved domains (Fig 1.4).

Figure 1.4. The organisation of functional domains shared by members of the STAT family.

C-terminal end carries a t̲ra̲nsa̲ctivation d̲omain (TAD), which underlies STATs functioning as positive regulators of transcription via interacting with co-activators such as TAFs (T̲BP-a̲ssociated f̲actors) and HATs (h̲istone a̲cetylt̲ransferases) (Paulson *et al.*, 1999; Goenka *et al.*, 2003). C-terminal truncated versions of STAT referred to as β forms (in contrast to full-length α forms) can serve as dominant negative factors likely due to the deletions in the TAD (Schaeffer *et al.*, 1997). However, recent studies have described the full-length STAT1α as a negative regulator of transcription in response to IFNγ (Horvath, 2000). Also in *Dictyostelium discoideum* STAT proteins lack the TAD and can function as transcriptional repressors (Fukuzawa *et al.*, 2001).

SH2 (S̲rc h̲omology 2̲) domain located upstream of the TAD plays a central role in STATs as it mediates high affinity binding to pY (reviewed in Vidal *et al.*, 2001; Schlessinger & Lemmon, 2003). Tyrosine residue in the intracellular domain of the receptor when phosphorylated by JAKs provides a docking site for the SH2 domain of STAT (De Souza *et al.*, 2002). However, it has been reported that STAT1 and STAT2 can bind to the receptor prior its phosphorylation (Li *et al.*, 1997).

Once bound to the receptor, and thus brought to the area of JAK activity, STAT undergoes phosphorylation on absolutely conserved Y around position 700bp on the C-terminus (Fig 1.2C; for review see Ihle *et al.*, 1995; Leaman *et al.*, 1996; Darnell, 1997; Leonard & O'Shea, 1998; Decker & Kovarik, 1999). Interestingly, STATs can also be phosphorylated by EGF-r (e̲pidermal g̲rowth f̲actor r̲eceptor) or PDGF-r

(platelet derived growth factor receptor) possessing intrinsic tyrosine kinase activity (reviewed in Ihle *et al.*, 1995; Leaman *et al.*, 1996).

Once activated, STAT molecules form homo- or heterodimers, with this dimerisation facilitated by reciprocal interaction between SH2 domain of one partner and pY of the other partner (Chen *et al.*, 1998; Mikita *et al.*, 1998). However, pre-existence of non-phosphorylated STAT1 and STAT3 homodimers, though incapable of DNA binding, has been also reported, and it has been proposed that the N-terminal domain of STAT (see below) is essential for stability of these dimers (Braunstein *et al.*, 2003).

In the canonical model, activated and dimerised STATs are transported to the nucleus. Nuclear translocation is enabled by importin-α of the nuclear pore complex that recognises nuclear localisation signal (NLS) within the DNA binding domain (DBD) of STAT (Fagerlund *et al.*, 2002; McBride *et al.*, 2002). However, mutational analysis shows that nuclear translocation of STATs is not linked to Y-phosphorylation (Johnson *et al.*, 1999; Fukuzawa *et al.*, 2001).

DNA binding motif located in the centre of the STAT molecule does not belong to any of the known classes of DBD and represents an individual group, though related to DBD of p53 and NF-κB (Horvath & Darnell, 1997; Chen *et al.*, 1998). All mammalian STATs recognise a DNA motif, termed GAS (γ-IFN activated sequence), representing a palindromic sequence with a general formula $TTCN_{3-4}GAA$ (N_3 for STATs 1, 3, 4 and 5, and N_4 for STAT6) (for review see Hoey & Schindler, 1998; Leonard & O'Shea, 1998). However, in some cases the recognition motif can comprise a non-palindromic site as reported for STAT1/STAT2 heterodimer that requires the DNA binding protein p48 for its activity (reviewed in Hoey *et al.*, 2003; Leonard & O'Shea, 1998; Aaronson & Horvath, 2002). STATs can also form complexes with other transcription factors such as Sp1, glucocorticoid receptor, c-Jun and SMAD (reviewed in Horvath & Darnell, 1997; Horvath, 2000; Levy & Darnell, 2002). Though the nature of those associations is not yet clear, the coiled-coil domain of the STAT molecule localised upstream of DBD (Fig 1.2C) is believed to mediate the protein-protein interactions (Chen *et al.*, 1998; Decker & Kovarik, 1999; Horvath, 2000). Alternatively, TAD can be involved in co-operation with other factors, as recently shown for STAT1 and BRCA1 (Horvath, 2000).

STAT dimers can further dimerise and bind DNA as tetramers, which is facilitated by the N-terminal domain. This domain is also known to be involved in STAT dephosphorylation and contains an important signal for export of STATs back to the cytoplasm (Vinkemeier *et al.*, 1998; John *et al.*, 1999; Levy & Darnell, 2002; Meyer *et al.*, 2004).

Among vertebrates, STATs are found in *Danio rerio* and other fishes, and in the frog *Xenopus laevis* (Nishinakamura *et al.*, 1999; Oates *et al.*, 1999b; Leu *et al.*, 2000; Pascal *et al.*, 2001; Lewis & Ward, 2004).

A single *Drosophila* STAT protein encoded by the *stat92E* gene is 37% and 34.7% identical to the human STAT5 and STAT6 (Hou *et al.*, 1996). Like other STATs it possesses the SH2 domain and the characteristic DBD (Sweitzer *et al.*, 1995; Hou *et al.*, 1996). High homology with mammalian STATs within DBD has been shown to be functionally significant, as STAT92E binding consensus <u>TTC</u>CCG<u>GAA</u> includes the GAS sequence (underlined) recognised by all STATs (Yan *et al.*, 1996b). A tyrosine residue located just downstream of the putative SH2 domain represents the conservative Y found in the mammalian STATs around position 700bp (Sweitzer *et al.*, 1995; Hou *et al.*, 1996; Yan *et al.*, 1996b).

Recently, another form of STAT92E derived from alternative splicing was characterised (Henriksen *et al.*, 2002). This N-terminally truncated STAT92E (ΔNSTAT92E), though being able to dimerise and bind DNA, fails to activate transcription of target genes and is proposed to represent a negative regulator of the pathway.

1.3 Negative regulation of the JAK/STAT pathway

Being there a way to activate the pathway, there should be a means to control it. So far, three major families of proteins that can negatively regulate the JAK/STAT pathway have been characterised.

1.3.1 SOCS (<u>s</u>uppressors <u>o</u>f <u>c</u>ytokine <u>s</u>ignalling) family

The first SOCS was discovered independently in three different screens focused on searches for proteins that: a) suppressed macrophage differentiation upon IL-6 stimulation (Starr *et al.*, 1997), b) interacted with the kinase domain of JAK2 (Endo *et al.*, 1997), and c) contained SH2 domain (Naka *et al.*, 1997). Eight members of SOCS

family are now known (reviewed in Larsen & Ropke, 2002). It is worth mentioning that these negative regulators also represent transcriptional targets for STATs.

All SOCS proteins have a central SH2 domain, flanked by a variable N-terminal domain and a highly conserved C-terminal motif, referred to as the SOCS-box (Fig 1.5), a domain also found in other proteins. Additionally, a <u>k</u>inase <u>i</u>nhibitory <u>r</u>egion (KIR), whose structure is close to that of the catalytic JH1 domain of JAK, is found in SOCS1 and SOCS3 (Yasukawa *et al.*, 1999).
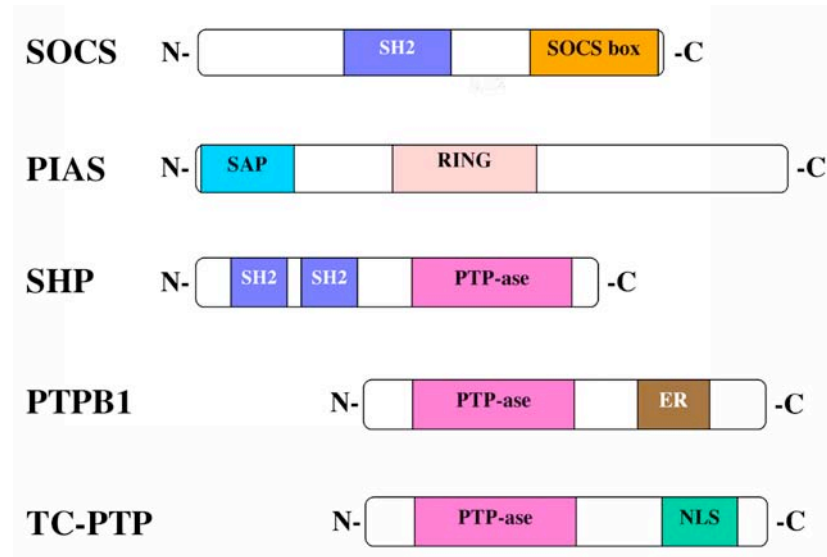
Figure 1.5. Domain structures of the known negative regulators of the JAK/STAT pathway.

For SOCS, PIAS and SHP see the text. Phosphatase domain is marked as PTP-ase. In addition to PTP-ase domain PTPB1 also contains a C-terminal motif for targeting to the endoplasmic reticulum (marked ER). TC-PTP carries NLS for transport to the nucleus.

Several mechanisms have been described, by which SOCS proteins can repress JAK/STAT signalling. Firstly, by means of either SH2 or KIR domains SOCSs can inactivate JH1 kinase domain of JAK (Yasukawa *et al.*, 1999; Saharinen & Silvennoinen, 2002). Secondly, SOCSs can bind to pY of the receptor thus competing for STATs (Yamamoto *et al.*, 2003). And finally, SOCSs can target JAKs for degradation through the SOCS box, which interacts with ubiquitin ligase complex (Kile *et al.*, 2002; Ali *et al.*, 2003).

The *Drosophila* gene SOCS36E shows the highest homology to the vertebrate SOCS-5 (29.7% overall identity, with up to 44% and 75% that within SOCS box and SH2 domains, respectively) (Karsten *et al.*, 2002). SOCS36E is expressed in Upd-dependent manner and can down-regulate JAK/STAT pathway activity (Callus &

Mathey-Prevot, 2002; Karsten *et al.*, 2002). Other similar genes, *socs16D* and *socs44A*, may also represent homologues of the mammalian SOCSs, though their functions have not yet been analysed (Bach & Perrimon, 2003).

1.3.2 PIAS (protein inhibitors of activated STAT) family

Originally identified as inhibitors of STATs, PIAS proteins are now known as a family of general repressors involved in the regulation of a variety of transcription factors (Schmidt & Müller, 2002; Liu & Shuai, 2003). Five PIAS members (PIAS1 and 3, PIASxα and β, PIASy) are known in humans. The molecule contains N-terminal SAP (scaffold attachment factor, acinus and PIAS) motif, which can bind chromatin and build up a higher-order chromatin structure (Fig 1.5; reviewed in Schmidt & Müller, 2002). Central part of the protein is occupied by a module related to zinc binding RING domain, implicated in protein degradation via attachment of SUMO (small ubiquitin related modifier) (reviewed in Jackson, 2001). Recent studies point out a potential function of PIAS family members as E3-like ligases that control the conjugation of SUMO to target proteins (Kotaja *et al.*, 2002; Schmidt & Müller, 2002). However, PIAS can also use a distinct mechanism. For instance, PIASy-mediated repression of androgen receptor neither requires RING domain nor involves SUMOylation, but is achieved by interaction with the histone de-acetylases HDAC1 and HDAC 2 (Gross *et al.*, 2004).

A single *Drosophila* homologue of mammalian PIAS is encoded by *zimp*, also called *Su(var)2-10 (suppresser of position-effect variegation 2-10)*. *zimp* pre-RNA is alternatively spliced and gives rise to 6 different transcripts. All known translated isoforms contain SAP domain and a zinc finger, found in the mammalian PIASs (see Section 1.1.2; Hari *et al.*, 2001). Zimp physically interacts with STAT92E and can suppress melanotic tumour formation (see below) caused by JAK/STAT pathway over-activation (Betz *et al.*, 2001). It is also involved in chromatin organisation and maintaining chromatin structures required for normal gene expression and chromosome inheritance (Hari *et al.*, 2001).

1.3.3 Tyrosine phosphatases

As JAK/STAT pathway signalling depends on Y-phosphorylation, removal of this modification was predicted to be a potential mechanism for pathway regulation. Indeed, tyrosine phosphatases implicated in negative regulation of other pathways

were also shown to down-regulate JAK/STAT signalling (reviewed in Matozaki & Kasuga, 1996; Streuli, 1996). Y-specific phosphatases, called SHPs (SH2-containing phosphatases), possess an N-terminal SH2 domain and a C-terminal phosphatase domain (Fig 1.5; reviewed in Matozaki & Kasuga, 1996). Binding of SHP to the receptor causes dephosphorylation of JAK, which blocks signal transduction (Streuli, 1996; Symes et al., 1997; Bartoe & Nathanson, 2002). Interestingly, pY within the JH1 domain of JAK2 can be bound by both SHP-2 and SOCS1. In this case dephosphorylation of JAK2 by SHP-2 inhibits the pathway, but simultaneously prevents SOCS1 from targeting JAK2 for ubiquitin-degradation (Ali et al., 2003). This implies the existence of "soft" (reversible) and "hard" (irreversible) repression.

A cytosolic phosphatase PTPB1 (protein-tyrosine phosphatase B1; Fig 1.5) has also been found to antagonise the JAK/STAT pathway via binding to and dephosphorylating STATs (Aoki & Matsuda, 2000).

Another class of phosphatases can inactivate STATs in the nucleus. Recent studies identified T-cell phospho-tyrosine phosphatase (TC-PTP; Fig 1.5) as an enzyme responsible for dephosphorylation of STAT1 and STAT3 (Hoeve et al., 2002; Yamamoto et al., 2002). Dephosphorylation is required for nuclear export of STAT back to the cytoplasm to allow it to partake in the next cycle of activation (Haspel & Darnell Jr., 1999; McBride et al., 2002).

Searches through *Drosophila* databases found one SH2-containing phosphatase Corkscrew, but its interaction with the JAK/STAT pathway remains to be studied (Perkins et al., 1992).

1.4 Functions of the JAK/STAT pathway in mammals

Cytokines control a variety of important biological processes related to hematopoiesis and immunity. The major importance of the JAK/STAT pathway, therefore, belongs to immune system, as lymphocytes and other immune competent cells are known to both proliferate and differentiate in response to various interleukins and interferons, or their combinations. Over 30 ligands are known to date, which signal through the JAK/STAT pathway. These also include growth factors and hormones essential for organogenesis and embryonic development.

1.4.1 Immune response

IFNs are cytokines that play central roles in the resistance of host organisms to pathogens, modulation of the immune response and antitumour activities (reviewed in Parmar & Platanias, 2003). All IFNs activate JAK1 and STAT1, while additional signalling through JAK2, Tyk2 and other STATs is characteristic for different INFs (reviewed in Hoey & Schindler, 1998; Parmar & Platanias, 2003). For instance, IFNγ produced by lymphocytes signals through JAK1, JAK2 and STAT1 (reviewed in Hanlon *et al.*, 2002; Parmar & Platanias, 2003), which results in expression of antimicrobal peptides and enhanced phagocytic activity of macrophages (reviewed in Hanlon *et al.*, 2002). IFNγ-induced Ig class switch in B-cells is mediated by STAT6 (reviewed in Boehm *et al.*, 1997).

Besides IFNs, interleukins are also important for the immune response. Biological impact of interleukins is very diverse as they can produce both pro- and antiproliferative effects and cause both pro- and anti-inflammarory events. Interleukins are essential for T-cell immune response, activities of natural killers (NK) and cytotoxic cells (reviewed in Conti *et al.*, 2003; Trinchieri, 2003; Watford *et al.*, 2003). For example, IL-12 signalling via JAK2, TYK2 and STAT4 induces IFNγ production by T-cells and NK, stimulates its own synthesis in dentritic cells, mediates T-cell proliferation, Th1 (T-helper 1) differentiation and cytotoxicity of NK (reviewed in Trinchieri, 2003; Watford *et al.*, 2003). In turns, expression of IL-12 in macrophages and dendritic cells is positively regulated by IFNγ (reviewed in Watford *et al.*, 2003). Anti-inflammatory effects are reported for IL-10 induced signalling that recruits STAT3 homodimers and up-regulates expression of SOCS3, which then antagonises IFNγ and IL-4 signalling (reviewed in Hanlon *et al.*, 2002).

All STATs are found to be involved in interleukin-induced signalling (Levy, 1999).

1.4.2 Hematopoiesis

The JAK/STAT pathway is also known to play roles in proliferation and differentiation of myeloid and lymphoid cell lineages. STAT1, 3 and 5 can be activated in response to hematopoietic cytokines such as erythropoietin (EPO), granulocyte-macrophage-colony stimulating factor (GM-CSF), stem cell factor (SCF), hepatocyte growth factor (HGF) and some interleukins (reviewed in IIhle *et al.*, 1995; Levy, 1999; Constantinescu & Moucadel, 2003). For instance, EPO induces signalling

through JAK2, STAT1, 3 and 5, which promotes proliferation and diferentiation of erythroid progenitors (reviewed in Constantinescu & Moucadel, 2003).

1.4.3 Mammary gland development

Requirements for the pathway in mammary gland development were predominantly shown in STAT5a deficient mice. Signal transduction via JAK2 and STAT5a induced by prolactin is critical for proliferation and differentiation of mammary epithelial cells and for lactation (reviewed in Davey *et al.*, 1999). STAT3 is also involved in mammary gland development as a regulator of apoptosis during morphogenesis (reviewed in Akira, 2000). Interestingly, constitutive activation of STAT3 is reported in prostate cancer and mediated by interactions with BRCA1 (<u>br</u>east <u>ca</u>ncer <u>1</u>) (Gao *et al.*, 2001).

1.4.4 Growth hormone response and embryonic development

STAT5b, which shares approximately 90% amino acid identity with STAT5a, is essential for <u>g</u>rowth <u>h</u>ormone (GH) signalling. STAT5b deficient animals demonstrate defects in loss of sexually dimorphic body growth rates (reviewed in Davey *et al.*, 1999). Growth defects are even more apparent in animals mutant for both STAT5a and STAT5b, that also show infertility in females (reviewed in Levy, 1999).

Implication of the JAK/STAT pathway in mouse embryonic development is concluded from expression of STAT3 in early post-implantation embryos and the observation that STAT3-deficient individuals die in embryogenesis prior to gastrulation. The embryonic lethality is assumed to result from insufficiency of nutrition, as timing of the STAT3$^{-/-}$ embryo degeneration coincides with the onset of STAT3 expression in the extra-embryonic visceral endoderm, which is the principal site of nutrient exchange between the maternal and embryonic environments (reviewed in Akira, 2000).

Animals lacking JAK/STAT pathway activity that do not die during embryogenesis suffer from severe diseases. While under-activation of the pathway results in various forms of immunodeficiencies, its over-activation has a transformation effect frequently leading to tumours such as leukemias, lymphomas, myelomas as well as breast and prostate cancers (reviewed in Schindler, 2002; Calò *et al.*, 2003).

1.5 Functions of the JAK/STAT pathway in *Drosophila melanogaster*

The canonical JAK/STAT pathway in *Drosophila* is identical to that described in mammalian system. To date, the fruitfly homologues for all core components are identified and characterised. Investigations over the past decade have found a requirement for the JAK/STAT pathway in diverse processes important during embryonic, larval and adult stages. Some of the roles are similar to those played by the pathway in vertebrates, whereas a number of functions appears to be unique for *Drosophila*. This chapter illustrates the importance of the JAK/STAT pathway in the fruitfly.

1.5.1 Role of the JAK/STAT pathway in spermatogenesis

Though the role of the JAK/STAT pathway in spermatogenesis is a fresh chapter of the pathway history, I decided to begin with gametogenesis, as this order seems chronologically reasonable.

The *Drosophila* testis is a long tube with straight apical and coiled basal ends (for review see Fuller, 1998; Zhao & Garbers, 2002). Self-renewing germline stem cells (GSC) are arranged around a hub, a group of specialised somatic cells located at the apical tip (Fig 1.6). Stem cells divide asymmetrically to give one proximal to the hub stem cell and one distal goniablast that differentiates and gives rise to future sperm cells.
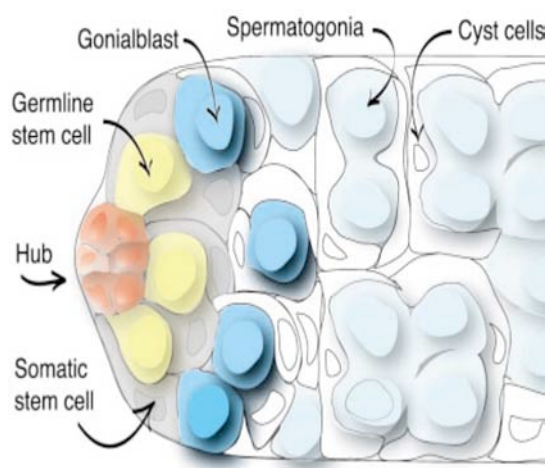
Figure 1.6. Apical end of the *Drosophila* tesits (from Tulina & Matunis, 2001).

GSCs (yellow) attach to the hub (orange). GSC daughters adjacent to the hub remain stem cells (yellow); daughters displaced from the hub differentiate into gonialblasts (blue). Gonialblasts undergo 4 mitotic divisions forming 16 interconnected spermatogonia (light blue). Later, spermatogonia enter meiosis and become spermatocytes. The cells move to the basal end as differentiation proceeds. Each gonialblast and its progeny are enveloped by two somatic supporting cyst cells (colorless) arising from asymmetric divisions of cyst progenitor cells (gray).

Yet in 1986 it was noticed that viable alleles of *hop* caused male sterility (Perrimon & Mahowald, 1986). However, not until 2001 the cause for this defect was uncovered. Recent investigations have shown that embryonic gonads in *hop* and *stat92E* mutants possess normal number of primordial cells, whereas adult testes contain no or almost no GSCs (Kiger *et al.,* 2001; Tulina & Matunis, 2001). Analysis of *stat92E* GLC shows that mutant spermatogonia are able to differentiate into a sperm, which implies that the JAK/STAT pathway is not required for differentiation. The pathway ligand Upd is expressed in and secreted by the hub cells, and its ectopic expression results in expansion of GSCs. Altogether these suggest that the essential function of the JAK/STAT pathway in the testis is to maintain the population of the germline cells.

1.5.2 Functions of the JAK/STAT pathway in oogenesis

The *Drosophila* ovary is composed of egg chambers, formed by a cyst and the surrounding it follicle cells (Fig 1.7; reviewed by Roth, 2001). The follicular epithelial differentiates into three populations of cells: a monolayer, encapsulating the cyst; polar cells, the most anterior and posterior cells within the monolayer; and, finally, stalk cells, connecting the chambers. Later, the follicular cells that are the most adjacent to the anterior polar cells differentiate into border cells, detach from the rest of the epithelium and migrate between the nurse cells towards the anterior pole of the oocyte.
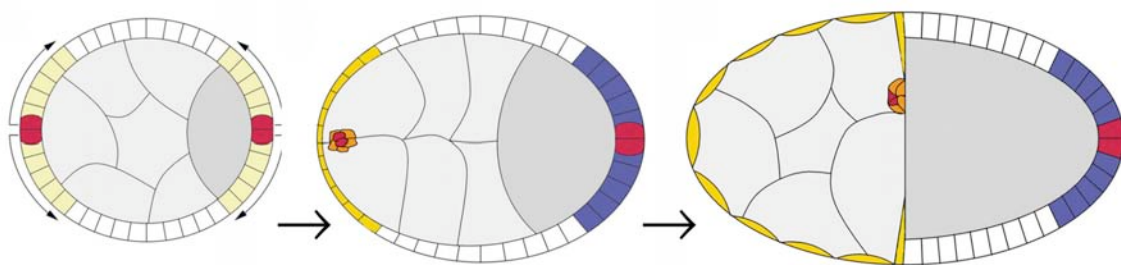
Figure 1.7. Composition of the *Drosophila* ovary (after Denef & Schüpbach, 2003).

Schematic representations of egg chamber development. Anterior is to the left, and posterior is to the right. Prior to stage 6 of oogenesis, the follicle cell layer becomes subdivided into terminal (light yellow) and mainbody (colourless) domains. The polar cells (red) differentiate within the terminal domain. A signal emanating from the polar cells specifies the terminal cell populations and organises them into anterior and posterior domains (yellow and blue). The differentiated border cells (orange) detach from the epithelium at stage 9 and migrate between the nurse cells (light grey) to reach the anterior end of the oocyte (dark grey) by the beginning of stage 10.

As discovered recently, the JAK/STAT is required for stalk and polar cell development (Baksa *et al.*, 2002; Beccari *et al.*, 2002; McGregor & Harrison, 2002; Xi *et al.*, 2003). Upd is secreted specifically by the precursors of stalk/polar cells and establishes a gradient of JAK/STAT pathway activity along the follicle epithelium. Mutations in *hop* cause fusions of the egg chambers due to the lack of the stalk cells, while over-activation of the pathway results in expanded population of the stalk cells at the expense of the polar cells. These suggest that the JAK/STAT pathway activity defines the fate of both the stalk and the polar cells. The posterior polar cells when lacking JAK/STAT pathway activity do not differentiate properly, which results in aberrant cytoskeleton reorganisation and mis-translocation of anterior-posterior determinants, processes that are normally triggered by signals from the posterior polar cells.

In the anterior follicle epithelium JAK/STAT pathway is also required for border cell migration, as in *hop*, *stat92E* and *upd* mutants the border cells are not able to migrate properly, while ectopic *upd* or *hop* promote additional cells to move.

1.5.3 Requirement for the JAK/STAT pathway in segmentation

Segmentation of the fruitly embryo is a breath-taking topic in developmental biology. During the last two decades a large number of genes involved in embryonic pattern formation have been identified, which advanced our understanding of mechanisms underlying early *Drosophila* development. Since a good deal of reviews are now available, I will try to make this introduction as brief as possible, though there is a large temptation to mention all intriguing facts that, unfortunately, lie beyond the topic of this study.

The *Drosophila* body plan is established by a cascade of interactions between genes falling into three co-operating groups: anterior-posterior (AP) polarity establishing system, dorso-ventral (DV) system and terminal group.

The initial AP polarity is determined by the **maternal determinants** – *bicoid* (*bcd*) and *hunchback* (*hb*), called "anterior" genes, and the opposing "posterior genes" *nanos* (*nos*) and *caudal* (*cad*) – which interact to subdivide the embryo into two broad regions: the anterior half containing Bcd and Hb^{mat} proteins, and the posterior half containing Cad and Nos (Fig 1.8, for review see Dearden & Akam, 1999; Lipshitz, 1991; St Johnston & Nüsslein-Volhard, 1992; Ephrussi & St Johnston, 2004).
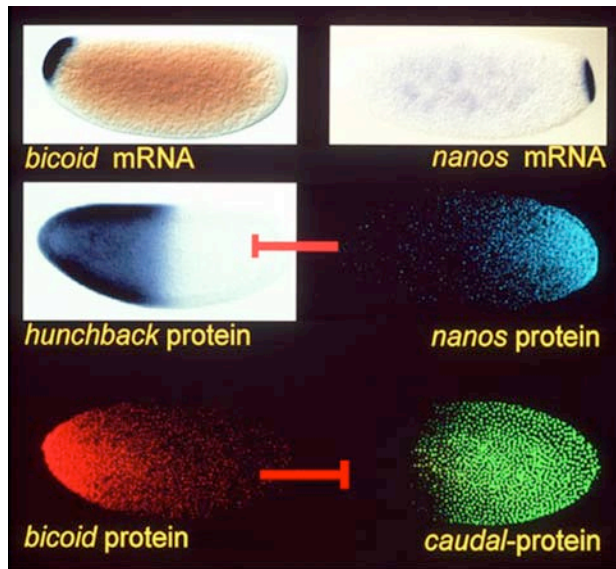
Figure 1.8. Maternal determinants (from lectures by U. Schmidt-Ott).

In the oocyte and early embryo *bicoid* and *nanos* mRNAs are tightly localised to the anterior and the posterior poles, respectively. By the end of the 9th cell cycle the domain of Nanos becomes established. Nanos represses translation from *hunchback* mRNA, which leads to Hunchback distribution only in the anterior half. Bicoid represses translation of *caudal*, therefore Caudal is restricted to the posterior half of the embryo. As a result, the embryo is subdivided into two domains: the anterior half, expressing Bicoid and Hunchback; and the posterior, containing Nanos and Caudal.

By the end of 10th cell cycle at the syncitial blastoderm stage, the domains of hb^{zyg}, *giant*, *Krüppel* and *knirps* that belong to the **gap gene** group are established in response to the early determinants (Fig 1.9). Precise expression pattern of the gap genes is achieved by activity of the maternal genes as well as interactions between the gap genes themselves (reviewed in Sanchez & Thieffry, 2001). The combined actions of the regulators encoded by the maternal genes and the gap genes then specify the domains of **pair rule** genes transcription by 13th mitotic cycle. The pair rule genes are expressed in seven stripes at the syncitial blastoderm stage and define the odd- or even-numbered parasegments (a parasegment (PS) corresponds to the posterior compartment of one segment and the anterior compartment of the adjacent segment). When cellularisation is completed, **segment polarity** genes are activated, whose expression marks the boundaries between parasegments (reviewed in Sanson, 2001). Finally, development of segment specific structures is determined by **homeotic genes** (Alonso, 2002).

The roles of DV and terminal systems in establishing the *Drosophila* body plan are reviewed in Lipshitz, 1991; Steward & Govind, 1993; Morgan & Mahowald, 1996; Nilson & Schüpbach, 1999; Stein & Stevens, 2001.

Segmentation gene cascade

maternal genes

gap genes

pair rule genes

segment polarity genes
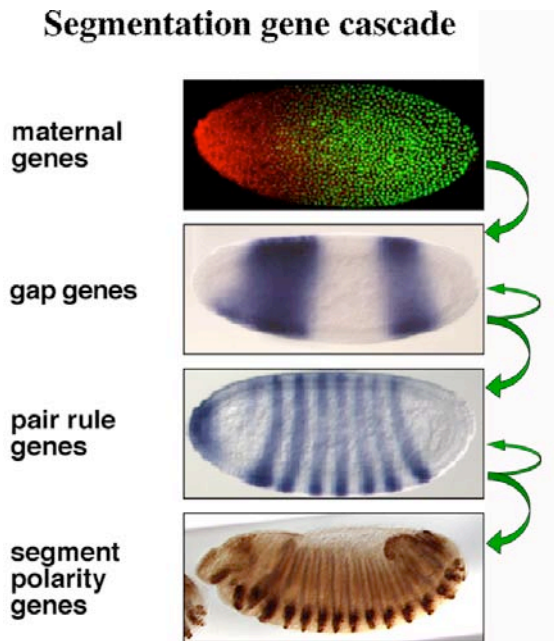
Figure 1.9. Segmentation gene cascade (from lectures by U. Schmidt-Ott).

The *Drosophila* body plan is established in several steps. First, anterior and posterior regions are defined by the maternal determinants of the AP system. Within these regions sub-domains are determined by the gap genes. The gap genes regulate their own expression and that of the downstream pair rule genes, which results in a regular parasegmental pattern of the embryo. In turns, pair rule genes affect parasegment-specific activation of the segment polarity genes which determine anterior and posterior regions within each parasegment.

In 1986 *hopscotch* was identified as a maternal effect gene required for embryonic segmentation. Though Hop is uniformly expressed in the embryo, its loss-of-function (LOF) mutaions show distinct segmentation defects, with the most prominent loss of the fifth abdominal (A5) segment and less consistant reduction of A4, A8 and the thorasic segments T3 and T2. In rare cases A6 and A7 are fused and defects in the posterior spiracles are observed (Perrimon & Mahowald, 1986). Identical defects are also seen in *stat92E* GLC (germ line clone) embryos (Fig 1.10). Since the JAK/STAT pathway was discovered and the ligand Upd identified, the segmentation effects of *hop* and *stat92E* LOF mutations have become clear.
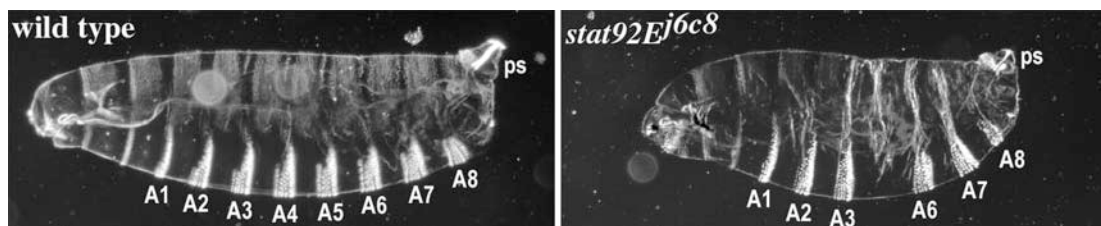
Figure 1.10. Segmentation defects in GLC derived *stat92E^{j6c8}* embryos.

Dark field images of the cuticles secreted by the wild type and mutant embryos lacking maternal *stat92E*. Eight abdominal denticle belts marked A1-A8 are clearly distinguished in the wild type embryos. In the *stat92E^{j6c8}* mutant A4 and A5 are missing. Defects in the posterior spiracle (ps) are also visible.

In embryogenesis *upd* is expressed zygotically in a very dynamic pattern (Fig 1.11; Harrison *et al.*, 1998; Karsten *et al.*, 2002). Loss of the early *upd* expression in the

mutants affects the segments that are most dependent of JAK/STAT pathway activity and phenocopies *hop* GLC mutants.
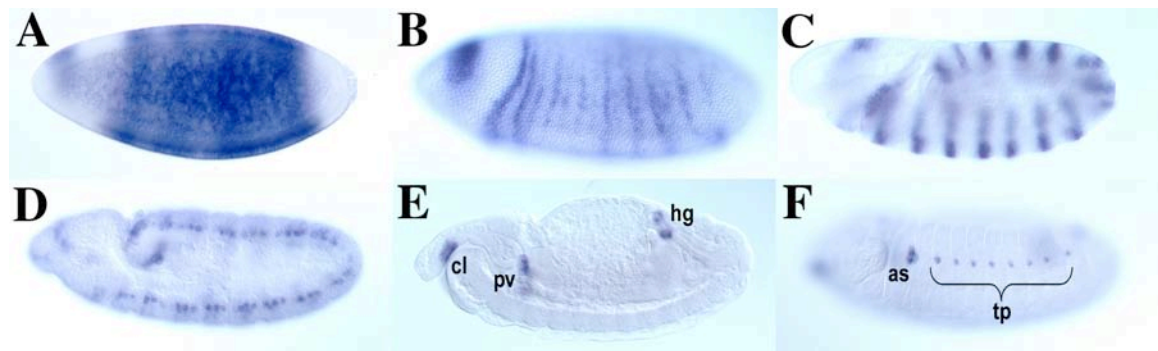
Figure 1.11. Expression of *upd* mRNA during embryogenesis (after Karsten *et al.*, 2002).

(A) At stage 5 the staining is seen in the dorsal anterior head region and 7 sripes resolving in the trunk region. (B) Stage 6 embryos show expression in the head region and 14 narrow stripes throughout the trunk. (C) Early stage 9 embryos express *upd* in the head region and in 14 stripes. (D) Stage 10, expression is transiently detected in three neuroblasts per hemisegment. (E) Expression in the stage 13 embryo is detected in the clypeolabrum (cl), the proventriculus (pv) and thehindgut (hg). (F) At stage 14, *upd* is expressed in the anterior spiracles (as) and the tracheal pits (tp).

Analysis of segmentation gene expression in the JAK/STAT mutants revealed that while gap genes being unaffected, expression of the pair rule genes *even-skipped* (*eve*), *runt* and *fushi tarazu* was reduced in stripe 5 with an additional weaker defect in the *eve* stripe 3 (Binari & Perrimon, 1994; Harrison *et al.*, 1998; Yan *et al.*, 1996b). Expression of the segment polarity genes *engrailed* (*en*) and *wingless* (*wg*) is also altered, with the *wg* stripe 9 corresponding to PS9 and the *en* stripe 10 (PS10) missing, although these defects reflect the changes in the pair rule gene expression (Binari & Perrimon, 1994).

Thus, the primary role of the JAK/STAT pathway in early embryogenesis is to specify the abdominal segment 5, while the pathway activity is also required for other abdominal as well as thoracic segments and posterior spiracle development.

1.5.4 The JAK/STAT pathway and sex determination

In *Drosophila* sex is determined at early stages of embryogenesis and defined by the ratio of X chromosomes to the number of autosomes (X/A) (for review see Lalli *et al.*, 2003; Penalva & Sanchez, 2003). X/A ratio equal to 1 produces females, while that of 1/2 results in male development. This ratio information is transmitted to the master switch gene *sex-lethal* (*sxl*), such that Sxl is expressed only in females (Fig 1.12). Its

activity results in transcription of female-specific genes, whereas in males absence of Sxl enables a dosage compensation mechanisms that hyperactivates X-linked genes in males.
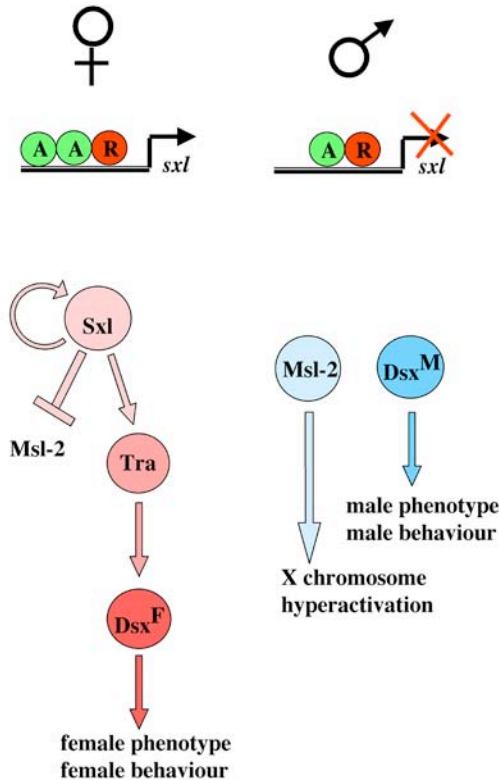
Figure 1.12. Interactions underlying sex determination in *Drosophila*.

In females, activators encoded from X chromosome trigger expression of Sxl, which maintains its own expression, negatively regulates *msl-2* (*male-specific lethal 2*) and specifies female splicing of *tra* (*transformer*) pre-RNA. The full-length female-specific Tra defines the female-specific splicing of *doublesex* (*dsx*). As a result, female-specific genes are activated giving rise to the female phenotype and behaviour.

In males, absence of Sxl enables expression of Msl-2, which is involved in dosage compensation mechanism via hyper-activation of X-chromosome. Male-specific Dsx^M regulates expression of male-specific genes, which results in the male phenotype and male behaviour.

The initial choice of *sxl* expression depends on a prevalence of either activators encoded by X-linked genes, or repressors coded for by autosomal genes. The identified activators are *sisterless-a* (*sis-a*), *sis-b*, *runt* and *sis-c*, of those the first three genes encoding transcription factors, whereas *sis-c* is now known as *unpaired* (reviewed in Zeidler & Perrimon, 2000). Activation of *sxl* expression by Upd has been confirmed using a reporter construct encompassing a part of the *sxl* promoter, in which STAT92E binding sites have been identified (Sefton *et al.*, 2000). However, lack of JAK/STAT pathway activity has a significantly weaker effect than mutations in *sis-a* and *sis-b* (Jinks *et al.*, 2000; Sefton *et al.*, 2000). Therefore, Upd is suggested to play a secondary role in X chromosome counting likely via enhancing activation of *sxl* induced by other modulators.

1.5.5 Embryonic gut formation

Drosophila digestive tract is composed of three major parts: fore-, mid- and hindgut. The embryonic gut is formed through invagination of the anterior and posterior midgut primordia. During the germband retraction, the anterior and posterior midgut anlagen move towards each other and finally fuse (Fig 1.13). Meanwhile, both the fore- and the hindgut undergo extensive morphological changes and regional specifications, so that by the end of embryogenesis the digestive tract represents a complex structure (reviewed in Skaer, 1993).
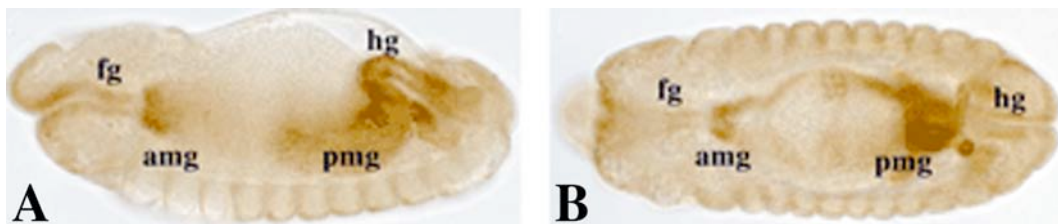
Figure 1.13. The structure of the embryonic gut (after Bauer *et al.*, 2002).

kropfP188 line embryos carrying P insertion in the *innexin 2* transcription unit, which is expressed in the embryonic gut, are stained with anti-ß-Gal antibody. The foregut (fg), the anterior and posterior midgut (amg and pmg, respectively), and the hindgut (hg) are visualised. Lateral (A) and dorsal (B) views are shown.

Recent studies have shown that the JAK/STAT pathway is required for proper morphology of both the fore- and the hindgut. In the foregut the JAK/STAT pathway, in co-operation with Notch signalling, controls cell movements critical for epithelial morphogenesis of the proventriculus (Josten *et al.*, 2004). In the hindgut, Upd is expressed in the most anterior region, referred to as small intestine, and promotes oriented cell rearrangements, termed "convergent extension", that lead to gut elongation. In *upd*, *hop* or *stat92E* mutant embryos the hindgut is short and wide (Johansen *et al.*, 2003).

1.5.6 Trachea development

Drosophila trachea formation begins with ten tracheal placodes invaginating in every segment from the second thoracic (T2) to the eighth abdominal (A8) on either side of the embryo (Fig 1.14; reviewed in Krause, 2003). The external openings of these invaginations – tracheal pits – obliterate by the late stages of embryogenesis, meanwhile tracheal placodes form branches. The tracheal branches migrate towards their target tissues and eventually fuse with each other to form the dorsal trunk, a

major airway, linking each tracheal metameres and the anterior spiracle in T1 to the posterior spiracle in A8. The spiracles are the terminal parts of the tracheal system that connect the tracheal network with the external environment.
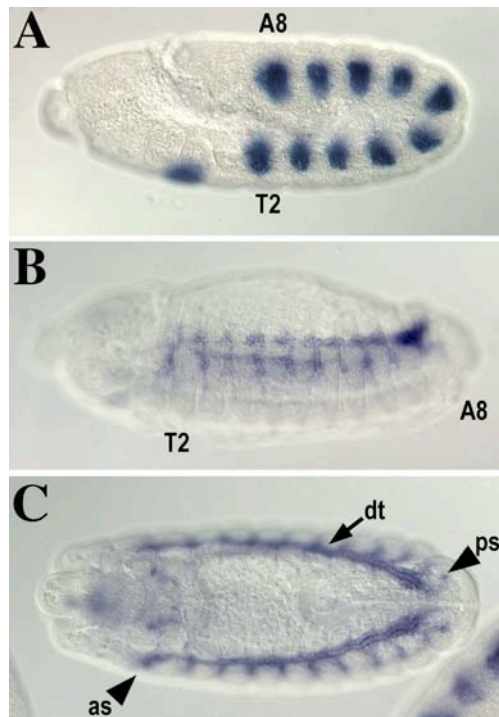
Figure 1.14. Development of the tracheal system traced by *trachealess* (*trh*) expression.

(A) Stage 10/11 embryo, lateral view. Tracheal placodes start invaginating in each segment from T2 to A8 (marked). (B) Stage 13 embryo, lateral view. At the end of germband retraction the branched tracheal invaginations fuse forming the larval tracheal tree. T2 and A8 segments are marked. (C) Stage 15 embryo, dorsal view. Dorsal trunk (dt) is formed and connects the anterior spiracles (as), the tracheal metameres and the presumptive filtzkörper of the posterior spiracles (ps)

The exact mechanism, whereby the JAK/STAT pathway controls trachea development, is not yet clear. However, expression of *upd* and presence of phosphorylated STAT92E in the tracheal and posterior spiracle placodes suggest a role for the JAK/STAT pathway in tracheal system formation (Harrison *et al.*, 1998; Li *et al.*, 2003). Furthermore, analysis of *dome* and *stat92E* mutants has shown that tracheal pits do not form in the absence of the JAK/STAT pathway, neither the posterior spiracles develop properly (Brown *et al.*, 2001; Chen *et al.*, 2002). Also expression of *trachealess*, the early marker of trachea, and, later, *knirps* is almost undetected in *dome* and *stat92E* mutants (Brown *et al.*, 2001).

1.5.7 Roles of the JAK/STAT pathway in blood cell development and immune response

One of the first indicators that the JAK/STAT pathway might be involved in the development of hemocytes came from the characterisation of dominant gain-of-function (GOF) alleles of *hop − Tum-l* (*tumourous lethal*) and *T42*. These are

characterised by constitutively hyperactivated kinase activity, which causes melanotic tumour formation and abnormalities in blood cell development (Harrison *et al.*, 1995; Luo *et al.*, 1997).

Drosophila hematopoiesis occurs in two major phases. First embryonic hematocytes originate from the anterior mesoderm and colonise the embryo where they function as phagocytes of apoptotic cells (reviewed in Tzou *et al.*, 2002; Meister & Lagueux, 2003). By the end of embryogenesis, the lymph glands (the larval hematopoietic organ) differentiate and give rise to three lineages of hemocytes: plasmatocytes, lamellocytes and crystal cells. Plasmatocytes represent approximately 90-95% of the blood cells and function as phagocytes. Lamellocytes are required for encapsulation of parasites, while crystal cells are involved in melanisation processes.

hop^{Tuml} mutants have 5- to 20-fold more plasmatocytes, many of which prematurely differentiate into lamellocytes and contribute to melanotic tumourigenesis (Sorrentino *et al.*, 2004). The precise mechanism, whereby the JAK/STAT pathway functions in blood cells, is not yet known. But it has been shown that hamocytes from hop^{Tum-l} larvae have an elevated level of D-eIF1A, a homologue of human eukaryotic initiation factor 1A (eIF1A) involved in protein translation initiation (Myrick & Dearolf, 2000).

Another organ essential for immune response is the fat body. Following parasitic invasion, signalling pathways provoke fat body cells to produce anti-microbial peptides (reviewed in Tzou *et al.*, 2002; Agaisse & Perrimon, 2004). Recent observations report that the JAK/STAT pathway is activated in the fat body cells upon immune challenge (Agaisse *et al.*, 2003). Furthermore, TotA, an anti-microbal peptide, and Tep-1, a protein related to human macroglobulins of the complement system, are expressed in response to JAK/STAT pathway activation (Lagueux *et al.*, 2000; Agaisse *et al.*, 2003). Strikingly, neither *upd* nor *upd2* levels are elevated upon bacterial infection, whereas expression of *upd3* in hamocytes is significantly increased (Agaisse *et al.*, 2003). It is, therefore, proposed that Upd3 secreted by circulating hamocytes upon infection mediates immune response via activating the JAK/STAT pathway in the fat body cells.

1.5.8 The JAK/STAT pathway and imaginal discs development

Imaginal discs form as groups of 10-50 cells that invaginate in the embryo and proliferate extensively during larval development (reviewed in Ramirez-Weber &

Kornberg, 2000; Gibson & Schubiger, 2001). In larva, the imaginal discs are flattened epithelial sacs with two opposing surfaces: a columnal epithelium, which will give adult structures, and a peripodial membrane, which is a provisory organ. Upon stimulation by the steroid moulting hormone ecdysone during the mid-third instar, the imaginal discs undergo a series of metamorphic changes, finally resulting in eversion, a process that unfolds the epithelial layer and results in transformation of the discs into adult structures.

The only documentation of requirement for the JAK/STAT pathway in wing imaginal disc development is a study by the laboratory of Charles Dearolf (Yan *et al.*, 1996a). The authors generated a hypomorphic *stat92E^{HJ}* mutation that, in addition to affecting embryonic segmentation, also exhibited defects in the wing. The *stat92E^{HJ}* homozygous adults show ectopic wing vein formation that can be suppressed by constitutively active Hop^{Tum-l}. Another phenotype that can link the JAK/STAT pathway to wing development is outstretched wings, a characteristic of some *upd* alleles (Harrison *et al.*, 1998). Interestingly, in *os^{1A}* homozygous flies *upd* is not expressed in one of the three domains within the prospective hinge region of the wing imaginal discs (M. Zeidler, unpublished observation).

A role for the JAK/STAT pathway in the eye imaginal discs has also been studied. The proliferative effect exercised by JAK/STAT signalling is necessary for eye development, as small eye phenotype is registered in *upd* and *hop* LOF mutants (Luo *et al.*, 1999; Tsai & Sun, 2004; Betz *et al.*, 2001). Reciprocally, ectopic expression of Upd in the eye imaginal discs results in eye overgrowth (Chen *et al.*, 2002; Bach *et al.*, 2003).

The JAK/STAT pathway is also implicated in ommatidia differentiation. Ommatidia are structural units of the *Drosophila* compound eye (reviewed in Voas & Rebay, 2004). Ommatidia differentiation begins in the early third instar larvae and occurs as a wave, moving from posterior to anterior. This wave is marked by an apical constriction of the disc epithelium, termed morphogenetic furrow. Differentiating ommatidia behind the furrow rotate 90° away from the dorso-ventral midline, with this rotation being differentially polarised in dorsal and ventral poles. The JAK/STAT pathway, in synergy with Notch and Wingless signallings, is involved in the establishment of DV polarity and ommatidia rotation most likely via regulating expression of *four-joined*, a gene encoding a transmembrane protein and shown to be

required for ommatidia rotation (Zeidler *et al.*, 1999a; Zeidler *et al.*, 1999b; Zeidler *et al.*, 2000).

1.6 Screen to identify new components of the JAK/STAT pathway

As described above the JAK/STAT pathway is implicated in many processes in various tissues and at different time points during *Drosophila* development. However, in contrast to mammals, the entire variety of functions is served by a relatively small number of proteins, so that the final step in the signal transduction – gene expression – is fulfilled by a single STAT92E. The question arises how the same molecules can underlie such a wide range of tissue- and stage-specific responses? It is very probable that JAK/STAT signalling must be involved in a large network of interactions, including cross-talk with other pathways, which allows precise and well-timed tuning of developmental processes. In order to reveal potential interaction partners of the JAK/STAT pathway a screen was undertaken based on the eye overgrowth phenotype (Fig 1.15A-B; Bach *et al.*, 2003). This phenotype is caused by over-expression of the pathway ligand Unpaired driven under control of *GMR* (Glass mulrimerised response) promoter containing multiple binding sites for the eye specific transcription factor Glass (Hay *et al.*, 1997). Over-proliferation of eye tissues caused by Upd results in overgrowth of the eye imaginal discs and, as a consequence, increased eye size in adults (Fig 1.15C-D). This phenotype is sensitive to the efficiency of the endogenous JAK/STAT signalling cascade and has been used to search for loci that interact with the pathway (Bach *et al.*, 2003). Mutations that reduce the efficiency of the signalling are expected to suppress the phenotype, while mutations in genes normally required to down-regulate the pathway should result in additional overgrowth (Fig 1.15E).

One small locus, defined by *Df(2R)Chi^{g320}* and removing the genomic region 60A3-7 to 60B4-7, has been found a moderate enhancer of the *GMR-updΔ3'* induced eye overgrowth. In order to identify the gene responsible for the interaction, available mutations of the loci missing from *Df(2R)Chi^{g320}* were tested for interaction. A potential candidate located in the genomic region 60A6 is *ken&barbie* (*ken*), which is the central focus of this thesis.
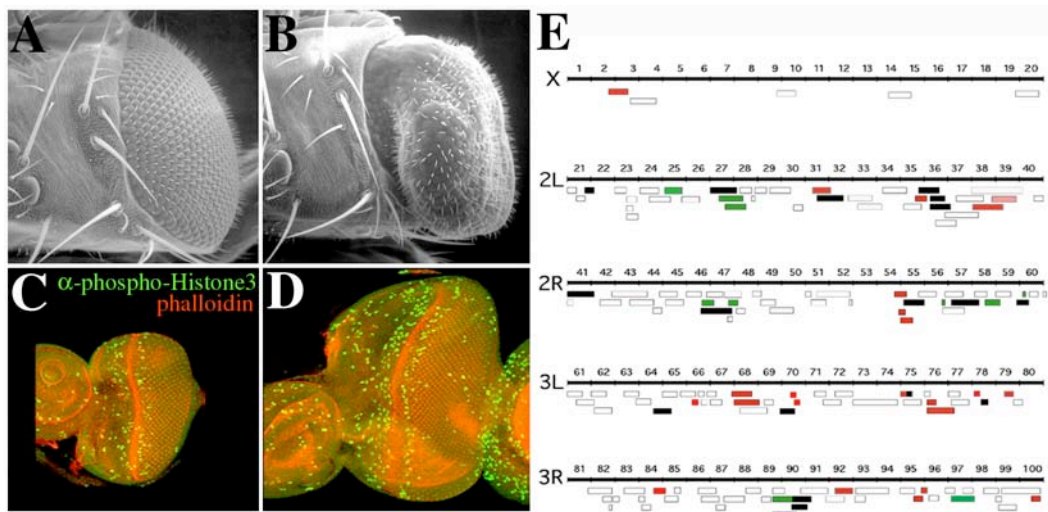
Figure 1.15. *GMR-updΔ3'* screen (from M.Zeidler, unpublished).

(A-B) Scanning electron micrographs of a wild type eye (A) and an enlarged eye of *GMR-updΔ3'* (B). (C-D) Third instar eye-antennal disc complexes were stained with an antibody to phospho-Histone3 (in green), which marks cells in mitosis, and with rhodamine-conjugated phalloidin (in red) at 96 hr after egg laid. Compared to wild type (C) the *GMR-updΔ3'* discs (D) are apparently bigger and contain more mitotic cells in the region anterior to the furrow. (E) A scheme representing the approximate genomic positions of the deficiencies examined. Suppressors of the large eye phenotype are marked by red boxes, enhancers are presented in green boxes. Non interacting deletions are colourless. Black boxes indicate lethal crosses.

2 Results

2.1 Mutations in *ken* locus enhance the *GMR-upd* eye overgrowth phenotype

As described in the section 1.6, *Df(2R)Chi^g320* has been identified in the *GMR-updΔ3'* screen as a region that potentially interacts with JAK/STAT pathway in *Drosophila melanogaster* (see Fig 1.15; Bach *et al.*, 2003). After having tested available mutations in candidate genes encompassed by this deficiency, several LOF mutations in *ken* locus were found to enhance the *GMR-updΔ3'* phenotype to a level similar to that initially observed for *Df(2R)Chi^g320* (Fig 2.1).
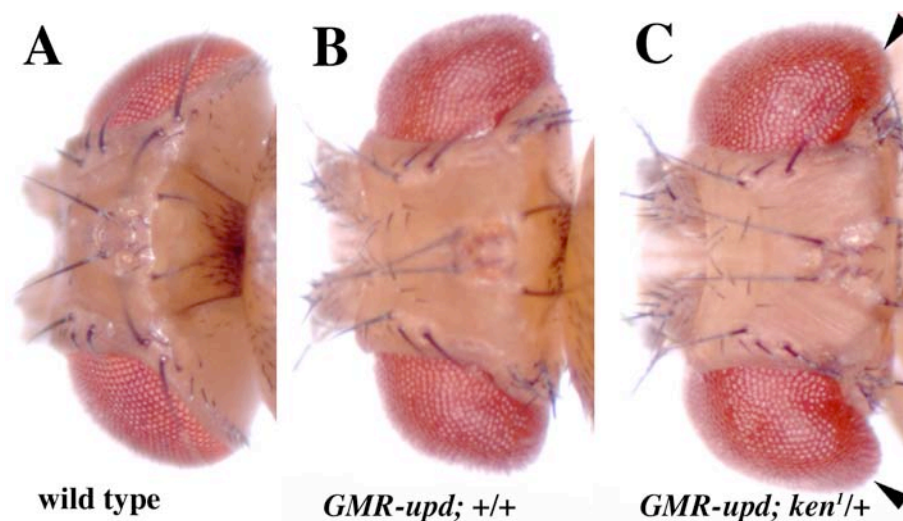
Figure 2.1. Genetic interactions between *ken* and *GMR-updΔ3'*.

Dorsal view on the head region of adult wild type (A) and *GMR-updΔ3'* flies, either carrying a wild type second chromosome (B) or heterozygous for *ken^1* allele (C). Note the additional eye overgrowth in flies lacking one copy of the *ken* locus (arrowheads in C).

The enhancement of the *GMR-updΔ3'* phenotype is potentially a consequence of either an interaction with the JAK/STAT pathway or an interaction with the *GMR* promoter itself. To test whether removal of one copy of *ken* can enhance the *GMR* driven mis-expression of other genes, *ken* mutants were crossed to stocks carrying *GMR-rho* and *GMR-yan* transgenes. Both of the lines are reported to generate rough eye phenotypes likely to be independent of the JAK/STAT pathway (Rebay & Rubin, 1995; Häcker & Perrimon, 1998). Introducing either *ken^1* or *ken^02970* alleles into

GMR-rho and *GMR-yan* flies had no effect on the eye phenotypes caused by the corresponding constructs (Fig 2.2). This indicates that loss of one copy of *ken* is unlikely to modulate the strength of the *GMR* promoter, and the gene rather interacts – directly or indirectly – with the JAK/STAT pathway.
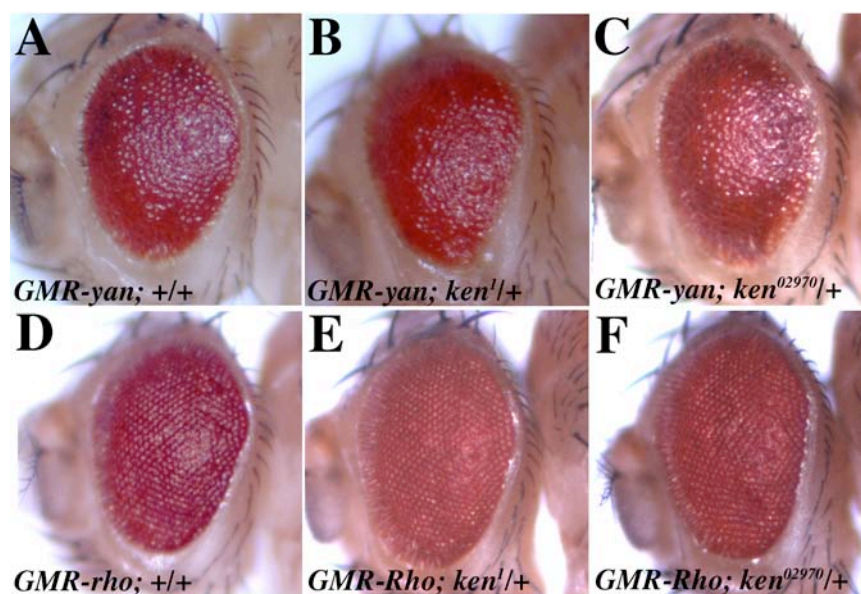
Figure 2.2. *ken* interacts with neither *GMR-rho* nor *GMR-yan*.

(A-C) Lateral view on the head region of *GMR-yan* flies. Severe rough eye phenotype caused by *GMR-yan* (A) is indistinguishable from that of the flies simultaneously heterozygous either for *ken[1]* (B) or *ken[02970]* (C) alleles. (D-F) Lateral view on the head region of *GMR-rho* flies. Weaker rough eye phenotype caused by *GMR-rho* (D) is not affected by one copy of *ken[1]* (E) or *ken[02970]* (F) alleles.

2.2 The *ken* locus

The *ken* transcription unit has been mapped to the 60A6 region of the right arm of the second chromosome and contains three exons, which encode a 601amino acid protein (Fig 2.3A; Kühnlein *et al.*, 1998; Lukacsovich *et al.*, 1999; Lukacsovich *et al.*, 2003). The protein possesses an N-terminal BTB/POZ (bric-a-brac, tramtrack, broad complex/Pox virus zinc fingers) domain extending from amino acid (AA) 17-131, and three C-terminal C_2H_2 zinc finger motifs from AA 502 – 590 (Fig 2.3B). BTB/POZ domains present in vertebrate transcription factors have been shown to mediate dimerisation and transcriptional repression via the recruitment of transcriptional co-repressors such as SMRT, mSIN3A, N-CoR and HDAC-1 (Dhordain *et al.*, 1997; Dhordain *et al.*, 1998; Huynh & Bardwell, 1998; Wong & Privalsky, 1998; Ahmad *et al.*, 2003). Searches for proteins similar to Ken identified the human BCL6 (B-cell lymphoma 6) as the closest overall homologue present in vertebrates (Baron *et al.*,

1993). BCL6 and Ken share the same domain structure and show 20.3% overall identity (Fig 2.3B; Chang *et al.*, 1996), and homologues of Ken are found in the genomes of *Drosophila pseudoobscura* and the mosquito *Anopheles gambiae*, which form a distinct, but related branch of the BCL6 family of proteins (Fig 2.3C).
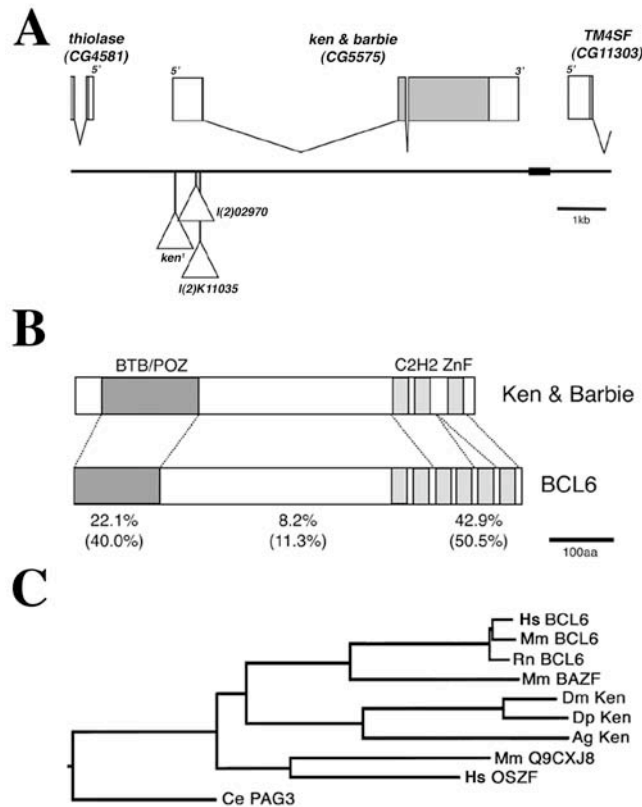
Figure 2.3. Scheme of the genetic region, protein structures and phylogeny of Ken.

(A) The *ken* genomic region is flanked by the *thiolase* and *TM4SF* loci. The position of the three P-elements inserted within the first exon of *ken*, which were used in this work, are shown below the line (not to scale). Coding regions are shown in grey and include also 3 AA encoded by exon1. (B) The predicted Ken protein contains an N-terminal BTB/POZ domain and three C-terminal Zinc fingers. The degree of identity (similarity) of a pairwise alignment generated using EMBOSS software (http://www.ebi.ac.uk/emboss/align/index.html) to human BCL6 is shown. (C) A phylogenetic tree shows the relationship between human (Hs), mouse (Mm) and rat (Rn) BCL6 genes, the close homologue BAZF, and the related invertebrate Ken-like proteins from *Drosophila malanogaster* (Dm), *Drosophila pseudobscura* (Dp) and *Anopheles gambiae* (Ag). More distantly related genes from humans, mouse and *Caenorhabditis elegans* (Ce) are also shown.

2.3 Analysis of *ken* alleles

P-element insertions, which generate ken^1, ken^{02970} and ken^{K11035} (Lukacsovich *et al.*, 1999; Spradling *et al.*, 1999), represent the only available alleles of this locus. In order to determine the relative strength of these alleles a genetic analysis was undertaken. Among the flies examined, 9.4% of the expected homozygous ken^1

mutants survive to adulthood (N=1353), many of which show external genitalia phenotypes (Fig 2.4), a characteristic that gave the locus its name. However, when crossed over the $Df(2R)Chi^{g320}$ deficiency chromosome that removes the *ken* locus, only 1% (N=610) of the expected number of trans-heterozygous $ken^1/Df(2R)Chi^{g320}$ individuals are recovered, indicating that ken^1 is a hypomorphic allele. While homozygous ken^{02970} animals never survive to adulthood, $ken^{02970}/Df(2R)Chi^{g320}$ trans-heterozygous flies showing ken^1 like phenotypes are recovered at 0.6% (N=932) of the expected frequency. This indicates that ken^{02970} also represents a hypomorphic allele and contains a second site mutation responsible for the lethality of the stock. Finally, ken^{K11035} contains a P-element close to the transcriptional start site (Fig 2.2A; Lukacsovich *et al.*, 1999) and does not give escapers when homo- or trans-heterozygous. When ken^1 LOF clones were induced in the second instar larvae no obvious phenotype was observed in the adult eyes within the clones marked by absence of w^+ marker. By contrast, induction of ken^{K11035} LOF clones caused lethality, and no flies eclosed. This implies that ken^{K11035} is a stronger allele than ken^1. However, the *ken* transcript is still present in $ken^{K11035}/Df(2R)Chi^{g320}$ trans-heterozygous embryos as detected by *in situ* hybridisation (see Fig 2.6J & K), with the levels of *ken* mRNA varying in the population of the trans-heterozygous mutant embryos. Though a large proportion of the embryos shows no staining, ken^{K11035} cannot be considered a null allele. Therefore, the strength of the *ken* alleles can be classified as $ken^1 \leq ken^{02970} < ken^{K11035} < Df(2R)Chi^{g320}$.
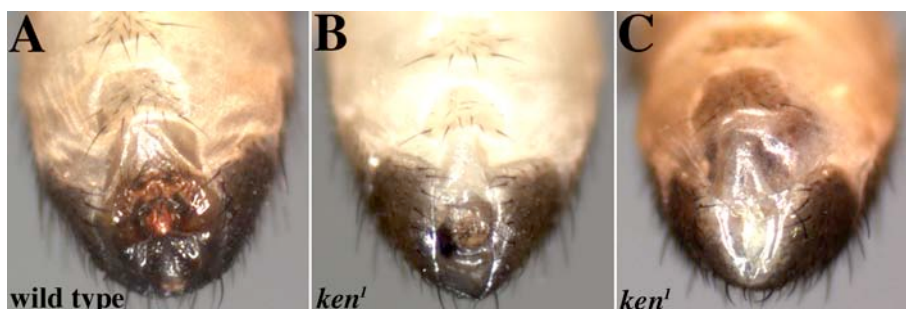
Figure 2.4. *ken* homozygous flies lack external genitalia.

Ventral view on the abdomen of wild type (A) and ken^1 homozygous males, lacking (B) or complete missing (C) the external genitalia structures.

2.4 *ken* interacts genetically with *stat92E^{HJ}*

So far, *ken* LOF mutations enhance the phenotype caused by *GMR-updΔ3'*, and this effect is specific for *upd* rather than for the *GMR* promoter. This implies that Ken normally functions by exerting a negative effect on the JAK/STAT pathway; in other words, Ken is a negative regulator of the pathway. If this is the case, *ken* must also interact with other components of the JAK/STAT pathway. To test this a genetic interaction between *ken* alleles and the hypomorphic *stat92E^{HJ}* allele was assayed. *stat92E^{HJ}* contains a point mutation within its first intron that inhibits normal mRNA splicing and results in the formation of a truncated negative protein (Yan *et al.*, 1996a). Homozygous *stat92E^{HJ}* mutants survive to adulthood and have wings that frequently contain an additional vein material (Fig 2.5). The frequency, with which ectopic veins are present in homozygous *stat92E^{HJ}* wings, was therefore assessed and compared to flies simultaneously heterozygous for *ken* (Table 2.1). All three *ken* alleles act as suppressors of the phenotype, an interaction consistent with both the proposed role of Ken as a negative regulator of JAK/STAT signalling and the allelic series described above.
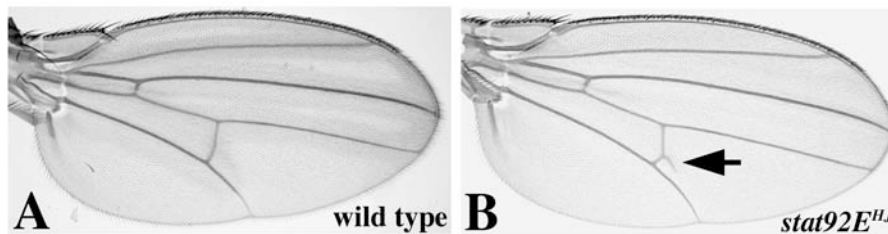
Figure 2.5. *stat92E^{HJ}* extra wing vein phenotype.

Adult wings of either wild type flies (A) or those homozygous for the hypomorphic *stat92E^{HJ}* allele (B), that frequently contain an additional wing vein material (arrow), a phenotype that can be modulated by changes in *ken* gene dosage.

Genotype	Vein Defects	
+ / + ; stat92E^{HJ} / +	0%	(n=93)
+ / + ; stat92E^{HJ} / stat92E^{HJ}	44.7%	(n=76)
ken^1 / + ; stat92E^{HJ} / stat92E^{HJ}	39.7%	(n=73)
ken^{02970} / + ; stat92E^{HJ} / stat92E^{HJ}	27.5%	(n=91)
ken^{K11035} / + ; stat92E^{HJ} / stat92E^{HJ}	9.7%	(n=41)

Table 2.1 Genetic interaction between *stat92E^{HJ}* and *ken* alleles.

Taken together, it appears that the *ken* locus genetically interacts as a negative regulator with both up- and downstream components of the JAK/STAT signalling pathway *in vivo*.

2.5 *ken* is expressed during development and in adult flies

Interactions with *GMR-updΔ3'* in the eye and *stat92E ^{HJ}* in the wing suggest that *ken* is active in these tissues. In order to determine where and when *ken* is expressed, especially with respect to the potential overlap with the pattern of JAK/STAT pathway activity, *in situ* hybridisation was performed.

ken anti-sense RNA probes detect the transcript as early as at pre-blastoderm stage, suggesting maternal accumulation of *ken* mRNA (Fig 2.6A). Zygotic *ken* is then expressed in two narrow stripes located approximately at 64% and 16% of the embryo length at stage 5 (Fig 2.6B). At this stage *ken* mRNA is abundant in the basal to the prominent cortical nuclei region (Fig 2.6G), in contrast to other genes, whose mRNA is actively apically localised during this stage of development (Bullock & Ish-Horowicz, 2001).

During gastrulation, the anterior stripe of *ken* subsequently weakens and finally vanishes by stage 9/10, while the posterior domain coalesces, such that *ken* is expressed at high levels in the presumptive hind gut/posterior spiracles, a region that maintains its relative position within the extending germband (Fig 2.6C).

At stage 14 *ken* expression is restricted to the presumptive posterior spiracles (Fig 2.6D), and by stage 15, the transcript is seen along the entire foregut (Fig 2.6E, F & H). Besides the foregut, *ken* is also expressed in the most anterior epithelial cells of each abdominal segment (Fig 2.6F & I).

During larval stages *ken* expression can be detected essentially uniformly throughout the imaginal discs (Fig 2.7A-C), with a region of higher expression present within the eye disc corresponding to the morphogenetic furrow (arrow in Fig 2.7A), and an anterior-posterior stripe in the antennal disc (arrowheads in Fig 2.7A). Identical pattern is observed when using *ken^1* enhancer trap detector expressing β-galactosidase under control of the endogenous *ken* promoter (not shown).
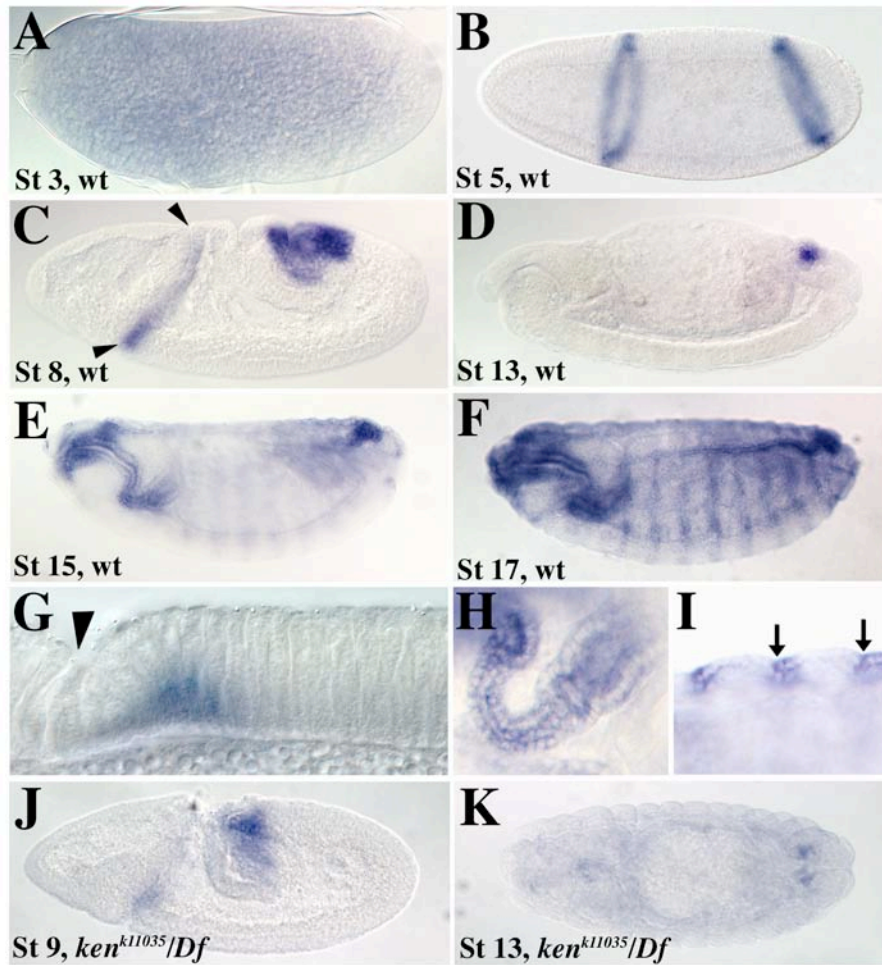
Figure 2.6. *ken* expression pattern in embryos.

(A-I) *In situ* hybridisation with *ken* anti-sense probe was performed on wild type embryos. (A) Stage 3/4 pre-blastoderm embryo shows maternally supplied *ken*. (B) At stage 5 *ken* is expressed in two narrow stripes. (C) The anterior stripe localises immediately posterior to the cephalic furrow (arrowheads), and posterior domain corresponds to the presumptive hindgut/posterior spiracles. (D) By stage 12, only the future posterior spiracles express *ken*. (E & F) Stage 15-17, expression is visible in the foregut, in the posterior spiracles, along the posterior region of the dorsal trunk and in weak stripes within the epidermis. (G-I) Higher magnification views. (G) Stage 6 cellular blastoderm, *ken* mRNA is abundant basely within the cells immediately posterior to the cephalic furrow (arrowhead). (H) At stage 15, *ken* is expressed along the entire foregut. (I) Expression is also detected in the most anterior epidermal cells of each segment. Arrows mark segment boundaries. (J & K) Low levels of *ken* transcript are seen in *ken^{K11035}/Df(2R)Chi^{g320}* trans-heterozygous embryos at stage 9 (J) and stage 13 (K). Embryonic staging is according to Campos-Ortega & Hartenstein, 1997. Here (except for K showing dorsal view) and further embryos and discs are oriented dorsal up and anterior to the left, unless otherwise specified.
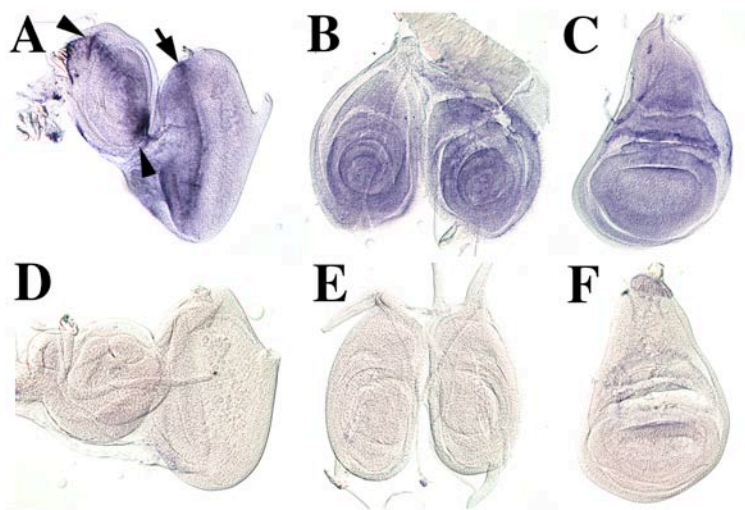
Figure 2.7. *ken* expression in imaginal discs.

Imaginal discs were derived from late third instar larvae. In situ hybridisation was performed with anti-sense (A-C) and sense (D-F) RNA probes against *ken*. (A) An eye-antennal imaginal disc complexe shows specific staining throughout the eye disc, with higher levels of *ken* expression immediately ahead of the morphogenetic furrow (arrow) and in a stripe through the antennal disc (arrowheads). Leg (B) and wing (C) imaginal discs show uniform expression. (D-F) Imaginal discs stained with sense probe remain blank.

Using Reverse Transcription-PCR (RT-PCR) *ken* mRNA was detected also at pupal and adult stages (Fig 2.8), which implies that Ken is expressed not only during embryonic and larval development, but its expression is maintained to adulthood. However, it is not clear whether *ken* shows equal distribution between genders, as RT-PCR reactions were performed on a population of both males and females. *ken* specific band was also detected in *ken¹* and *ken⁰²⁹⁷⁰* homozygous larvae, pupae and imagoes (not shown), which confirms the alleles as being hypomorphic.
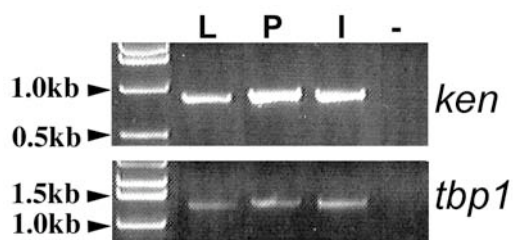
Figure 2.8. *ken* transcript is revealed by RT-PCR.

RT-PCR was performed with *ken* and *tbp-1* specific primers. Total cDNA was obtained from wild type larvae (L), pupae (P) and imagoes (I). The upper panel shows 926bp band specific for *ken*. The emount of cDNA in all samples is normalised as the 1230bp specific product derived from the constitutively expressed *tbp-1* shows equal intensity in each lane. DNA is visualised by ethidium bromide staining in 1% TBE agarose gel.

2.6 *ken* expression pattern overlaps regions that require JAK/STAT pathway activity

Visualisation of *ken* expression pattern identifies regions where Ken can potentially co-operate with the JAK/STAT pathway. As early as at stage 8, the anterior domain (AD) of *ken* is localised posterior to the developing cephalic furrow (arrow in Fig 2.9A), a region where *upd* transcript is expressed (arrow in Fig 2.9B). As Upd is a secreted molecule capable of diffusing from the source of its expression, this cephalic furrow region may represent a potential overlap between activities of Ken and the JAK/STAT pathway.

Later at stage 13, the expression of *ken* in the presumptive posterior spiracles (arrowheads in Fig 2.9C), which are known to require JAK/STAT pathway activity (Brown *et al.*, 2001), overlaps with the *upd* expression pattern, as the *upd* transcript is observed in the centre of the posterior spiracle primordia (arrowheads in Fig 2.9D). Furthermore, at stage 15 *ken* is expressed in the foregut including the proventriculus (Fig 2.6E, F & H), a structure known to express and require all components of the JAK/STAT pathway (Josten *et al.*, 2004).
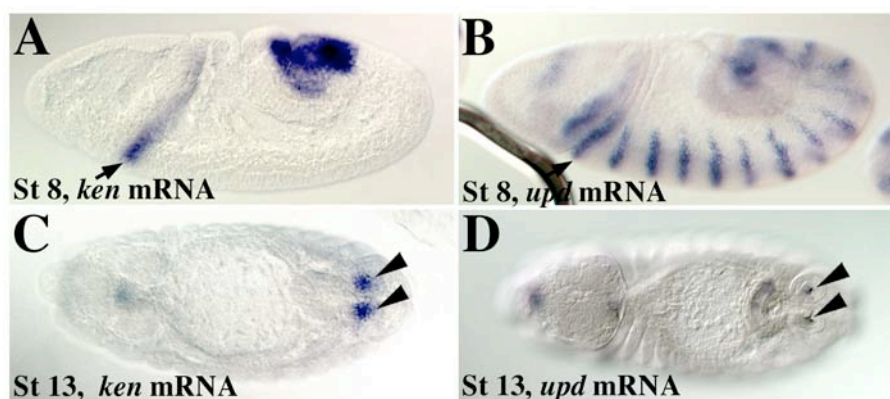
Figure 2.9. *ken* expression pattern overlaps that of *upd*.

ken and *upd* transcripts are visualised by *in situ* hybridisation. At stage 8, *ken* AD (A) is expressed very close to the region of the second stripe of *upd* (B, arrow). At stage 13, *ken* expression (C) overlaps the region of *upd* transcript (arrow) in the posterior spiracle primordia (D). C and D show dorsal views.

The presence of *ken* in the developing wing and eye imaginal discs is also consistent with the genetic interactions of *GMR-updΔ3'* and *stat92E^{HJ}* observed in these tissues, and with requirements for the JAK/STAT pathway in the imaginal discs (Yan *et al.*, 1996a; Zeidler *et al.*, 1999b; Zeidler *et al.*, 1999a). Furthermore, *ken* is expressed in

the adult flies, and the JAK/STAT pathway has been shown to be active at adult stages as well, when it is involved in follicle cell differentiation (Baksa *et al.*, 2002; Xi *et al.*, 2003), spermatogenesis (Kiger *et al.*, 2001) and immune response (Agaisse *et al.*, 2003).

2.7 *ken* interacts with *dome* in the posterior spiracles, and extra Ken phenocopies *dome* mutants

An overlap between *ken* expression and JAK/STAT pathway activity was found in the posterior spiracles (Fig 2.9C & D). It is known that mutations in *domeless* affect posterior spiracle development, and several *dome* alleles of different strengths have been characterised (Brown *et al.*, 2001). Moreover, changes in the structures, which comprise the posterior spiracles, can be clearly monitored in prepared embryonic cuticles (Fig 2.10A). Given these three aspects, genetic interactions between the weak *dome*^{367} allele and the strongest available *ken*^{K11035} mutation were assessed. When *dome*^{367}/FM7 virgin females being out-crossed to wild type males, 25% of the progeny are potentially hemizygous mutant (Table 2.2) and secrete cuticles with either weak phenotypes (Fig 2.10B), in which the external stigmatophore is missing, but the filtzkörper are still present, or strong phenotypes that almost completely lack both the stigmatophore and filtzkörper (Fig 2.10C). When crossed to *ken* alleles or the *Df(2R)Chi*^{g320} deficiency, half of the *dome*^{367} mutant embryos also lack a copy of *ken*. Under these conditions the frequency of the strong posterior spiracle phenotypes are clearly reduced for each *ken* allele with a concomitant increase in the weak phenotypes (Table 2.2).

dome^{367}/FM7 crossed to:	Posterior spiracle defects	
	weak	**severe**
wt	13.3%	10.1% (N=157)
ken^{1}/+	18.0%	6.9% (N=261)
ken^{k11035}/+	18.2%	8.0% (N=176)
Df(2R)Chi^{g320}	19.8%	7.0% (N=324)

Table 2.2. Genetic interactions between *dome*^{367} mutants and *ken* alleles.

As an alternative approach, the consequences of Gal4/UAS driven Ken over-expression were also tested. To express *ken* ectopically the *daughterless-GAL4* (*da-*

GAL4) line, which gives a uniform expression in the developing embryo (Wodarz *et al.*, 1995), was used.
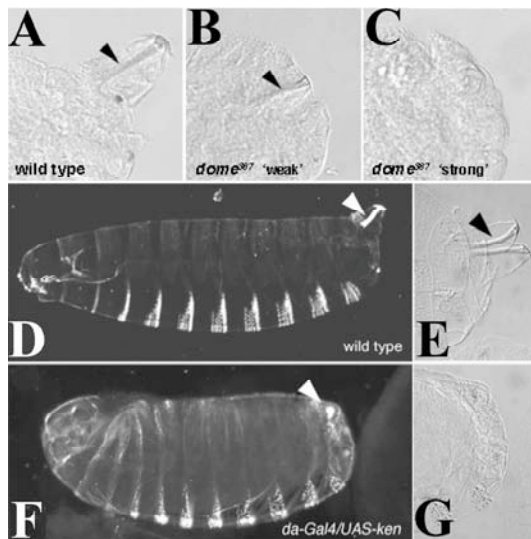
Figure 2.10. Ken mis-expression affects posterior spiracle formation.

(A-C, E & G) Terminal region of cuticles visualised by differential interference contrast microscopy. (D & F) Dark field images of entire embryonic cuticles.

The posterior spiracles in the wild type (A) and *dome367* mutants showing weak (B) and severe defects (C). Arrows indicate the filtzkörper. (D) The wild type cuticle shows normal head skeleton, denticle belts and posterior spiracles. (E) The posterior spiracles in the wild type embryo. (F) A cuticle secreted by the *da-GAL4/UAS-ken* embryo shows a head defect and under-developed posterior spiracles. (E) The posterior spiracles in the *da-GAL4/UAS-ken* embryo.

Examination of the cuticles in *da-GAL4/UAS-ken* embryos shows that, by comparison to wild type (Fig 2.10A, D & E), mis-expression of *ken* results in defects in the head skeleton (Fig 2.10F), occasional fusion of the abdominal denticle belts (not shown) and a consistent posterior spiracle phenotype (arrow in Fig 2.10F & G). In the *da-GAL4/UAS-ken* embryos, the tubular filtzkörper are often missing or thin, and the external stigmatophore is significantly smaller and shorter than in wild type (Fig 2.10G). This defect is also observed when *Act-GAL4*, *nullo-GAL4* and *nos-GAL4.NGT40* lines are used to drive Ken mis-expression (not shown), and represents a phenotype essentially indistinguishable from that caused by strong *dome468* allele (Fig 2.10C).

It therefore appears that mis-expression of *ken* in the posterior spiracles is sufficient to phenocopy a specific developmental defect caused by loss of JAK/STAT signalling. When considered in conjunction with the LOF interaction, these findings support the proposed role of Ken as a negative regulator of the JAK/STAT pathway during development.

2.8 Intracellular localisation of Ken

The presence of three Zn-finger motifs suggests that Ken is likely to be a DNA binding protein and thus probably localises to the nucleus. To visualise Ken protein

within living cells fusion constructs were generated where EGFP (Clontech) sequence was attached to either N- (GFPKen) or C-termini of Ken (KenGFP). Both *UAS-GFPken* and *UAS-kenGFP* were first tested *in vivo* and compared to *UAS-ken*. When mis-expressed under the control of *Mj21A-GAL4* line, which drives expression in the presumptive dorsal blade of the wing disc, *UAS-ken* and both of the EGFP-fused constructs showed a similar folded wing phenotype (not shown). When using the *GMR-GAL4* line, expression of either construct caused a high degree of lethality. The flies that did not die and eclosed had a dramatically reduced, degenerative eyes (Fig 2.11B-D).
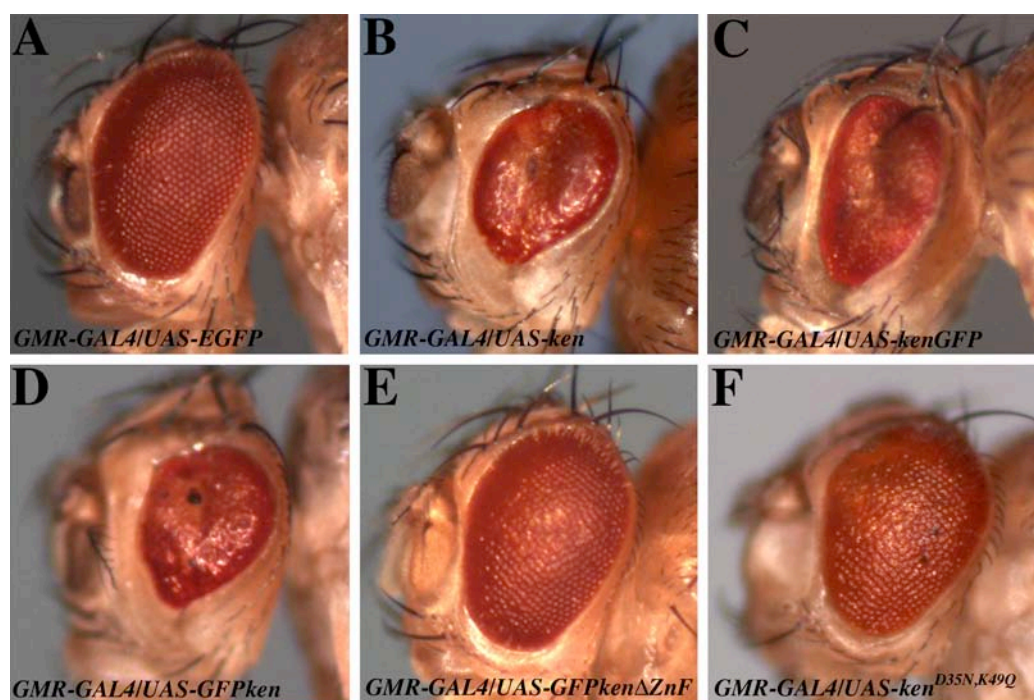
Figure 2.11. Misexpression of Ken, GFPKen, KenGFP and GFPKenΔZnF.

Lateral view on the head region of adult flies mis-expressing EGFP (A), Ken (B), KenGFP (C), GFPKen (D), GFPKenΔZnF (E) and Ken^{D35N,K49Q} (F) driven by *GMR-GAL4* line. Flies mis-expressing full-length wild type Ken (B-D) have greatly reduced eyes with almost no ommatidial structure, whereas flies expressing the truncated (E) or mutant (F) forms of Ken have normal sized eyes similar to the control flies expressing EGFP (A).

This phenotype is identical for all full-length Ken constructs including EGFP-fused those, which indicates that adding EGFP to either terminus of Ken does not destroy protein functions. Interestingly, a truncated form of *GFPKen* lacking the Zn-finger domain, when mis-expressed by the same driver, does not give the phenotype (Fig 2.11E), which implies the absolute requirement of the DNA binding domain for the proper function, stability or folding of Ken. Similarly, no reduction in the eye size

was observed in the flies mis-expressing Ken^{D35N,K49Q} that contained two point mutations in the conserved positions within the BTB/POZ domain. These positions are known to be required for association with co-repressors and repressional activity (Fig 2.11F; Melnick *et al.*, 2000; Melnick *et al.*, 2002).

The functionality of the constructs having been confirmed, EGFP-fused Ken was expressed in *Drosophila* S2R$^+$ cells under control of *Act-GAL4* driver. As shown in Fig 2.12, GFPKen accumulates in the nuclei, as GFP fluorescence co-localises with DNA specifically stained with DRAQ5. Interestingly, each nucleus contains a dark spot free of GFPKen, which potentially corresponds to nucleoli. Lower levels of GFPKen are also seen in the cytoplasm.
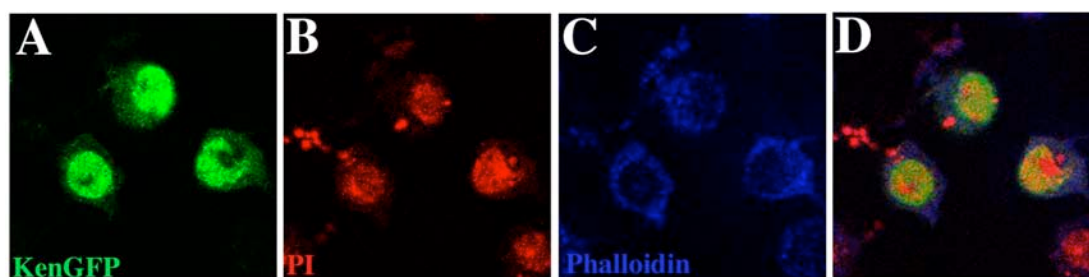
Figure 2.12. Intracellular localisation of KenGFP in S2 cells.

S2R$^+$ cells expressing KenGFP. (A) Green channel shows KenGFP, (B) red channel represents the nuclei stained by propidium iodide (PI), (C) blue channel demonstrates the actin filamentous network visualised by TRITC-labelled phalloidin. (D) Overlay of all three channels.

However, the level of protein expression in S2R$^+$ cells was very low, while cells transfected with equivalent amounts of EGFP alone showed much higher levels of fluorescence (not shown). Moreover, it was noticed that increasing the concentration of *UAS-EGFP* expressing plasmid in the transfection mixture resulted in higher fluorescence, while different concentrations of *UAS-GFPken* gave only low, relatively constant levels of GFPKen. On Western-blot stained with anti-GFP antibody, no GFPKen protein could be detected, whereas EGFP or STAT92E-GFP were clearly detectable (Fig 2.13). These observations suggest the existence of an intracellular mechanism, which maintains an approximately constant level of Ken mis-expression in this cell type.
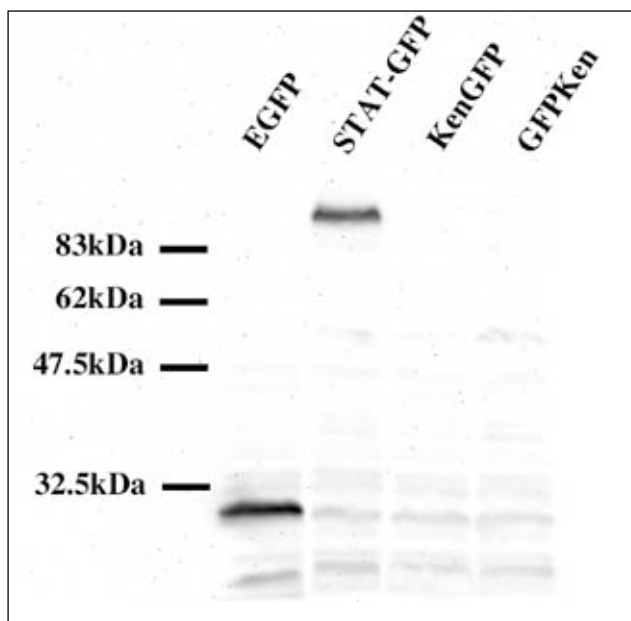
Figure 2.13. KenGFP expressed in S2R⁺ cells cannot be detected on Western-blot.

S2R⁺ cells expressing EGFP, STAT92E-GFP, KenGFP, GFPKen as indicated. EGFP (~27kDa) and STAT92E-GFP (~113kDa, marked as STAT-GFP) are clearly detected on Western-blot stained with anti-GFP antibody. No band corresponding to Ken fused to GFP (approximately 94kDa) is seen.

Nuclear accumulation of GFPKen is also observed following mis-expression *in vivo* by the salivary gland specific *sgs3-GAL4* line (Cherbas *et al.*, 2003). In these cells GFPKen is primarily located to the nucleus, although it is also enriched at the cell membrane (Fig 2.14). The reason for this membrane localisation is as yet unknown.
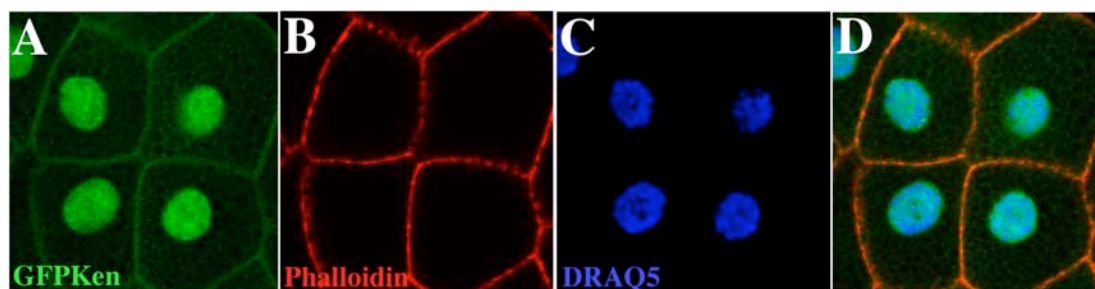
Figure 2.14. Intracellular localisation of GFPKen in the salivary gland.

GFPKen was expressed in the salivary glands under *sgs3-GAL4* driver. (A) GFPKen (green channel) is primarily located in the nuclei, stained with the DNA dye DRAQ5 (blue channel, B) and enriched at the cell membrane as visualised by TRITC-phalloidin (red channel, C). All three channels are shown separately (A-C) and merged (D).

2.9 Ken binds DNA *in vitro*, and its consensus overlaps that of STAT92E

Given the presence of potentially DNA binding C_2H_2 zinc finger domains (Iuchi, 2001) and nuclear accumulation of Ken, an *in vitro* selection technique, termed SELEX (Systematic Evolution of Ligands by EXponential enrichment; Tuerk & Gold, 1990), was applied to determine the potential DNA binding properties of Ken. For this a DNA library has been synthesised that contains 20bp randomised core, representing 2^{40} potential binding sequences. This core is flanked by two 21-nucleotide primers allowing amplification of the library. The Ken Zn-finger domain was tagged with GST and expressed in *E. coli*. A multi-stage selection procedure comprising DNA-protein binding, removing free oligonucleotides and amplification of the recovered DNA, was used to generate enriched population of oligonucleotides that could be bound by Ken Zn-finger domain. This selected population was then used for the next round of selection. After ten rounds the resulting oligonucleotide pool was subcloned and sequenced. Alignment of 43 independent clones showed that all recovered plasmids were unique and each contained one, or occasionally two, copies of the motif GNGAAAK (K = G/T; Table 2.3).

position →	-2	-1	1	2	3	4	5	6	7	8	9	10
T	5	8	2	9	4	4	1	3	15	12	11	10
A	4	9	4	17	1	39	47	45	4	11	7	14
G	9	9	32	11	44	2	0	1	24	14	11	8
C	3	6	4	10	1	5	2	1	3	7	12	9
↑ nucleotide	N	N	G	N	G	A	A	A	G/T	N	N	N

Table 2.3. Alignment of Ken DNA binding sites identified by SELEX.

The specificity of the selected consensus was confirmed by electroforetic mobility shift assays (EMSA), in which GFPKen derived from a transfected S2R$^+$ cells lysate was allowed to complex with a radioactively labelled probe containing the wild type (WT) consensus GAGAAAG identified by SELEX. This binding results in a specific band shift, which can be super-shifted by an anti-GFP antibody (Fig 2.15A) and is therefore believed to represent a GFPKen/DNA complex. In order to identify positions essential for DNA binding a competition assay was performed, in which unlabelled oligonucleotides containing single substitutions in each position from 1 to 7 (Table 2) were added to the binding reactions. 10-fold excess of the unlabelled WT

oligos greatly diminishes the intensity of the GFPKen band, while 50- and 100-fold excess totally ablates the original signal (Fig 2.15B). By contrast, competition with the unlabelled M3 oligonucleotides containing G → A substitution at position 3 fail to significantly reduce the intensity of the band even when added at 100-fold excess (Fig 2.15C). Using this approach the mutant oligonucleotides M1 and M7 are found to be able to compete for Ken protein, implying that changes in the positions 1 and 7 do not affect the ability of Ken to bind DNA. By contrast, the oligonucleotides containing mutations in position 3 to 6 cannot compete for the binding of Ken, indicating that the central GAAA core is absolutely required (Fig 2.15C). Similar results are obtained with the converse experiment using labelled mutant probes, although in this case the WT probe produces a signal noticeably stronger than the M1 and M7 mutant oligonucleotides (Fig 2.15D).
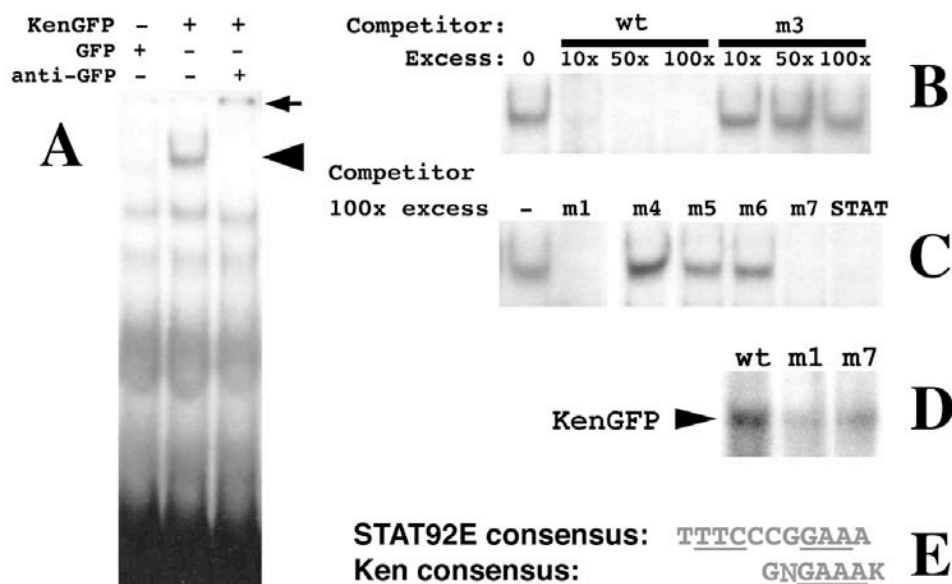
Figure 2.15. Ken binds DNA *in vitro*.

EMSA analysis of Ken DNA binding. (A) Indicated proteins are derived from S2R$^+$ cells transfected with pUC18-Act-GAL4 and pUAST-EGFP or pUAST-KenGFP. KenGFP specifically binds to the radioactively labelled consensus sequence and gives the specific band (arrowhead) that is super-shifted, when anti-GFP antibody added. Arrow indicates the super-shifted band. (B & C) Cold DNA competition assays. Unlabelled oligonucleotides are indicated: wt contains the GAGAAAG consensus; m1, m3 and m7 contain G → A substitutions in positions 1, 3 and 7 respectively; m4 to m6 have A → T substitutions in the corresponding positions. Loss of the specific band implies that the mutant oligonucleotides are capable of binding to Ken. (D) Radioactively labelled wt, m1 and m7 probes are used. Arrowhead indicates KenGFP band, which is stronger in case wt probe than in m1 or m7. (E) STAT92E and Ken consensus binding sites. The minimal sequences required for Ken and STAT92E (Yan *et al.*, 1996b) protein binding are underlined.

Taken together these experiments not only define the core sequence for Ken binding, but also demonstrate the specificity of Ken as a site specific transcription factor.

Strikingly, the core GAAA of the Ken consensus overlaps the consensus sequence bound by STAT92E (Fig 2.15E), and a 100-fold excess of unlabelled oligo containing this STAT92E consensus site is sufficient to fully compete Ken (Fig 2.15C).

2.10 Ken affects expression of luciferase reporter, whose promoter contains STAT92E binding sites

As described so far, (i) *ken* interacts genetically with *upd*, *dome* and *stat92E in vivo*, (ii) when mis-expressed during embryogenesis ectopic Ken phenocopies specific defects in the posterior spiracles known to be caused by loss of JAK/STAT pathway activity, (iii) *in vitro* Ken binds DNA, with its consensus overlapping STAT92E binding site. These results propose a function of Ken as a negative regulator of JAK/STAT pathway signalling, which potentially mediates transcriptional repression of the pathway target genes.

It has been reported that the JAK/STAT pathway is involved in regulation of the *D-raf* gene (Kwon *et al.*, 2000). Furthermore, a 2x*Draf*-STATwt-luc reporter construct containing firefly luciferase coding gene and a *D-raf* promoter region containing two STAT92E recognition sites, was shown to be specifically activated by STAT92E when co-transfected in *Drosophila* S2 cells (Kwon *et al.*, 2000).

In this study, the 2x*Draf*-STATwt-luc reporter construct kindly provided by Dr. Yamaguchi, was co-transfected in S2 cells together with EGFP-fused STAT92E and constitutively active kinase Hop^{TumL}. To monitor transfection efficiency in each experiment, cells were also co-transfected with a plasmid constitutively expressing *Renilla* luciferase (pUP-RL), and values of firefly luciferase activity were divided by those of the *Renilla* enzyme to normalise for actual reporter activation. Expression of STAT92E-GFP alone produces no activation over background levels, while co-expression together with Hop^{Tuml} results in approximately 5-fold response (Fig 2.16). Reporter activation seen in cells expressing Hop^{TumL} alone is likely due to the activation of endogenous STAT92E.
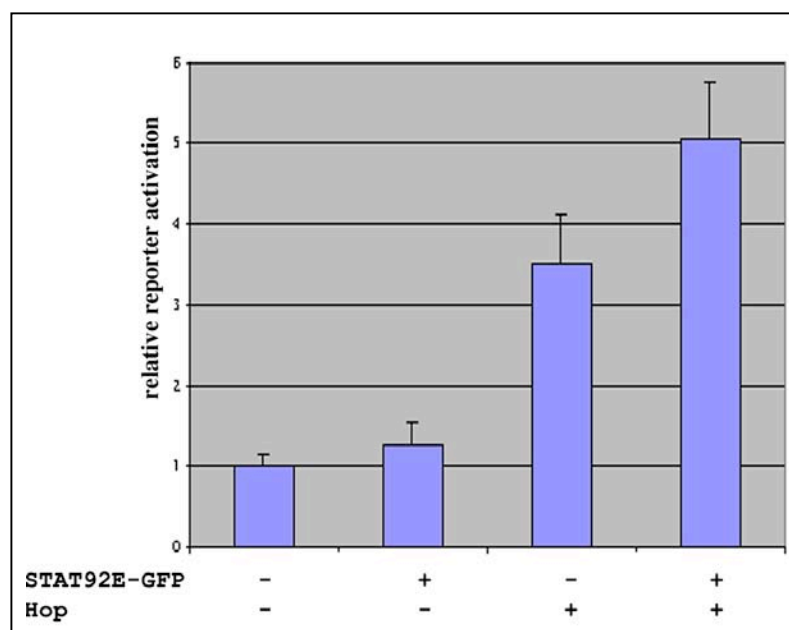
Figure 2.16. Effects of co-transfecting Hop^{TumL} and STAT92E-GFP on 2x*Draf*-STATwt-luc reporter expression.

S2 cells are co-transfected with 2x*Draf*-STATwt-luc, pUP-RL, pUC18-Act-GAL4 and pUAST-Hop^{TumL}, pUAST-STAT92E-GFP as indicated on the axis X. For mock transfections pUAST-Hop^{TumL} and pUAST-STAT92E-GFP plasmids were substituted by equal amount of empty pUAST vector. Here and in next charts, values are normalized to mock transfected cells. Axis Y represents fold activation of 2x*Draf*-STATwt-luc reporter relative to the mock transfected control.

The STAT92E site ATTCGCG<u>GAAA</u>G derived from the *D-raf* promoter and present in the 2x*Draf*-STATwt-luc reporter potentially represents a suitable sequence for Ken binding. It is therefore expected that Ken can repress transcription of the reporter. Surprisingly, when co-expressed together with STAT92E-GFP and Hop^{TumL} Ken does not suppress, but appears to enhance the reporter activation (Fig 2.17). This effect seems to be specific for the functional domains of Ken, as removal of either the Zn-finger or BTB/POZ domains restores luciferase activity approximately to the level of STAT92E activated by Hop^{TumL}.
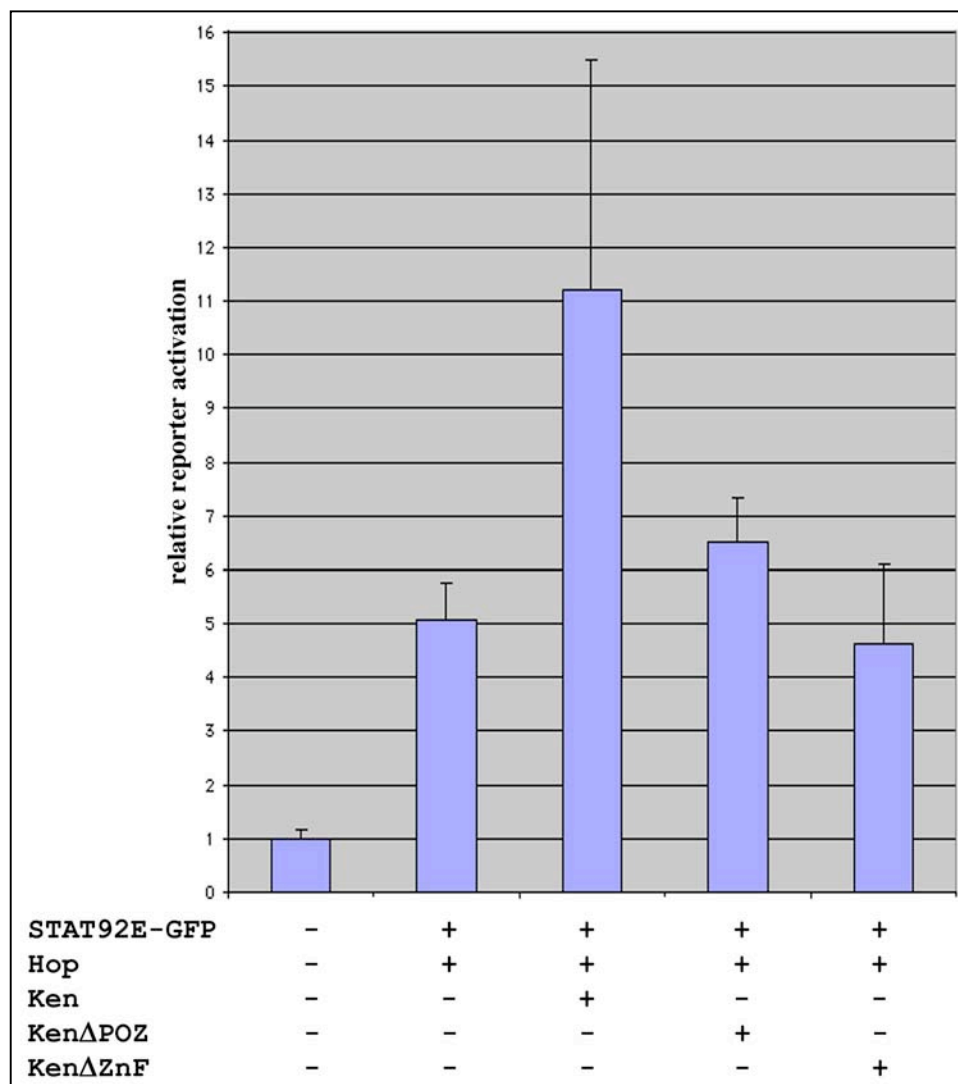
Figure 2.17. Effects of the full-length and truncated forms of Ken on 2x*Draf*-STATwt-luc reporter when co-transfected with STAT92E-GFP and Hop^TumL.

S2 cells are expressing the indicated proteins. Notice that neither KenΔPOZ lacking the BTB/POZ domain nor KenΔZnF activate the reporter above the level achieved by activated STAT92E-GFP.

Interestingly, co-transfection of Ken with Hop^TumL was as effective as activated STAT92E-GFP (Fig 2.18). This activation may be mediated by endogenous STAT92E. If this is the case, Ken seems to affect the reporter expression only in presence of active STAT92E. In contrast, the truncated forms did not activate the reporter above the level produced by Hop^TumL itself.
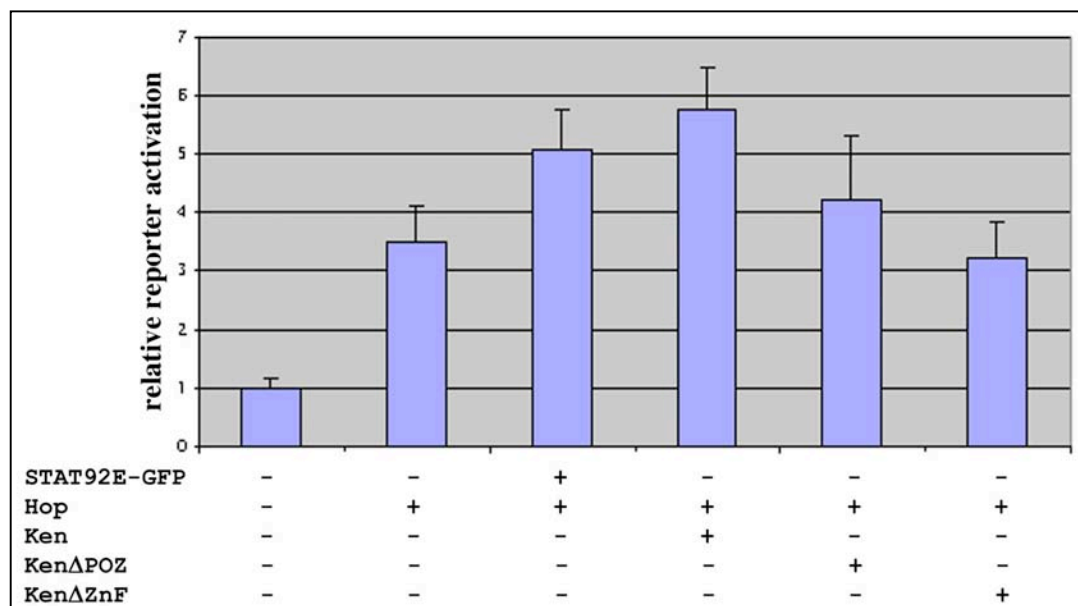
Figure 2.18. Effects of the full-length and truncated forms of Ken on 2x*Draf*-STATwt-luc reporter when co-transfected with Hop^{TumL}.

S2 cells are expressing the indicated proteins. Full-length Ken, but not KenΔPOZ or KenΔZnF activates the reporter, when Hop^{TumL} co-expressed.

As shown in Fig 2.19, no reporter activation is detected when either Ken forms were expressed alone or with STAT92E-GFP.
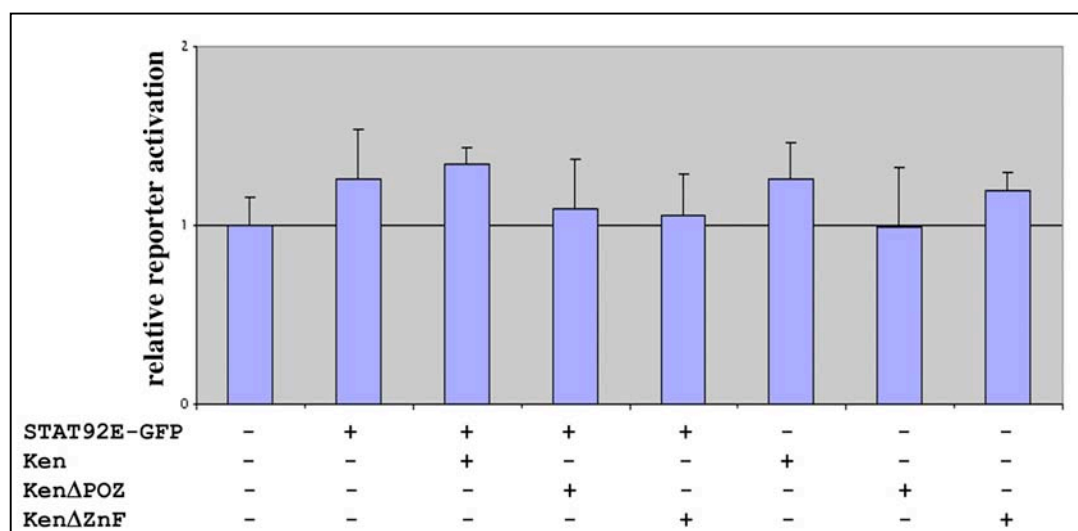
Figure 2.19. Neither the full-length nor truncated forms of Ken activate 2x*Draf*-STATwt-luc reporter when expressed alone or together with STAT92E-GFP.

S2 cell are expressing the indicated proteins. Without Hop^{TumL} no activation of the reporter is seen.

Finally, neither combination of STAT92E-GFP, Hop^{TumL} or Ken produce the activation when the mutant reporter 2x*Draf*-STATmut-luc, in which the STAT92E

sites were mutated in positions essential for both STAT92E and Ken binding, was used (Fig 2.20; Kwon *et al.*, 2000).
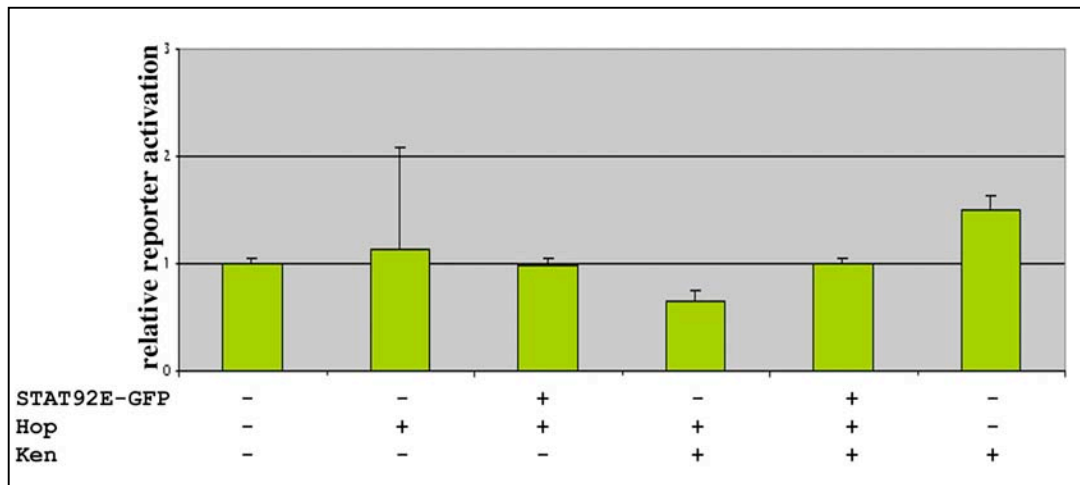
Figure 2.20. Mutations in the STAT92E binding site do not allow STAT92E-GFP and Ken to activate 2x*Draf*-STATmut-luc reporter.

S2 cells are expressing the proteins indicated on the axis X. 2x*Draf*-STATmut-luc reporter contains mutant sites AT$\underline{G}$CGCG$\underline{C}$AAAGT (mutated nucleotides are underlined).

In summary, Ken activates expression of the 2x*Draf*-STATwt-luc reporter, whose promoter contains STAT92E sites derived from the promoter of the *D-raf* gene. This activation is specific, first, to the DNA sequence, as the mutant reporter does not response to Ken transfection, and second, to the functional domains of Ken, as the truncated forms do not activate the reporter. Moreover, activation by Ken is seen only in presence of activated STAT92E or Hop^{TumL}.

2.11 *smrter* coding for a transcriptional co-repressor interacts genetically with *ken* and *stat92E*

A number of tissue culture based studies have indicated that the transcriptional repression associated with BCL6, a vertebrate protein related to Ken, is mediated by binding of the transcriptional co-repressor SMRT to specific residues within the BTB/POZ domain (Dhordain *et al.*, 1997; Melnick *et al.*, 2000). A highly conserved SMRT homologue, named *smrter* (*smr*), has also been identified within the *Drosophila* genome (Tsai *et al.*, 1999). To reveal a potential genetic interaction between *smr* and the JAK/STAT pathway, the *smr*^{G036} allele was introduced into *stat92E*^{HJ} homozygous flies. Interestingly, removal of one copy of *smr* reduces the

frequency, with which ectopic wing vein material is formed in *stat92E^HJ* homozygotes (Table 2.3), an effect similar to that shown for *ken* alleles (see Table 2.1). This genetic interaction is consistent with the physical interactions reported between BCL6 and SMRT in vertebrate systems (Dhordain *et al.*, 1997; Melnick *et al.*, 2000) and implies that a similar mechanism of transcriptional co-repression between Ken and SMRTER may also exist in *Drosophila*.

Genotype	Vein Defects			
	males		females	
+ / + ; stat92E^HJ / stat92E^HJ	22.0%	(n=41)	72.1%	(n=68)
ken^K11035 / + ; stat92E^HJ / stat92E^HJ	2.5%	(n=40)	29.6%	(n=71)
w,smr^G0361 / + ; stat92E^HJ / stat92E^HJ	NA		21.3%	(n=75)

Table 2.3. Genetic interactions between *stat92E^HJ*, *ken* and *smr*.

A similar genetic assay was undertaken for *ken*. The frequency, with which adult *ken^1* homozygous individuals from a newly out-crossed stock survive to adulthood, is also increased following the removal of a single copy of *smr*. While 48.5% of the expected number of *ken^1* homozygous adults eclose from control crosses (n=341), this rate rises to 70% of the expected number of flies that are simultaneously heterozygous for *smr*.

2.12 Ken does not associate with STAT92E *in vitro*

A proposed function of Ken as a negative regulator of JAK/STAT pathway that potentially mediates transcriptional repression of the pathway target genes can suggest two models.

In the "competition" model (Fig 2.21A), Ken as mono- or dimer, possibly bound to a co-repressor, occupies STAT92E binding site, thus preventing the latter to activate transcription. Alternatively, in the "heterodimerisation" model (Fig 2.21B), Ken and STAT92E contact each other at the DNA site. The latter model requires physical interaction between the proteins.
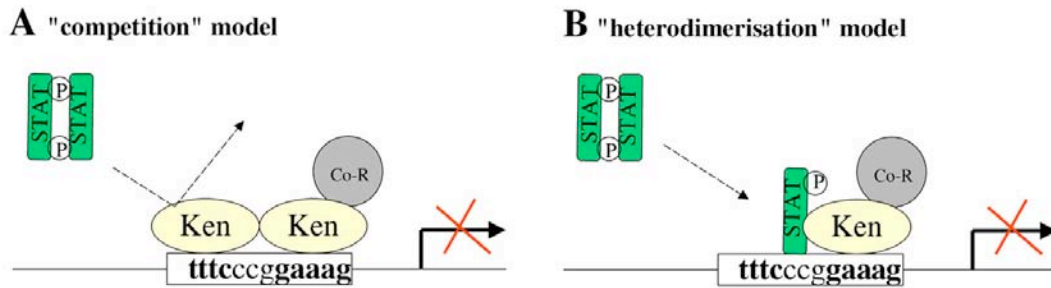
Figure 2.21. Models for Ken and STAT92E interaction.

One of the techniques to reveal protein-protein interactions is <u>co</u>-<u>i</u>mmuno<u>p</u>recipitation (co-IP) assay, in which a protein of interest is precipitated by a specific antibody, and the precipitate is tested for the presence of additional associated proteins. The latter can be detected following separating by SDS-PAGE and immunoblotting with a second antibody, which recognises the associated protein. Using this method STAT92E was successfully co-immunoprecipitated together with STAT92E-GFP when both versions were co-transfected in *Drosophila* S2 cells (Fig 2.22).
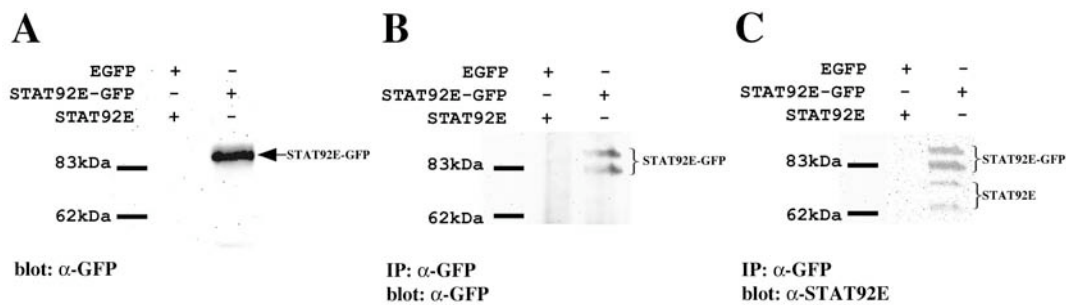
Figure 2.22. Western-blot showing STAT92E-GFP/STAT92E heterodimer precipitated with anti-GFP antibody.

Co-IP was performed on S2 cells. Cells were co-transfected either with EGFP/STAT92E or STAT92E-GFP/STAT92E. (A) 1/5 of the nuclear extracts prepared from the cells expressing the indicated proteins was loaded on 10% acrylamide gel, resolved by SDS-PAGE and immunoblotted with anti-GFP antibody. The detected band corresponds to STAT92E-GFP (marked by arrow). The rest volumes of the nuclear extracts were precipitated with anti-GFP antibody and the resulting fractons were resolved by SDS-PAGE and immunoblotted either with anti-GFP (B) or anti-STAT92E antibody (C) (see text).

Nuclear extracts of cells transfected with STAT92E and STAT92E-GFP express detectable levels of STAT92E-GFP when blotted with anti-GFP antibody (Fig 2.22A). Following immunoprecipitation two bands are detected as specifically stained with anti-GFP antibody, which are likely to represent precipitated STAT92E-GFP. As the biggest band of approximately 113kDa size probably corresponds to the full-length STAT92E-GFP, it is believed that the additional band observed (Fig 2.22B) may

result from the activity of site-specific proteases, which were not fully inactivated during co-IP. The same bands are also seen when the blot is probed with anti-STAT92E antibody (Fig 2.22C). Taken together with the absence of those bands in the negative control, this suggests that both of the bands represent STAT92E-GFP. The other pair of bands, detected on the Western-blot probed with anti-STAT antibody (Fig 2.22C), are likely to represent the intact and cleaved untagged STAT92E molecules co-precipitated with STAT92E-GFP as a heterodimer. This result confirms that using S2 cell lysate STAT92E can be successfully co-immunoprecipitated with STAT92E-GFP.

As KenGFP could not be expressed in S2 cells at a level detectable on Western-blot (see above, Fig 2.13), for co-IP assay Ken was translated *in vitro* and simultaneously labelled by ^{35}S-methionin incorporation. Nuclear extracts containing STAT92E-GFP were incubated with *in vitro* translated Ken, followed by washing, SDS-PAGE and autoradiography. However, under the conditions suitable for co-immunoprecipitation of STAT92E with STAT92E-GFP the technique failed to reveal Ken in complex with STAT92E-GFP, either inactive or activated by Hop^{TumL} (Fig 2.23). A faint band of approximately 67kDa size most likely represents ^{35}S-Ken that is non-specifically bound to anti-GFP antibody.
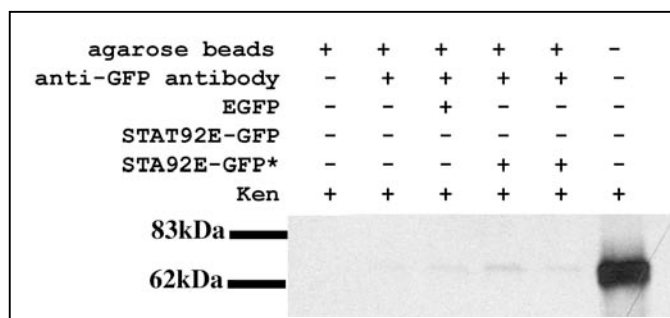
Figure 2.23. Ken does not co-precipitate with STAT92E-GFP.

EGFP and STAT92E-GFP were derived from S2 cell lysates. Ken was translated *in vitro* and labelled by ^{35}S-methionin incorporation. The lysates were mixed with translated Ken, allowed to form complexes, washed and resolved by SDS-PAGE (10% polyacrylamide gel). Presence of ^{35}S-Ken in the resulting fractions was revealed by autoradiography. Asterisk marks STAT92E-GFP activated by co-transfected Hop^{TumL}. The last lane represents ^{35}S-Ken loaded in 1/10 amount of that used for co-IP.

2.13 Mis-expression of Ken is sufficient to down-regulate a subset of JAK/STAT pathway target genes

The genetic interactions between *ken* and *upd, dome* and *stat92E,* in conjunction with the overlap between Ken and STAT92E DNA binding sequences, suggest a model, in which both proteins could compete *in vivo* for available DNA binding sites. In this model a subset of functional STAT92E binding sites contain sequences, with which Ken can also associate, while other STAT92E binding sites do not allow Ken binding. The question arises whether Ken can function as a transcriptional repressor of JAK/STAT pathway target genes *in vivo*.

Recent studies have identified a number of genes that represent putative transcriptional targets for activated STAT92E. These include the JAK/STAT dependent expression of the fifth stripe of *even-skipped* (*eve*) in the early embryo (Yan *et al.*, 1996b), the hindgut specific expression of *ventral vein lacking* (*vvl*) (Brown *et al.*, 2003), the expression of *trachealess* (*trh*) and *knirps* (*kni*) in the tracheal placodes during embryogenesis (Brown *et al.*, 2001), and a gradient of *four-jointed* (*fj*) within the developing eye imaginal disc (Zeidler *et al.*, 1999a). A potential influence of Ken mis-expression on these genes has been tested.

2.13.1 *even-skipped*

Expression of *eve* is restricted to seven stripes in stage 5 embryos (Fig 2.24A). Previously it has been shown that in *stat92E* or *hop* GLC the fifth stripe of *eve* is greatly reduced (Binari & Perrimon, 1994). Reduction of the third eve stripe has been reported when dominant negative ΔNSTAT92E was mis-expressed under control of *nos-GAL4.NGT40* driver that expresses GAL4 during oogenesis (Henriksen *et al.*, 2002). Therefore, the same maternal driver has been used to check whether Ken expressed ectopically during early stages of embryogenesis is capable of repressing *eve*. However, neither in *nos-GAL4.NGT40/UAS-ken* embryos nor in those mis-expressing dominant negative ΔNSTAT92E (Henriksen *et al.*, 2002) and truncated DomeΔCyt lacking the intracellular domain (Brown *et al.*, 2001), any changes in the expression level of *eve* stripes are seen (Fig 2.24B-D).
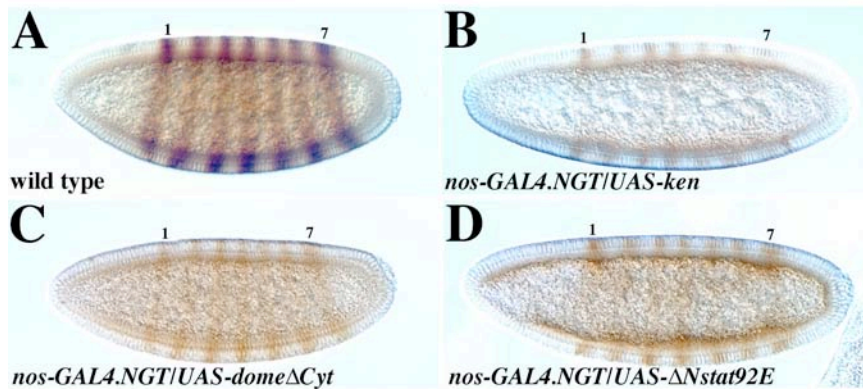
Figure 2.24. *eve* expression is affected neither by Ken nor by dominant negative DomeΔCyt or ΔNSTAT92E.

Stage 5 embryos were stained with anti-Eve antibody. (A) In wild type, Eve is expressed in 7 stripes (the 1st and the 7th stripes are marked). In *nos-GAL4.NGT40/UAS-ken* (B), *nos-GAL4.NGT40/UAS-domeΔCyt* (C) and *nos-GAL4.NGT40/UAS-ΔNstat92E* (D) the relative intensity of all 7 stripes remains unchanged.

2.13.2 *four-jointed*

To analyse *fj* expression in the eye imaginal discs, groups of cells over-expressing full-length Ken and the marker gene GFP were generated by FLP/FRT technique (Ito *et al.*, 1997). Using the *fj^{P1}* enhancer detector expressing β-galactosidase (β-Gal) under control of the endogenous *fj* promoter, changes in signal transduction that affect *fj* expression can be monitored. With this technique alterations in Notch, Wingless and JAK/SAT signalling have been shown to influence *fj* expression in the eye disc (Zeidler *et al.*, 1999a). However, analysis of multiple Ken expressing clones present in the regions that either express (in the central part of the eye disc) or lack *fj* (on the periphery), failed to identify any consistent or reproducible effect (Fig 2.25).
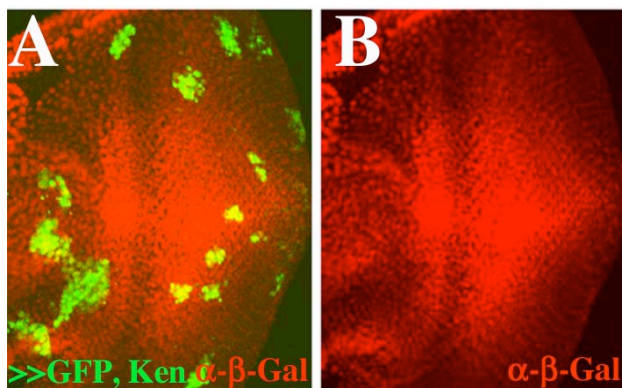
Figure 2.25. *ken* flip-out clones do not affect *fj* expression in the eye disc.

Eye imaginal disc of 3d instar larva. The *fj^{P1}* enhancer detector visualised by anti-β-Gal antibody is expressed in a gradient (red in A and B). *ken* flip-out clones are marked by EGFP (green in A). Panel B shows only the red channel from panel A. No changes in *fj* enhancer detector are seen in *ken* over-expressing clones.

2.13.3 *ventral vein lacking*

Possible modulation of the JAK/STAT dependent *vvl* expression in the hindgut (Brown *et al.*, 2003) by Ken has also been examined. By contrast to wild type (Fig 2.26A), amounts of *vvl* transcript in embryos ubiquitously expressing Ken under control of the *daughterless-GAL4 (da-GAL4)* driver line (Wodarz *et al.*, 1995) are significantly reduced to a level similar to that observed in *upd*[OS1A] mutant embryos, which lack all detectable JAK/STAT signalling activity (Fig 2.26B & C).
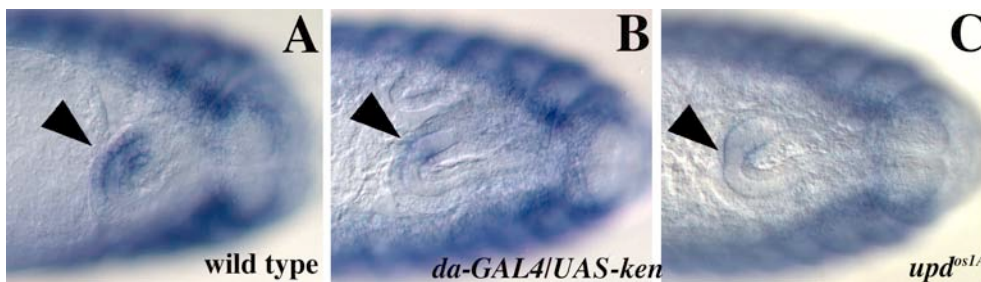
Figure 2.26. Ken down-regulates the expression of *vvl* in the hindgut.

In situ hybridisation of stage 14 embryos against the *vvl* transcript focused on the hindgut (arrowheads). (A) Expression visible in both the lateral body wall and the hindgut of the wild type embryo. The *da-GAL4/UAS-ken* (B) and *upd*[OS1A] (C) embryos show reduced levels of *vvl* in the hindgut.

2.13.4 *trachealess*

A potential effect of Ken on the JAK/STAT pathway target gene *trh* was also addressed. From stage 10/11 *trh* expression proceeds the formation of the tracheal pits in each of the embryonic segments T2 to A8 (Fig 2.27A; Boube *et al.*, 2000). Strikingly, levels of *trh* in *da-GAL4/UAS-ken* embryos are greatly reduced (Fig 2.27B). Many tracheal placodes express little or no *trh*, and tracheal pits fail to form even in the presence of residual *trh* (Fig 2.27B & E). Similar effects are seen in *upd*[OS1A] mutant embryos (Fig 2.27C & F), which completely lack JAK/STAT pathway signalling activity.
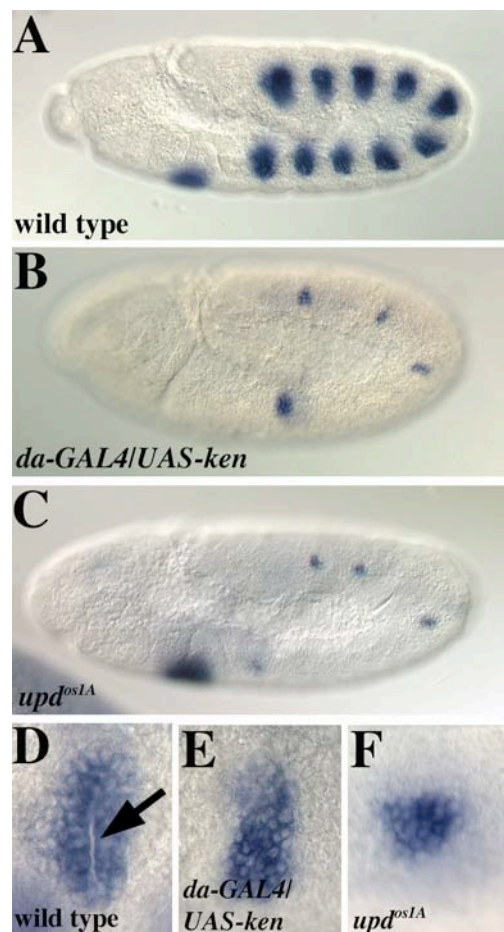
Figure 2.27. *trh* is suppressed by *ken* mis-expression.

In situ hybridisation is performed on stage 10/11 embryos to visualise *trh* expression (A) Wild type embryo showing expression in the 10 tracheal placodes and the salivary gland primordium. *da-GAL4/UAS-ken* embryo (B) and an embryo mutant for the strong *upd^{OS1A}* allele (C) contain only weakly stained regions in a few tracheal placodes. (D-F) High magnification views. The tracheal pit invaginations formed in the wild type embryo (arrows in D) are missing in the *da-GAL4/UAS-ken* (E) and *upd^{OS1A}* mutants (F).

2.13.5 Knirps

Kni is expressed in the tracheal pits in a pattern similar to that of *trh*, and this expression has also been shown to depend on JAK/STAT pathway signalling (Brown *et al.*, 2001). Likewise, a down-regulation of Kni is observed in the embryos mis-expressing *ken* (Fig 2.28).
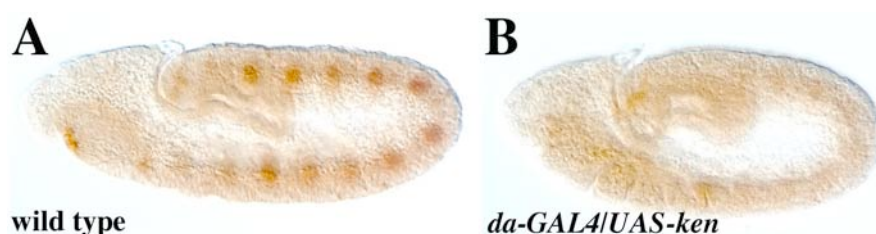
Figure 2.28. Kni expression is ablated in *ken* misexpressing embryos.

Stage 10/11 embryos stained with anti-Kni antibody showing wild type tracheal staining (A) not detectable in the embryo expressing *da-GAL4/UAS-ken* (B).

Taken together, these results illustrate that Ken mis-expressed during embryonic development is capable of down-regulating the expression of several known JAK/STAT pathway target genes. This repressional activity is consistent with both the genetic interactions observed and the repressor activity of homologous BTB/POZ domain containing transcription factors (Chang *et al.*, 1996; Ahmad *et al.*, 2003). Furthermore, Ken only appears to be able to suppress a subset of STAT92E targets, a finding that is consistent with the overlap of their DNA binding sequences, and supports the idea of a differential regulation of the JAK/STAT pathway by Ken.

2.13 *ventral vein lacking* is up-regulated in *ken* mutants

As pointed out above, Ken mis-expression can down-regulate a subset of the known JAK/STAT pathway target genes. The question arises whether this down-regulation takes place during normal development. Therefore, expression of the genes repressed by ectopic Ken was examined in embryos lacking *ken*, with a particular interest in the posterior spiracles, a region where both Ken and Upd are expressed (Fig 2.9).

At stage 14/15, *vvl* is expressed in the hindgut in a JAK/STAT pathway dependent manner (Fig 2.26), but not in the presumptive posterior spiracles (Fig 2.29A), despite the pathway activity in this region (Brown *et al.*, 2001). Strikingly, in the $ken^{K11035}/Df(2R)Chi^{g230}$ trans-heterozygous embryos that express much lower levels of *ken* than the wild type those, up-regulation of *vvl* in the posterior spiracles is observed (Fig 2.29B).
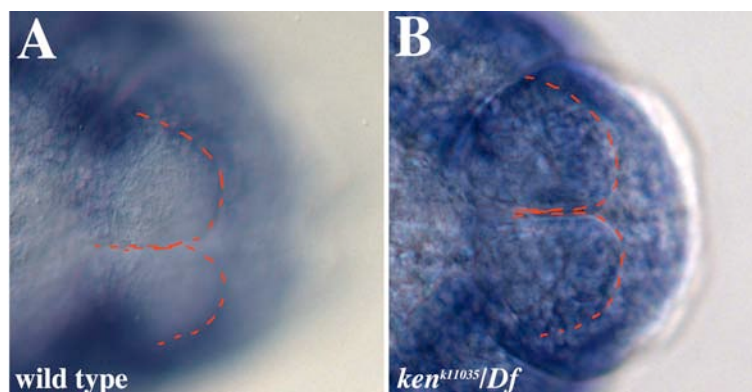
Figure 2.29. Ectopic *vvl* expression in *ken* LOF mutant embryos.

In situ hybridisation of stage 14/15 embryos for the *vvl* transcript focused on the most terminal part of the abdomen that contains the posterior spiracles (marked by dashed red line). (A) In wild type embryos, the posterior spiracle region does not contain *vvl* mRNA and looks empty. (B) By contrast, *vvl* expression is up-regulated in this region of $ken^{K11035}/Dr(2R)Chi^{g230}$ trans-heterozygous embryos.

These results show that Ken is required for regulation of *vvl* expression in the posterior spiracles, and that ectopic *vvl* activation in the embryos lacking Ken is likely a consequence of de-repression of endogenous STAT92E activity.

2.14 Ectopic Ken and embryonic segmentation

Given the lethality caused by Ken mis-expressed under control of a number of Gal4 driver lines such as *Act-GAL4*, *da-GAL4*, *nullo-GAL4* and *nos-GAL4.NGT40*, an analysis of phenotypes brought about by mis-expression of Ken during embryonic development was undertaken. To restrict the time gap of ectopically expressed Ken activity to the earliest stages, maternal Gal4 drivers have been chosen, which cause accumulation of GAL4 mRNA during oogenesis and result in an early embryonic expression of paternally supplied UAS transgenes (Rorth *et al.*, 1998).

As a result, driven by *mat-α-tub-GAL4* line Ken mis-expression gives rise to a variety of phenotypes such as head defects (arrows in Fig 2.30B-D), reduced posterior spiracles (marked by asterisk in Fig 2.30C) and occasional fusion of abdominal segments (not shown). The most intriguingly, in a proportion of embryos head structures are frequently underdeveloped and, in the most severe case, even replaced with abdominal structures. This phenotype is termed "bicaudal" or "double-abdomen". The umber of abdominal segments in those bicaudal embryos may vary. A proportion of embryos has almost complete abdomen (A2-A8) and, additionally, one or two mirror-inverted ectopic abdominal segments present at the anterior end (arrowheads in Fig 2.30D). However, a number of embryos show absolute symmetry, with two identical abdomens carrying from 3 to 5 abdominal segments formed in a mirror image (arrowheads in Fig 2.30E). Analysis of the hatching rate of the *mat-α-tub-GAL4/UAS-ken* embryos shows that 95% of them (N=340) hatch, though approximately 14% of those die at the 1st instar larva stage. Among the unhatched embryos 43% demonstrate the double-abdomen phenotype, 42% show anterior defects without the replacement with the abdominal structures, and 15% secrete wild type cuticle (N=120).

These observations suggest that ectopically expressed Ken interferes with the system establishing anterior-posterior polarity in the early embryos.
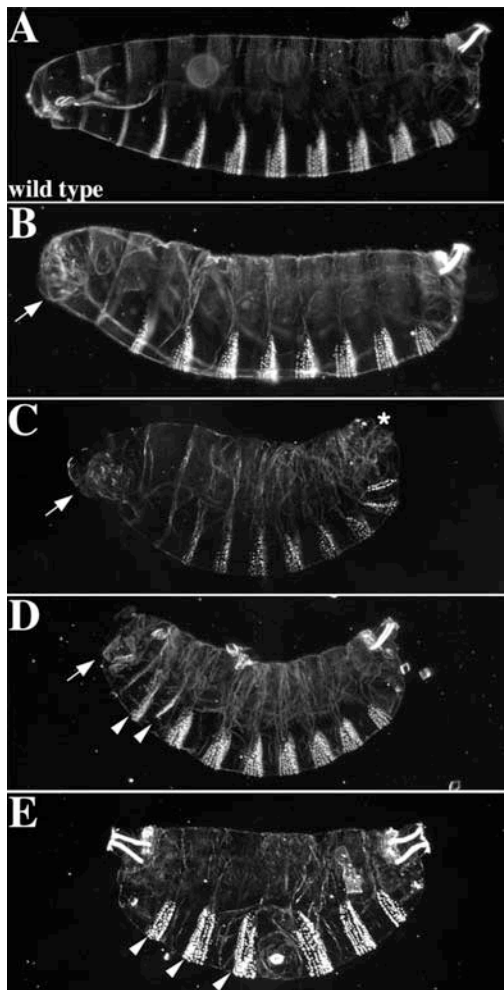
Figure 2.30. Early mis-expression of *ken* under control of maternal Gal4 driver.

Cuticle preparations of wild type (A) and *mat-α-tub-GAL4/UAS-ken embryos* (B-E).

Mutant embryos show head defects (B-D), asymmetrical (D) and symmetrical bicaudal phenotypes (E). Arrows point to head structure defects, asterisk marks defects in the posterior spiracle. Arrowheads mark the ectopic abdominal segments.

2.13 Krüppel expression is affected in *mat-α-tub-GAL4/UAS-ken* embryos

The bicaudal phenotype is characteristic for embryos lacking *bicoid* (*bcd*) and maternal *hunchback* (*hb*) (Bull, 1966; Lehmann & Nüsslein-Volhard, 1986; Hülskamp *et al.*, 1990). Since alterations in the level of Bcd and Hb activity must affect downstream target genes, expression of Krüppel (Kr) was used as an indicator of Bcd/Hb activity. Kr is normally up-regulated by low levels of Hb and Bcd, but down-regulated by high concentrations of both proteins in the most anterior region (Hülskamp *et al.*, 1990). In early wild type embryos the Kr domain occupies a central region of approximately 22% of egg length, with the anterior border (AB) estimated to localise at 58% of the embryo, and the posterior border (PB) at 36% (Fig 2.31A).

mat-α-tub-GAL4/UAS-ken embryos show a range of Kr distributions that fall into 4 groups.

i)   Wild type expression of Kr, which probably represents the 95% embryos that hatch.

ii)   Broadened domain (27%) shifted anteriorly with AB at 70% of the egg length and PB at 43% (Fig 2.31B). A detailed analysis of Kr expression in a number of mutants (Huelskamp *et al.*, 1990) has shown that a similar broad domain shifted anteriorly is observed in the embryos lacking zygotic Hb (Hb^{zyg}). Expression of Hb^{zyg} covers the same anterior half of the embryo where maternally supplied Hb (Hb^{mat}) is localised, though at lower levels. In those embryos Kr domain is activated only by Hb^{mat} and Bcd and, therefore, expressed in a broader region extended anteriorly to the position where level of Hb^{mat} is high enough to repress its expression.

iii)   Weak Kr expression, with the width of the domain occupying 19% of the egg length from 60% to 41% (Fig 2.31C). A similar phenotype is seen in double *hb^{mat}*, *hb^{zyg}* mutants where Kr expression is driven only by Bcd, whose lower concentration allows a broader domain of Kr (Hülskamp *et al.*, 1990).

iv)   No (or almost no) Kr expression (Fig 2.31D), an observation also reported for *bcd*, *hb^{mat}* double mutant embryos (Hülskamp *et al.*, 1990). As *hb^{zyg}* is not expressed in the absence of *bcd*, those double mutants lack all anterior determinants required to activate Kr (Driever & Nüsslein-Volhard, 1989).

Thus, the variety of Kr expression patterns in the *mat-α-tub-GAL4/UAS-ken* embryos appears to reflect a variability in the strength of anterior determinant activities and is consistent with the range of the phenotypes observed in the cuticle preparations. Kr central domain corresponds to the position of the presumptive T2 and T3 thoracic segments and A1-A4 abdominal those (Gaul & Jäckle, 1990). Therefore, embryos that show no Kr expression (Fig 2.31D) apparently represent the most severe phenotype with only 3-4 abdominal segments formed (Fig 2.30E). Moreover, at early stages two almost equivalent invaginations, typical for the posterior pole of the wild type embryo, are occasionally seen at both poles of the embryos lacking detectable central domain of Kr expression. Similarly, a broad Kr domain (Fig 2.31B) seems to correspond to the cuticles that show a complete endogenous abdomen and lack the

most anterior segments replaced by extra mirror-inverted abdominal segments (Fig 2.30D).
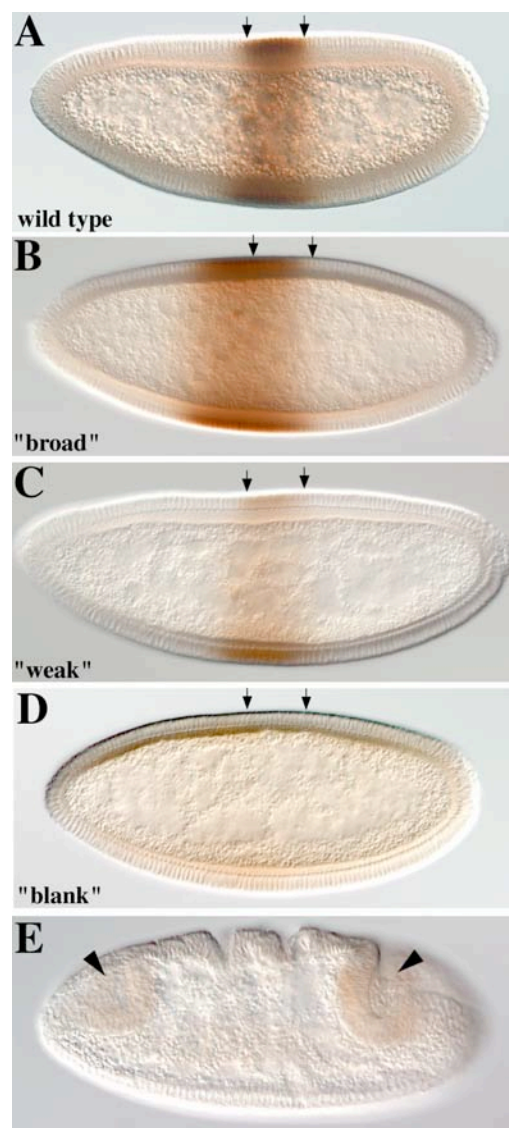
Figure 2.31. Kr expression is changed in the *mat-α-tub-GAL4/UAS-ken* embryos.

Early embryos of stage 5 (A-D) and stage 7/8 (E) are stained with anti-Kr antibody.

(A) Kr expression in the wild type embryo (arrows mark AB and PB of the domain corresponding to the wild type expression). (B-D) *mat-α-tub-GAL4/UAS-ken* embryos show distinct variations in Kr expression such as "broad" domain (B), "weak" domain (C) or no Kr expression (D). (E) In a gastrulating *mat-α-tub-GAL4/UAS-ken* embryo invagination of the polar cap (arrowheads) is seen at both the anterior and posterior poles of the embryo.

2.14 Expression of *hb* in the bicaudal embryos mis-expressing Ken

The data shown above argue that Ken mis-expressed at early stages reduces or even ablates Bcd and Hb activities. Since the maternal forms of these proteins are transcribed during oogenesis ectopic Ken expressed zygotically cannot repress transcription of either *bcd* or hb^{mat}. The translation of maternally provided transcripts occurs by the end of 9th mitotic cycle (Foe *et al.*, 1993). Assuming GAL4 mRNA is translated at the same time point as endogenous maternal mRNAs, and given the time

required for newly synthesised Gal4 protein to induce Ken expression, it is not possible for Ken to function at the level of protein translation. Therefore Ken is most likely to act in parallel or downstream of Bcd and Hb.

Early zygotic expression of *hb* at the anterior pole is Bcd-dependent (Driever & Nüsslein-Volhard, 1989). Therefore, expression of *hb^zyg* was tested in *mat-α-tub-GAL4/UAS-ken*. Staining with anti-Hb antibody showed no or almost no alteration in the anterior domain of Hb, though its border may be slightly shifted from 49% of the egg length seen in wild type (Fig 2.32A) to 53% in the mutant embryos (Fig 2.32B).

However, the domain of Hb^mat expression coincides with that of the early Hb^zyg, and the apparent level of Hb detected with anti-Hb antibody represents both Hb^zyg and Hb^mat. Therefore, expression of Hb was next examined at mRNA level. *In situ* hybridisation with *hb* anti-sense probe shows that in *mat-α-tub-GAL4/UAS-ken* embryos total level of *hb* mRNA present in the anterior half of the embryo is lower then in the wild type embryos of the same stage. Relatively high levels of *hb* expression observed in 60% of the wild type embryos (Fig 2.32C) are not seen in the mutants, two thirds of which show slightly reduced levels of *hb* mRNA (Fig 2.32D). Similarly low level of staining is only observed in 20% of the wild type embryos. In the remaining one third of the mutants anterior expression of *hb* is restricted to two stripes (Fig 2.32E), which are known to be Bcd-independent (H. Jäckle, personal communication). This *hb* mRNA distribution is observed in 33.3% of the mutant and 20% of the wild type embryos.

The fact that all *mat-α-tub-GAL4/UAS-ken* embryos examined contain levels of Hb protein as high as in wild type confirms the proposal that Ken does not affect transcription and translation of maternal Hb. However, lower levels of *hb* transcript suggest that Bcd activity may be suppressed to a certain extent in the *mat-α-tub-GAL4/UAS-ken* embryos.

Although the bicaudal phenotype caused by Ken mis-expression represents an artificial situation, it might be a clue to other JAK/STAT independent Ken functions.
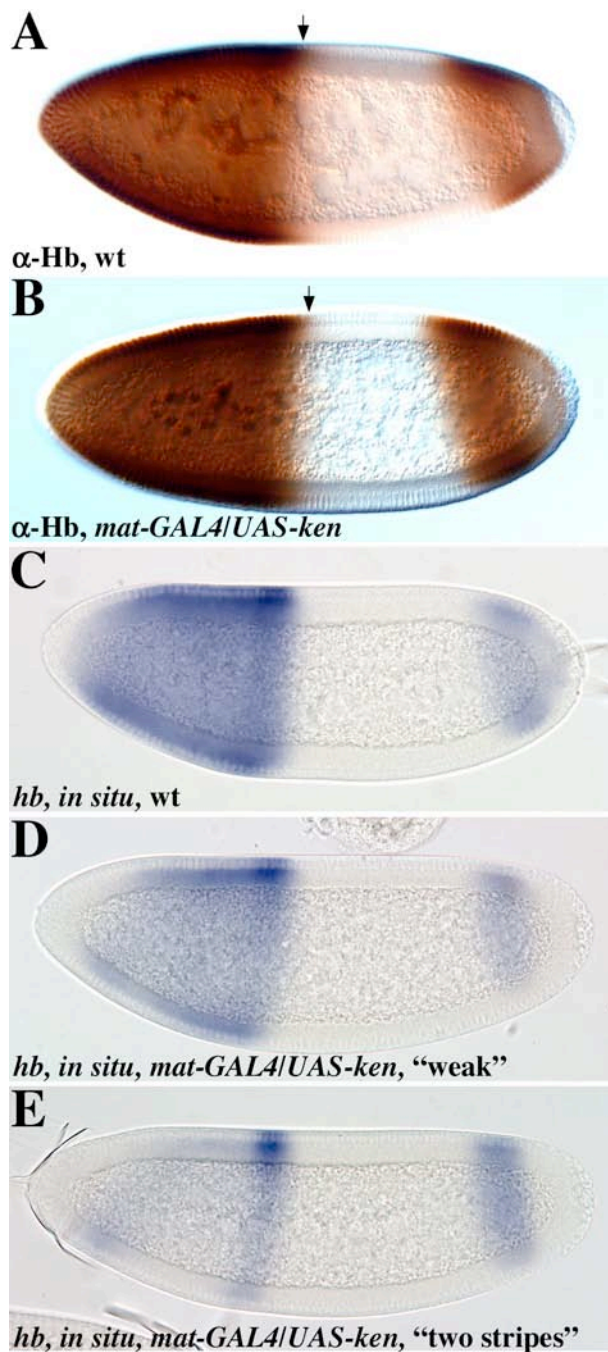
Figure 2.32. Expression of *hb* protein and mRNA in the *mat-α-tub-GAL4/UAS-ken* embryos.

Stage 5/6 embryos are either stained with anti-Hb antibody (A-B) or hybridised with *hb* anti-sense probe (C-E).

The wild type (A) and the *mat-α-tub-GAL4/UAS-ken* (B) embryos demonstrate similar localisation of Hb protein. Arrows mark the posterior border of the wild type Hb anterior domain. (C) In the wild type embryo, *hb* mRNA is expressed in two domains: the broad anterior domain covering the anterior half of the embryo, and a narrow stripe in the posterior end. In the *mat-α-tub-GAL4/UAS-ken* embryos the anterior domain of *hb* shows two types of distribution: (D) weaker levels of the transcript in the entire anterior half, or (E) the anterior domain represented only by two stripes.

2.15 Expression of *abd-B* is altered in *ken¹* mutants

Ken appears to be required for genitalia development as *ken¹* homozygous survivors have severely reduced or completely absent external genitalia structures (Fig 2.4; Castrillon *et al.*, 1993). At the cellular blastoderm stage *ken* is expressed in two stripes (Fig 2.6), with the posterior domain overlapping the 7th stripe of the *fushi tarazu* embryonic expression (Kühnlein *et al.*, 1998), a region that corresponds to the parasegments (PS) 14/15 (Jürgens & Hartenstein, 1993). The parasegments 14 and 15

contribute to formation of female genital primordium, male genital primordium and anal primordium (reviewed in Sanchez & Guerrero, 2001). The identity of PS13-15 is specified by the homeotic gene *abd-B* (Estrada & Sánchez-Herrero, 2001). *abd-B* pre-RNA is alternatively spliced and gives rise to two distinct forms: a morphogenetic form (mAbd-B) expressed in PS13 and a regulatory form (rAbd-B) expressed in PS 14/15 (Boulet *et al.*, 1991). Given the overlap between *ken* and *r-abd-B* expression in the PS14/15, and genitalia defects observed in both *ken* and *abd-B* mutants, expression of *abd-B* was examined in *ken[1]* homozygous mutants. To distinguish different forms of *abd-B* mRNA two specific probes were synthesised specific to *m-abd-B* and *r-abd-B*. Strikingly, a large proportion of early gastrulating *ken[1]* embryos contains no *r-abd-B* transcript (Fig 2.33A & B), whereas expression of *m-abd-B* remains unchanged (Fig 2.33C & D).
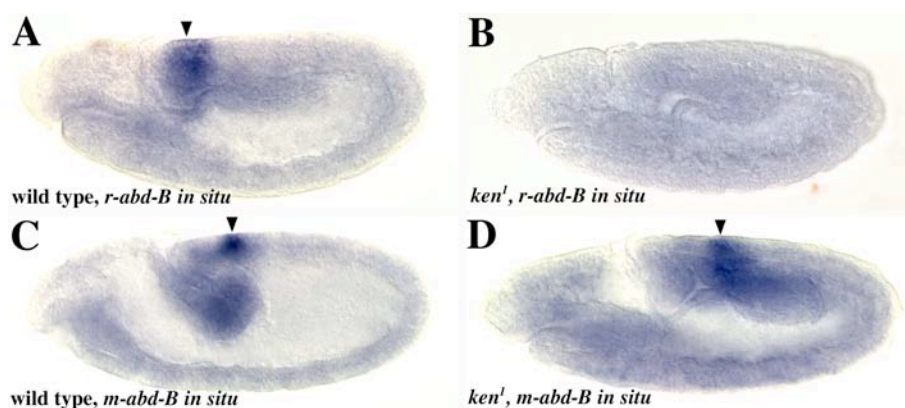
Figure 2.33. Expression of *r-abd-B*, but not *m-abd-B* is changed in *ken[1]* mutant embryos.

Stage 9/10 embryos are hybridised *in situ* using *r-abd-B* and *m-abd-B* specific anti-sense probes. Expression of the transcripts is indicated by arrowheads. *r-abd-B* mRNA seen in PS 14/15 of the wild type embryo (A) is not detected in the *ken[1]* homozygous embryo (B). In contrast, the wild type (C) and *ken[1]* mutant embryo (D) show similar levels of the *m-abd-B* expression.

This observation suggests that Ken may be involved in the regulation of *abd-B* expression, and potentially explain the genitalia defects seen in *ken[1]* mutant individuals. However, further investigations are required to establish the role that *ken* plays in Abd-B functions and genitalia development.

3 Discussion

The JAK/STAT pathway plays a central role in orchestrating the immune system as it transduces signals from interleukins and growth factors to co-ordinate proliferation and differentiation of immune competent cells (reviewed in Hanlon *et al.*, 2002; Parmar & Platanias, 2003). Uncontrolled JAK/STAT pathway activity is often implicated in severe diseases including tumours and cancers. The pathway also plays a vital role during development, with its under-activation leading to organ dysfunction or embryonic lethality (reviewed in Imada & Leonard 2000; Schindler, 2002; Calò *et al.*, 2003).

The JAK/STAT pathway has been conserved throughout evolution, and all known components are present in the genome of the fruit fly *Drosophila melanogaster* (reviewed in Castelli-Gair Hombria & Brown, 2002). Requirements for the pathway in haematopoiesis and immune system functions have also been shown in flies (Hanratty & Dearolf, 1993; Agaisse *et al.*, 2003). Investigations over the past ten years have shown the importance of the JAK/STAT pathway for many diverse processes during embryonic and larval development. However, this entire variety of functions is dependent on a relatively small set of proteins. Moreover, be it hindgut elongation upon the JAK/STAT pathway stimulation, or migration of the follicular border cells, these effects are triggered by the activation of the very same transcription factor, STAT92E. The question, therefore, arises as to how STAT92E molecules activated at a particular time in a particular place can bring about the expression of the appropriate set of responsive genes to produce the desired developmental response.

On the one hand, STAT92E transcription factor can function in synergy with other activators, as it is shown for *four-jointed*, whose gradient expression in the eye imaginal disc is determined by co-ordinated activities of Notch, Wingless and JAK/STAT pathways (reviewed in Zeidler *et al.*, 2000). On the other hand, presence of specific repressors can down-regulate the promoters that potentially can, but should not be induced. For example, stripe 7 of *eve* expression requires *tailless*, with its posterior border defined by Hunchback, which does not allow *eve* activation even in the presence of Tailless (Frasch & Levine, 1987; Small *et al.*, 1996).

This study describes Ken as a regulator that functions at the level of DNA binding and represents the identification of a novel mechanism by which JAK/STAT signalling is modulated *in vivo*.

3.1 Identification of *ken&barbie*

Deficiency $Df(2R)Chi^{g230}$ and LOF mutations in *ken&barbie* were identified as moderate enhancers of the eye overgrowth phenotype caused by over-expression of the pathway ligand Upd (Fig 2.1). *ken* LOF mutations also suppress the phenotypes caused by $stat92E^{HJ}$ (Table 2.1) and $dome^{367}$ (Table 2.2) LOF mutations, suggesting that Ken may function as a negative regulator of the pathway.

Structurally, Ken has two distinct domains. The C-terminus carries three C_2H_2 Zn-finger motifs shown in other proteins to mediate either DNA or RNA binding, or to be involved in protein-protein interactions (Iuchi, 2001; Laity *et al.*, 2001). Though no data are available about Ken Zn-finger domain interacting with RNA or proteins, its ability to specifically bind DNA *in vitro* is shown in this study. The N-terminal part of the Ken protein contains an evolutionary conserved BTB/POZ domain found in up to 10% of human zinc finger proteins (Collins *et al.*, 2001) and involved in protein-protein interactions (Bardwell & Treisman, 1994; Albagli *et al.*, 1995; Collins *et al.*, 2001; van den Heuvel, 2003). BTB/POZ containing proteins are implicated in a variety of processes such as transcriptional regulation, DNA remodelling, cytoskeleton binding and ubiquitin-mediated protein degradation (Albagli *et al.*, 1995; Geyer *et al.*, 2003; van den Heuvel, 2003). However, proteins harbouring BTB/POZ domain in a combination with Zn-finger motifs are more frequently involved in transcriptional repression and, therefore, grouped into a distinct subclass of transcriptional repressors (Albagli *et al.*, 1995). Given the ability to bind DNA *in vitro* (Fig 2.15) and nuclear accumulation shown using EGFP-fused constructs *in vivo* (Fig 2.14), Ken may well be considered as a transcription factor.

3.2 *Drosophila* Ken is similar to human BCL6

Searches through human and mouse databases for potential Ken homologues have identified BCL6 that shares 20.3% overall identity to Ken (Fig 2.3). Up-regulation of BCL6 is seen in up to 70% of non-Hodgkin's lymphomas (Dent *et al.*, 1997), while mice homozygous for BCL6 LOF mutations do not contain germinal centres and so

have diminished B-cell dependent immune responses (Dent *et al.*, 1997; Ye *et al.*, 1997; Niu, 2002). Molecular studies have shown that BCL6 binds to a DNA sequence containing a core GAAAG (Kawamata *et al.*, 1994; Baron *et al.*, 1995; Chang *et al.*, 1996), and that only four of six zinc fingers are required for this recognition (Mascle *et al.*, 2003). Interestingly, the four Zn-fingers of BCL6 involved in DNA recognition demonstrate 42.9% identity (50.5% similarity) to the Zn-fingers of Ken. Using SELEX technique the Ken DNA binding consensus GNGAAAGK has been identified, and the GAAA core has been confirmed by EMSA to be absolutely required for Ken binding to DNA. Moreover, this core overlaps the consensus sequence bound by each molecule of STAT92E within the STAT92E dimer (Fig 2.15).

3.2.1 Requirement for co-repressors

Cell culture based studies have shown that BCL6 acts as a potent transcriptional repressor recruiting co-repressors such as SMRT, mSIN3A, N-CoR and HDAC-1 are required for BCL6 activity (Dhordain *et al.*, 1997; Dhordain *et al.*, 1998; Huynh & Bardwell, 1998; Wong & Privalsky, 1998; Ahmad *et al.*, 2003). Though homologues of a number of co-repressors are identified within the fruitfly genome (Burke & Baniahmad, 2000), no physical interactions between Ken and any of them have yet been described by genome-wide interaction analysis (http://portal.curagen.com/cgi-bin/interaction/flyHome.pl). Interestingly, *smrter*, a *Drosophila* homologue of SMRT, shows a genetic interaction with both, *stat92E* and *ken*. In this respect further studies will be helpful to find out the nature of these interactions.

3.2.2 DNA binding

In vitro assays have shown that BCL6 can bind to STAT6 sites derived from STAT6 target genes (Harris *et al.*, 1999; Hartatik *et al.*, 2001), suggesting that BCL6 and STAT6 may compete for DNA binding. Similarly, Ken may occupy the STAT92E binding sites thus preventing the activation of transcription. Since the core of the Ken consensus overlaps only half of the palindromic STAT92E site, an alternative model can be proposed, in which the two proteins may heterodimerise and bind to DNA as a complex. *In vitro* co-immunoprecipitation assay failed to detect any association between Ken and STAT92E. However, given that the co-IP assay was based on heterologous system using *in vitro* translated Ken and STAT92E-GFP expressed in

Drosophila cell culture, the possibility that Ken may associated with STAT92E when expressed *in vivo* cannot be excluded. Also the luciferase assay suggests a link between these proteins. In the transfection experiments Ken alone does not influence the reporter expression, yet does when co-expressed together with activated STAT92E (Fig 2.18 & 2.19). A similar effect observed in Ken/Hop co-transfection may be brought about by Ken association with endogenous STAT92E. Alternatively, a direct interaction between Hop and Ken may take place, with Ken being activated by phosphorylation mediated by Hop. This possibility represents an object of especial interest, as nothing is known about potential phosphorylation or any other modifications of Ken. As for BCL6, it has been shown that phosphorylation targets BCL6 to ubiquitin-mediated degradation (Niu, 2002), while acetylation inhibits BCL6 functions (Bereshchenko *et al.*, 2002).

3.2.3 Transcriptional repression

Transcriptional repression by BCL6 is mediated by its BTB/POZ domain. A crystallographic analysis of BTB/POZ domain revealed several notable features including a highly conserved charged "pocket", which enables association with co-repressors (Melnick *et al.*, 2000). Mutations in the conservative negatively charged aspartic acid D35 and positively charged arginine R49 prevent binding to co-repressors and result in a loss of repressional activity by BCL6 (Melnick *et al.*, 2002). Interestingly, while the position D35 in the Ken BTB/POZ domain remains unchanged, arginine in the position 49 is substituted for positively charged lysine. Strikingly, mutations in these positions exchanged into structurally similar, but uncharged N35 and Q49, seem to make Ken non-functional, as Ken[D35N,K49Q] mis-expressed under *GMR-GAL4* driver does not show the eye reduction phenotype observed following mis-expression of the wild type protein (Fig 2.11). This suggests that the conserved charged pocket of BTB/POZ domain is also essential for Ken functions.

Of particular interest are reports showing that in tissue culture experiments BCL6 can repress a subset of STAT6 target genes induced by interleukin-4 stimulation (Harris *et al.*, 1999). Unexpectedly, in *Drosophila* S2 cells Ken over-expression does not suppress, but enhances the luciferase reporter activation induced by STAT92E. Moreover, this effect seems to be specific to DNA sequence, as the reporter with the mutated STAT92E site shows no response either to STAT92E or Ken. Besides, both

the Zn-finger and the BTB/POZ domains of Ken are required, as the truncated forms of Ken do not activate the reporter. It appears that removal of these functional domains interferes either with activity or folding of the Ken molecule.

It should be noted that the observed activation of the reporter by Ken contradicts the results obtained *in vivo*, which all consistently indicate that Ken functions as a negative regulator of the JAK/STAT pathway. A potential explanation why Ken over-expression in cell culture enhances the STAT92E induced reporter activation comes from the studies of BTB/POZ domain derived from PLZF, a transcriptional repressor related to Ken and BCL6 (Melnick *et al.*, 2000). It has been shown that the mutations in the positions D35 and R49, required for association with co-repressors (see above), may not only abolish repressional activity, but are also able to convert the protein from a repressor into an activator. This implies that repression by the BTB/POZ domain is entirely mediated by the associated co-repressors. If that is the case, then in a system lacking the required co-repressors, a BTB/POZ domain may become non-functional or even acquire an activator function. In cell culture experiments over-expression using the Gal4/UAS system may well generate amounts of proteins significantly greater than the physiological level. Though co-repressors potentially interacting with Ken are not yet identified, it seems likely that the level of Ken over-expression may be greatly in excess to the required co-repressors. As a result co-repressor molecules may only be available for a small portion of Ken, whereas the larger proportion of Ken not associated with co-repressors serves as an activator.

By contrast, a negative regulation by Ken is clearly seen in *in vivo* assays illustrating that Ken mis-expressed during embryogenesis is able to knock-down transcription of *ventral vein lacking*, *trachealess* and *knirps* in the regions known to require JAK/STAT pathway activity for their expression (Brown *et al.*, 2001; Brown *et al.*, 2003).

Taken together, the similarities between Ken and BCL6 at the level of their protein sequence composition, the domain structure, the ability to bind similar DNA sites and to repress a subset of JAK/STAT pathway target genes, suggest that Ken represents a functional orthologue of BCL6.

3.3 Differential regulation of JAK/STAT targets by ectopic Ken

In vitro techniques identified a DNA sequence specifically bound by Ken that resembles a STAT92E half-site. The fact that the Ken consensus only partially overlaps that of STAT92E suggests that not all STAT92E sites in the promoters of target genes may also allow Ken binding. First of all, the minimal recognition sequence for Ken is GAAA (Fig 2.15), whereas a STAT92E half-site does not require the last A (Yan *et al.*, 1996b). Secondly, the additional positions, though dispensable, are likely to modify the affinity, with which Ken binds to DNA. Therefore, among a variety of sequences that can be successfully bound by STAT92E only a subset is also suitable for Ken. The selective effect of Ken on the expression of putative JAK/STAT pathway target genes observed in the mis-expression experiments is consistent with this selective site hypothesis. However, lack of available information on the promoters of those genes represents a serious obstacle for testing this hypothesis. For many of the putative STAT92E target genes neither detailed analysis of the regulatory regions has been undertaken, nor direct binding of STAT92E to the promoters has been demonstrated.

Among the target genes examined in this study only the promoter of *even-skipped* is partly characterised and shown to contain two putative STAT92E binding sites. Cis-regulatory elements that direct *eve* expression in the stripes 2, 3 and 7 have been mapped (Goto *et al.*, 1989) and a *lac-Z* reporter construct containing a 500bp fragment of the *eve* promoter demonstrates that this fragment is sufficient to drive β-gal in the position of *eve* stripe 3 (Small *et al.*, 1996). Moreover, this stripe of β-gal expression is almost eliminated in *hop* GLC mutant embryos (Binari & Perrimon, 1994). Analysis of the 500bp promoter region revealed two potential STAT92E binding sites. Binding of the activated STAT92E to both of those sites was confirmed *in vitro* (Yan *et al.*, 1996b). However, the endogenous *eve* stripe 3 is only weakly reduced in *hop* and *stat92E* mutant embryos. This suggests that other activators can drive stripe 3 *eve* expression, probably via interaction with the promoter outside the 500bp region. STAT92E binding sites required for *eve* expression in the stripe 5, which is eliminated in *hop* or *stat92E* mutants, have yet to be characterised.

Though one of these STAT92E sites (TTCCCC<u>GAAA</u>, Yan *et al.*, 1996b) also contains the core required for Ken binding (underlined), ectopically expressed Ken

failed to change *eve* expression. Unexpectedly, neither DomeΔCyt nor ΔNSTAT92E, both of which shown to serve as negative regulators of the pathway (Brown *et al.*, 2001; Henriksen *et al.*, 2002), could suppress any stripe of *eve* (Fig 2.24). However, *runt* mis-expressed by the same driver is capable of affecting the stripes 1, 2 and 4 of *eve*, which implies that the ectopic expression driven by *nos-GAL4.NGT40* is early and strong enough to suppress *eve* (Tracey *et al.*, 2000). However, while it has been shown that endogenous *runt* is essential for refinement and maintenance of the *eve* expression pattern, and in *runt* LOF mutants all *eve* stripes are affected (Frasch & Levine, 1987), ectopic *runt* is only able to down-regulate three stripes, whereas the stripes 3, 5, 6 and 7 remain unaffected. This suggests that some of *eve* stripes, though sensitive to endogenous repressors, cannot be affected by ectopically expressed repressors. Similarly, the ectopic expression of the negative regulators DomeΔCyt and ΔNSTAT92E does not appear to be strong enough to influence the *eve* promoter region required to drive the expression of the stripes 3 and 5 that are repressed in JAK/STAT mutants.

The promoters of other putative JAK/STAT pathway target genes are not yet characterised. However, computer searches through a 6kb region flanking the *vvl* locus revealed a single potential STAT92E binding site A<u>TTCAGC<u>GAA</u>A</u>T located 825bp upstream of the translation start. Intriguingly, this site contains <u>GC<u>GAAAT</u></u> motif representing a perfect Ken binding sequence (double underlined). Cloning the *vvl* promoter and further *in vivo* investigations of Ken and STAT92E DNA binding will be required to determine whether this sequence (and potentially others) represents a functional binding site for both of the proteins.

3.4 Endogenous Ken antagonises the JAK/STAT pathway

As already discussed above, ectopic Ken is able to down-regulate a number of JAK/STAT pathway targets. However, endogenous Ken is expressed neither in the hindgut nor in the tracheal pits where the consequences of its mis-expression were observed. Therefore, the question arises whether this regulation also takes place during normal development, and whether the genes affected by ectopic Ken represent its natural targets.

The *ken* expression pattern shows overlap with the pattern of JAK/STAT pathway activity (Fig 2.9). These overlapping areas are of particular interest, as they identify

regions of potential co-operation between Ken and STAT92E. It can be proposed that presence of Ken in these tissues may be required to prevent expression of targets normally induced by STAT92E in different tissues or at different stages. As shown in the mis-expression assays, not all of the tested genes can be down-regulated by Ken. This implies that presence of ectopic Ken enables repression of some genes without affecting others within the same cells, which supports the proposed hypothesis.

Three putative JAK/STAT pathway target genes – *trh*, *kni* and *vvl* – are shown to be affected by Ken (Fig 2.26-28). Interestingly, though stimulated by Upd in the posterior spiracles, STAT92E is not able to activate *vvl* and *kni* in these tissues. Strikingly, in the mutant embryos lacking a large proportion of Ken *vvl* is up-regulated in the presumptive posterior spiracles (Fig 2.29). This suggests that one of the Ken functions in the posterior spiracles is to prevent expression of *vvl*, and its ectopic activation in *ken* mutants is potentially a result of de-repression of JAK/STAT pathway activity. However, further analysis using double mutants for both *dome* and *ken*, is required to confirm this.

Another consequence of this observation is a fine balance that must exist between STAT92E and Ken activities. Apparently, endogenous level of Ken is sufficient to repress *vvl*, but not other, as yet unidentified, JAK/STAT pathway targets that are essential for posterior spiracle development. Extra levels of Ken can phenocopy the posterior spiracle defects observed in *dome^{468}* (Fig 2.10). While it is possible that these abnormalities caused by additional Ken may be independent of JAK/STAT pathway activity, it seems more likely that Ken acts in a dosage dependent manner and extra Ken is able to further antagonise JAK/STAT pathway target genes.

While expression of *kni* has not yet been examined, *trh* expression restricted to the region of the presumptive filtzkörper (Fig 1.14 and reviewed in Hu & Castelli-Gair, 1999) does not appear to be altered in the posterior spiracle primordia in the *ken* mutants.

In summary, *ken* interacts with multiple aspects of the JAK/STAT pathway during development to antagonise signalling. Its ectopic expression can phenocopy developmental defects known to be caused by loss of JAK/STAT pathway activity. Also Ken can down-regulate a subset of known pathway target genes, and given the overlap between Ken and STAT92E consensus sequences, this selective regulation is

likely to occur at the level of gene expression. Furthermore, in the posterior spiracles endogenous Ken is required to repress the JAK/STAT pathway target gene *vvl*, whose expression is up-regulated in the *ken* mutants (Fig 3). The pattern of *ken* expression and its modulation of a subset of known JAK/STAT pathway targets suggests that Ken acts as a selective regulator of the signalling and is implicated in tissue- and stage-specific control of transcriptional output generated by activation of JAK/STAT signalling.
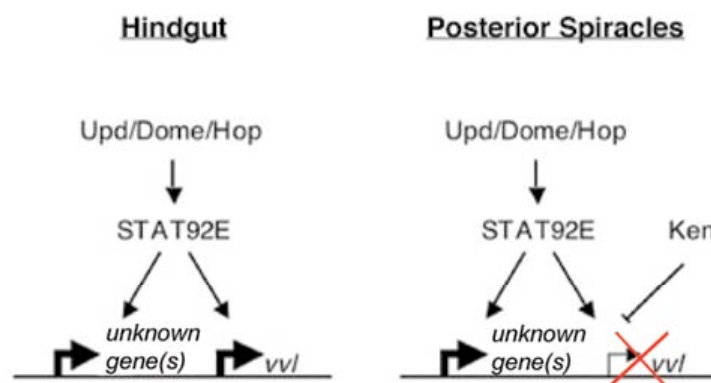
Figure 3. A scheme illustrating co-operation between Ken and the JAK/STAT pathway.

In the hindgut, STAT92E induced by Upd activates the expression of *vvl* and, potentially, other, yet unidentified genes. In the posterior spiracles, STAT92E is able to activate the expression of genes proposed to be essential for posterior spiracle development. However, presence of Ken prevents the expression of *vvl* by activated STAT92E.

3.5 Other Ken functions: the bicaudal phenotype

While Ken is involved in the regulation of the JAK/STAT signal transduction, it may also function in other developmental processes. This is indicated by its broad embryonic expression pattern (Fig 2.6 & 2.7), the genital defects present in the hypomorphic *ken* mutants (Fig 2.4), and the bicaudal phenotype caused by Ken mis-expression at early stages (Fig 2.30).

The bicaudal phenotype indicates that ectopic Ken is capable of regulating the anterior determinants Bcd and Hb, most probably in JAK/STAT pathway independent manner as no evidence exists that the JAK/STAT pathway can regulate Bcd, Hb or their target genes. Indeed, neither Hb nor Kr gap genes are affected in *hop* GLC embryos (Binari & Perrimon, 1994). Furthermore, like the pair rule genes Upd is unlikely to be expressed before the 13th mitotic cycle of embryogenesis, whereas

expression domains of the gap genes become defined by the end of 10th cell cycle (Foe *et al.*, 1993). Therefore, changes in Kr expression observed in the embryos mis-expressing Ken (Fig 2.31) cannot be caused by JAK/STAT pathway activity, and it is possible to exclude the JAK/STAT pathway as a cause for this phenotype.

The bicaudal phenotype was originally discovered in dominant GOF mutants for *bicaudal-C* and *bicaudal-D* loci (Bull, 1966). *Bic-D* is a cytoskeleton protein involved in the posterior localisation of *oskar*, *nanos* and other determinates during oogenesis. Its dominant mutations responsible for the bicaudal phenotype contain single amino acid substitutions, which causes the accumulation of the Bic-D protein in the anterior part of the oocyte (St Johnston, 1993). The resulting anterior mis-localisaion of *nos* mRNA leads to repression of *hb* and *bcd* translation mediated by Nos-response elements (NRE) present in 3'-UTR of *hb* and *bcd* transcripts (Wharton & Struhl, 1989; Wharton & Struhl, 1991). Once bound to NRE, Nos blocks translation of the corresponding mRNAs (Chagnovich & Lehmann, 2001).

The bicaudal phenotype can be also generated experimentally by localising *oskar* mRNA to the anterior half of the embryo, which results in the anterior mis-localisation of *nos* transcript (Lehmann & Nüsslein-Volhard, 1986).

Finally, the bicaudal phenotype was observed in the double mutants for the maternal genes *bcd* and *hb* (Hülskamp *et al.*, 1990). It is worth mentioning that in the embryos lacking only *bcd*, some posterior structures are formed in the anterior part of the embryo (Frohnhöfer *et al.*, 1986), whereas for the symmetrical, mirror-imaged bicaudal phenotype the loss of both Bcd and Hb is critical.

Together these results imply that Ken mis-expressed under the early *mat-α-tub-GAL4* driver must down-regulate both Hb and Bcd, but the mechanism of this repression is not fully understood. Obviously, Ken cannot regulate the maternal transcription of these genes that occurs during oogenesis. Furthermore, translation from maternally supplied mRNAs begins by the end of 9th mitotic cycle (Foe *et al.*, 1993), which implies that Gal4 protein can only be translated not earlier than Hb and Bcd. Given the time required for the subsequent transcription and translation of ectopic Ken, it is apparent that Ken cannot be involved in translational regulation of Hb and Bcd either. Therefore, Ken is likely to act at the same level or downstream of Hb and Bcd in the bicaudal embryos.

Given its DNA binding activity, Ken may be proposed to repress transcription of their target genes. However, neither Bcd (TCTAATCCC, Gao & Finkelstein, 1998; Zhao *et al.*, 2000) nor Hb ($^G/_A$$^C/_C$ATAAAAAA, Stanojevic *et al.*, 1989) consensus sequences overlap that of Ken (Fig 2.15E). Zn-finger domains are also known to mediate RNA binding and protein-protein interactions (Iuchi, 2001). However, ability to serve for both DNA and RNA binding has been observed in proteins with long Zn-finger domains, whereas Ken molecule contains only three Zn-finger motifs. Finally, presence of the BTB/POZ domain that is known to mediate protein-protein interactions (Bardwell & Treisman, 1994; Albagli *et al.*, 1995; Collins *et al.*, 2001; van den Heuvel, 2003) suggest that Ken may physically associate with Bcd and Hb. This possibility requires further investigations.

Nevertheless, the information elicited from the bicaudal phenotype is not enough to determine the potential functions of Ken in regards to Bcd and Hb. Moreover, mis-expression experiments represent an artificial situation, which may not reflect processes that take place during normal development. However, if the observed phenotype is based on real interactions between Ken, Hb and Bcd, it can be hypothesised that Ken, whose anterior expression domain is the only region where Bcd and Ken can potentially interact, may be involved in regulation of Bcd targets in this region. With regard to *hb*, its expression pattern shows more overlaps with that of *ken*, and, therefore, at this point it is not possible to address the significance of their potential interactions.

3.6 Other Ken functions: genitalia development

Ken is required for genitalia development as it is shown by the genitalia phenotype effected by some *ken* alleles. *ken¹* homozygous flies that do not die during development show external genitalia abnormalities. These defects may constitute a complete loss of the external genitalia (Fig 2.4 and Castrillon *et al.*, 1993) or, vice versa, duplications of the terminalia arranged in a mirror image (Lukacsovich *et al.*, 2003).

The *Drosophila* terminalia originate from the genital imaginal disc. Early in embryogenesis the presumptive genitalia region consists of three primordia: the female genital primordium (FGP) corresponding to A8 (PS13/14), the male genital primordium (MGP) developing from the A9 (PS14/15) and the anal primordium that

corresponds to A10/11 (PS15 and telson) (reviewed in Sanchez & Guerrero, 2001). Interestingly, at the cellular blastoderm stage *ken* is expressed in two stripes (Fig 2.6), with the posterior domain overlapping the 7th stripe of the *fushi tarazu* embryonic expression (Kühnlein *et al.*, 1998), which corresponds to the PS14/15 known to give rise to the genitalia primordia (Jürgens & Hartenstein, 1993). It is therefore possible that the genitalia phenotypes of the *ken[1]* mutants may result from the lack of Ken in the genitalia primordia at this stage.

The identity of PS13-15 is specified by the homeotic gene *abd-B*. Abd-B promotes genital development by changing how positional information is interpreted, with the genital primordia transforming into legs or antennae in the absence of Abd-B (Estrada & Sánchez-Herrero, 2001). Alternative splicing of *abd-B* pre-RNA gives rise to two distinct forms: morphogenetic Abd-B (mAbd-B) expressed in PS13 and regulatory Abd-B (rAbd-B) expressed in PS14/15 (Boulet *et al.*, 1991). Differential control of Wg, Dpp and Hh signalling by mAbd-B and rAbd-B in synergy with the female and male forms of Double-sex control proper development of the female and male terminalia (reviewed in Sanchez & Guerrero, 2001).

Strikingly, expression of the *abd-B* transcript encoding the r-form appears to be ablated in a proportion of the *ken[1]* homozygous embryos (Fig 2.33). Though these preliminary data need to be further investigated, it seems that Ken may be involved in the regulation of the *abd-B* expression. If this is the case, it may explain the genitalia defects shown for both *ken* and *abd-B* mutant. Also, *ken* and *abd-B* are both expressed in the genital disc of the larva (Freeland & Kuhn, 1996; Lukacsovich *et al.*, 2003) and, potentially, can interact also at this stage.

Abd-B is also expressed in the pupa where it is involved in sex-specific differentiation of the abdominal epithelium. Interestingly, at this stage regulatory input of Abd-B is integrated by Bric-a-brac1, another BTB/POZ domain transcription factor (Kopp *et al.*, 2000).

Further studies in this direction will be helpful to find out whether Ken implication in genitalia development is based on co-operation with Abd-B.

4 Materials and methods

4.1 Bacterial culture

4.1.1 Media and growth conditions

The *E.coli* strain XL1-blue (Stratagene) was used. Bacterial cells were grown either in LB$^+$ medium with vigorous shaking (200 rpm) or on agar plates at 37°C, unless otherwise specified.

Solutions:

LB$^-$(per 1l of medium)	10g bacto-tryptone, 5g bacto-yeast extract, 10g NaCl, pH 7.0, autoclaved 45min at 120°C
LB$^+$ medium	LB$^-$ with 50μg/ml of ampicillin or 34μg/ml of chloramphenicol
1000x ampicillin	50mg/ml in water, stored at –20°C
1000x chloramphenicol	34mg/ml in ethanol, stored at –20°C
LB-agar	15g agar-agar, 1l of LB$^-$, autoclaved and stored at room temperature (T$_{room}$)

To prepare plates LB-agar was melted, cooled down to 50°C and supplemented with antibiotics to the same final concentration as in LB$^+$.

4.1.2 Induced expression in bacteria

For protein expression in bacteria, cells carrying the desired plasmids (pGEX-kenDBD and pRSET-C-ken) were grown in LB$^+$ supplemented with 1μM ZnCl$_2$. At OD A$_{600}$ of 0.5, the culture was induced with 0.5mM IPTG and grown for 4h at 30°C. The cells were centrifuged at 6000rpm (Sorvall RC-5B, GS-3 rotor) for 15min at 4°C. The pellet was frozen and stored at –80°C.

4.1.3 Preparing competent cells

Heat-shock transformation competent *E.coli* cells were prepared as follows. The cells were grown in LB$^-$ over night (o/n). The resulting cell suspension was diluted 1:100

in LB⁻ and grown to A_{600} of 0.5. The culture was incubated on ice for 10-60min (from here all the steps were undertaken at $4^{o}C$ with ice-cold reagents and materials!), followed by centrifugation at 6000rpm (Sorvall RC-5B, GS-3 rotor) for 10min. The resulting pellet was resuspended in Rf1 buffer in a volume equal 1/3 of the cell culture volume and incubated for 15-120min followed by re-centrifugation. The pellet was resuspended in Rf2 buffer in a volume equal 1/4 of the volume Rf1. Following incubation for 15min the cells were aliquoted and frozen in liquid nitrogen. Aliquots were stored at $-80^{o}C$.

Buffers:

Rf1 buffer	100mM RbCl, 50mM $MnCl_2$, 30mM K-acetate, 10mM $CaCl_2$, 15% glycerol, pH adjusted to 5.8 with 1M acetic-acid
Rf2 buffer	10mM MOPS, 10mM RbCl, 75mM $CaCl_2$, 15% glycerol, pH adjusted to 6.8 with 1M NaOH

4.2 Nucleic acid manipulation

4.2.1 Molecular cloning

ken cDNA was derived from EST clones GH12495 and LD29702 (pOT2T-ken, BDGP). In order to generate constructs to be expressed in *Drosophila* cells, several constructs containing *ken* ORF (open reading frame, 1803bp) were cloned into pUAST vector (Brand & Perrimon, 1993) (for cloning scheme see table 4.1). The ORF was amplified by PCR (see section 4.2.1.1) using primers that contained *ken*-specific region and restriction sites of choice (for primers sequences see table 4.2). EGFP-fused constructs were produced in two steps: *ken* ORF was first cloned into pBS-EGFPA or pBS-EGFPB vectors (MPZ unpublished), and then re-cloned into pUAST vector. For the truncated versions GFPkenΔZnF (AA 1-503) and ΔPOZken (AA 129-601), the regions 1-1509 and 386-1803 of the ORF, respectively, were amplified.

Full-length *ken* with point mutations in BTB/POZ domain was generated by site-directed mutagenesis (see section 4.2.1.2).

ken and *vvl* ORFs were also cloned into pCR®II-TOPO® vector (see section 4.2.1.3).

To tag Ken DBD with GST, the region 1423-1803 (AA 475-601) of *ken* ORF was amplified and cloned into pGEX-4T-3 vector (Amersham).

Table 4.1 Schemes for molecular cloning.

Construct	Primers	Template	Restriction sites in polylinker
pUAST-ken	Ken-BglII-5' Ken-XbaI-3'	pOT2A-ken	*BglII* *XbaI*
pBS-SK(-)ken	Ken-Kpn1-5' Ken-BglII-3'	pOT2A-ken	*Asp718* BamHI
pCRII-ken	Ken-Kpn1-5' Ken-BglII-3'	pOT2A-ken	-
pBS-EGFPA-ken	Ken-BglII-5' Ken-XbaI-3'	pOT2A-ken	*BamHI* *XbaI*
pBS-EGFPB-ken	Ken-Kpn1-5' Ken-BglII-3'	pOT2T-ken	*Asp718* *BamHI*
pUAST-GFPken	-	pBS-EGFPA	*Asp718* **XbaI**
pUAST-kenGFP	-	pBS-EGFPB	*Asp718* *XbaI*
pUAST-kenΔPOZ	Ken-ΔPOZ-5' Ken-Xba1-3'	pOT2A-ken	*BglII* *XbaI*
pUAST-GFPkenΔZnF	T3 Ken-ΔZnF-3'	pBS-EGFPA	*Asp718* *XbaI*
pBS-SK(-)ken^{D34N,K49Q}	KenBTBmut-F KenBTBmut-R	pBS-SK(-)ken	-
pUAST-ken^{D34N,K49Q}	-	pBS-SK(-)kenD34N,K49Q	*Asp718* *BamHI*
pGEX-4T-3-kenZnF	GSTken-F GSTken-R	pBS-SK(-)ken	*BamHI* *XhoI*
pRSET-C-ken	Ken-Kpn1-5' Ken-HindIII-3'	pBS-SK(-)ken	*Asp718* *HindIII*
pcDNA3.1(+)ken	-	pCRII-ken	*HindIII* *XbaI*
pCRII-vvl	Vvl-F Vvl-R	genomic DNA	-

After PCR performed as described in the section 4.2.1.1, an aliquot of the resulting product was analysed by electrophoresis on 0.8-1.5% agarose gel (Invitrogen) in 0.5x TBE buffer. The DNA fragments were stained with ethidium bromide and visualised

with UV-transilluminator (Raytest) at 366nm. In case extra fragments had been amplified, the desired band was excised from the gel and purified with Gel Extraction Kit (Qiagen). When a single specific band had been synthesised, the entire volume of PCR reaction was precipitated with ethanol (salting agent 500mM NaCl), vacuum-dried and dissolved in TE buffer.

For subsequent cloning, both isolated the fragment and vector DNA were digested with restriction enzymes (New England Biolabs or Fermentas). The digestion reactions were carried out in 30μl volume on the excessive amount of DNA (up to 17μl of PCR mixture depending of the yield) for 1h at 37°C, unless otherwise suggested. After restriction the resulting DNA fragments were either purified by gel-extraction or ethanol-precipitation (see above).

For ligation, 200ng of the cut vector DNA was mixed with 2-3 molar excess of the isolated fragment and incubated with 1U of T4-DNA ligase (Roche) in ligation buffer (supplied by Roche) in 20μl of total volume o/n at 16°C.

In order to introduce the constructed plasmids into bacterial cells, heat-shock transformation was used. The entire volume of the ligation mixture was added to 100μl of competent *E.coli* cells (see section 4.1.3) and incubated on ice for 30min. The cells were heated for 45-50sec at 42°C, cooled down on ice and allowed recovering for 45min in 1 ml of LB^{-}. Afterwards the bacterial suspension was spread out on agar plates with an appropriate antibiotic and grown o/n (see section 4.1.1).

Colonies potentially containing the desired plasmid DNA were inoculated in 2ml LB^{+} medium and grown o/n (see section 4.1.1). 1.5ml of bacterial suspension was used for analytical DNA preparation by Miniprep Kit (Qiagen). Presence of the cloned DNA fragments was checked by restriction analysis and, if necessary, confirmed by DNA sequencing.

The bacterial colonies containing appropriate DNA constructs were inoculated into 300-500ml of LB^{+} medium and grown o/n (see section 4.1.1). Plasmid DNA preparation was performed using the Qiagen Maxiprep Kit.

Buffers:

0.5xTBE buffer	44.5mM Tris-base, 44.5mM boric acid, 1mM EDTA, pH 8.0

TE buffer   10mM Tris-HCl pH 8.0, 1mM EDTA

4.2.1.1 PCR (polymerase chain reaction)

In this study PCR amplification was used for molecular cloning (section 4.2.1), site-directed mutagenesis (section 4.2.1.2), analysis of *ken* expression by RT-PCR (section 4.2.5), synthesis of templates for *in situ* probes (section 4.2.6) and for SELEX experiments (section 4.5.1).

All primers used for PCR are summarised in table 4.2.

Table 4.2. Primers used for PCR.

Primer	Sequence	T$_{melting}$
For cloning:		
Ken-BglII-5' - *Bgl*II site - start codon - in frame	AAA-A↓GATCT-G-ATG-AAAGAGTTTCAAAGAATGTTG	62
Ken-KpnI-5' - *Kpn*I site - start codon	AA-GGTAC↓C-CTTA-ATG-AAAGAGTTTCAAAG	54
Ken-ΔPOZ-5' - *Bgl*II site - start codon - first 3 codons	ACTGTAA -A↓GATCT-CTTA-ATG-AAA-GAG-ACCGACTCCGCCTATCTGAG	64
Ken-ΔZF-3' - *Xba*I site - stop codon	ATAACTA -T↓CTAGA-CTA-TCGATACTCCCGGACCGAGG	66
Ken-BglII-3' - *Bgl*II site - no stop codon - in frame	ATA-A↓GAT-CTTCGCGCAGATTCTTTGTC	56
Ken-XbaI-3' - *Xba*I site - stop codon	A-T↓CTAGA-CTA-TTCGCGCAGATTCTTTG	58
GSTKen-F *BamH*I site	AA-G↓GATCC-GGACGCAGTGGGTCGGCCTC	70
GSTKen-R *Xho*I site	CG-C↓TCGAG-CTATTCGCGCAGATTCTTTGTCAGC	74
Ken-HindIII-3' *Hind*III site	CC-A↓AGCTT-ATTCGCGCAGATTCTTTGT	54

(table 4.2, continue)

Primer	Sequence	$T_{melting}$
For cloning:		
Vvl-F	ATCTCAATCGGCATCGAATC	58
Vvl-R	GGTCGTCTGGGAGAACACAT	62
For site-directed mutagenesis:		
KenBTBmut-F point mutations	GAGCACCCGGCGAACCTGACCATCGTCTGCGAGAACAA AGTAAAGCTGCACGCCCACCAGTTGGTCCTG	>75
KenBTBmut-R point mutations	CAGGACCAACTGGTGGGCGTGCAGCTTTACTTTGTTCTC GCAGACGATGGTCAGGTTCGCCGGGTGCTC	>75
For sequencing:		
Ken-1-F	ATGAAAGAGTTTCAAAGAATGTTG	62
Ken-468-R	ATCCGGCTCCAAATTCTGTG	60
Ken-441-F	ACCAGCCCACAGAATTTGGAG	60
Ken-963-R	GAAGAACAGGCCCTTCCGTTTC	64
Ken-925-F	AGCGAGCGAAAGCACGAAAC	62
Ken-1366-R	GATTGGGCATTGCGGACATG	62
Ken-1348-F	CATGTCCGCAATGCCCAATC	62
Ken-1797-R	CAGATTCTTTGTCAGCAGCAG	62
For *in situ* probe synthesis		
mAbdB-F	GGTCTTGTGTTGTCGGTGTG	62
T7-mAbdB-R T7 promoter	GAATTAATACGACTCACTATAGGGAGA-CAGTCGTTGTTGTTGCTGCT	60
rAbdB-F	CGTCACTGGAAGTGAGCAAA	60
T7-rAbdB-R T7 promoter	GAATTAATACGACTCACTATAGGGAGA-CTGACGCTGGAGGGAGAAAT	62
cAbdB-F	GCCAATCAGCAGAACAACAA	58
T7-cAbdB T7 promoter	GAATTAATACGACTCACTATAGGGAGA-GTCGGTTGGTCACACATCAG	62
For *tbp-1* RT-PCR:		
Tbp-1-F1	CAGATCAGGTGACCATTTAAAG	62
Tbp-1-R1	TTCCAGGAGAGGCGATTCC	60
Tbp-1-F2-nested	GATCAGGACGGGATAAGTTC	60
Tbp-1-R2-nested	CAATTATCGATGAAGTAGTGTAG	62
For SELEX:		
Sellib-F	CTCCTATACTGAGTTCATGAT–N_{20}–TGATATCGAACTGTATCGATG	
Sel-F	CTCCTATACTGAGTTCATGAT	58
Sel-R	CATCGATACAGTTCGATATCA	58

General composition of ingredients for 30μl of PCR reaction was the following:

1x PCR buffer (supplied by manufactory)

1.5-2.5mM $MgCl_2$

0.25mM dNTPs

0.2μM primer

1U *Taq* or 2.5U *PfuTurbo* polymerase

DNA from 1pg (plasmid) to 1μg (genomic DNA).

For analytical PCR and to amplify templates used for subsequent *in situ* probe labelling, *Taq* polymerase (Fermantas or Roche) was used. To produce templates for constructs to be expressed in *Drosophila* cells *PfuTurbo* DNA polymerase (Stratagene) was chosen. Because of its proofreading activity *PfuTurbo* synthesises DNA with the error rate 1.3×10^{-6}, whereas that of *Taq* is 8.0×10^{-6}.

General PCR cycling parameters were as follows. Pre-denaturation 7min at $95^{o}C$; 30 cycles: denaturation 1 min at $95^{o}C$, renaturation 1min at temperature appropriate for a pair of primers, synthesis 1min per kb at $72^{o}C$; 10min for complete synthesis at $72^{o}C$. Renaturation temperature was calculated as $(T_{melting} - 2)$ for *Taq* polymerase and $(T_{melting} - 5)$ for *PfuTurbo*.

For SELEX experiments the PCR reaction was mixed in 50μl volume and had slightly different composition of components:

1x PCR buffer (supplied by manufactory)

2.5mM $MgCl_2$

0.2mM dNTPs

1μM primers Sel-F and Sel-R

5U *Taq*

The cycling parameters were 1 min at $94^{o}C$, 19 cycles – 30sec at $94^{o}C$, 44sec at $50^{o}C$, 1min at $72^{o}C$ and complete synthesis for 2min at $72^{o}C$.

4.2.1.2 Site-directed mutagenesis

To generate point mutations at positions AA34 and AA49 of Ken BTB/POZ domain, a site-directed mutagenesis was performed. Specific primers were designed that were complementary to the region 88-156bp of the *ken* ORF and carried two nucleotide substitutions G →A and A →C at positions 100bp and 145bp, respectively (for sequence see table 4.2). These point mutations converted the triplets GAC →AAC and AAG →CAG resulting in exchange 34D →34N and 49K → 49Q known to abolish interaction of the BTB/POZ domain with co-repressors (Melnick *et al.*, 2000; Melnick *et al.*, 2002). Following 7-10 cycles of PCR amplification of pBS-KS(+)ken by *PfuTurbo* (see section 4.2.1.1), the resulting mixture containing the template and the newly synthesised plasmid was treated with *Dpn*I (Stratagen), a restriction endonuclease recognising a 4bp methylated DNA site. *Dpn*I digestion destroyed the parental template, and the mutated plasmid was transformed into bacteria. The resulting clones were analysed and the *ken* ORF carrying the desired mutations was re-cloned into pUAST vector (see section 4.2.1).

4.2.1.3 TOPO-cloning

For TOPO-cloning (TOPO TA Cloning® Kit by Invitrogen) no restriction or ligation is required. The technique is based on a non-template-dependent terminal transferase activity of *Taq* polymerase that adds a single deoxy-adenosine to the 3'-ends of PCR products. The linearised pCR®II-TOPO® vector has single overhanging 3'-deoxy-thymidine residues. This allows PCR product to ligate with the vector, with the reaction catalysed by Topoisomerase I.

When *PfuTurbo* polymerase lacking terminal transferase activity used, 3'-A-overhangs were generated by adding *Taq* polymerase to the PCR product and incubating for 8-10min at 72°C.

To transform bacterial cells, 0.5-5µl of PCR product was mixed with 1µl of pCR®II-TOPO® vector and incubated for 5min at T_{room}. Next, 2µl of this reaction was mixed with One Shop Chemically competent cells (supplied by Invitrogen). Transformation procedure was the same as described above for heat-pulse transformation (see section 4.2.1).

4.2.2 Preparing DNA for subsequent injections into *Drosophila* embryos

The DNA constructs cloned into pUAST vector (see section 4.2.1) and extracted with Qiagen Kit were additionally purified by phenol/chloroform extraction and precipitated with ethanol (salting agent 300mM Na-acetate, pH 5.5). Following centrifugation the resulting pellet was washed with 70% ethanol, vacuum-dried and dissolved in TE buffer at 60$^\text{o}$C for 5min.

12μg of the purified DNA construct was mixed with 4μg "helper DNA" and co-precipitated by ethanol (300mM Na-acetate, pH 5.5). The precipitate was centrifuged, washed twice with 70% ethanol, vacuum-dried and dissolved in 20μl of injection buffer at 60$^\text{o}$C for 5min. DNA concentration was adjusted to 400ng/μl.

Buffers:

TE buffer   10mM Tris-HCl pH 8.0, 1mM EDTA

Injection buffer   0.1mM Na-phosphate buffer pH 6.8, 5mM KCl

4.2.4 DNA isolation from flies

Approximately 50 flies per sample were frozen and ground in a 1.5ml Eppendorf tube, using a plastic Eppendorf pestle, in 400μl of DNA extraction buffer. Additional 400μl of DNA extraction buffer can help to rinse the pestle. Homogenate was incubated at 65$^\text{o}$C for 30min. 120μl of 8M K-acetate was added followed by incubation on ice for 30min. The supernatant resulted after centrifugation at maximal speed (Haeraus microfuge) for 5min was transferred into a fresh tube and precipitated with 50% ethanol (equal volume of 100% ethanol added). Following centrifugation the pellet was washed with 70% ethanol, dried and resuspended in 400μl of TE. RNAs were removed by RNAse treatment (final concentration 2μg/ml) at 37$^\text{o}$C for 30min. DNA fraction was isolated by phenol/chloroform extraction followed by ethanol precipitation. Finally, the DNA was dissolved in 50μl of TE with approximate DNA concentration 1μg/μl.

Buffers:

Extraction buffer   0.1M NaCl, 0.2M sucrose, 0.1M Tris-HCl pH 9.0,
                                             50mM EDTA, 0.5% SDS

TE buffer   10mM Tris-HCl pH 8.0, 1mM EDTA

4.2.5 RNA isolation and Reverse Transcription PCR (RT-PCR)

Total RNA was isolated from larvae, pupae and adult flies with using RNeasy® Mini Kit (Qiagen). 5-8μg of total RNA was used for one reaction of first strand cDNA synthesis performed with oligo(dT)$_{12-18}$ primer and SuperScript™ Choice (Gibco BRL). Total cDNA was diluted 1:10 and used for subsequent PCR reaction with *tbp-1-* and *ken*-specific primers (see table 4.2).

For semi-quantitative RT-PCR, the amount of cDNA produced in different samples was normalised by amplification of *tbp-1* specific band. *tbp-1* is expressed ubiquitously in cells. Therefore, varying the amount of total cDNA taken for *tbp-1* amplification, equal intensity bands can be obtained. The number of PCR cycles is to be established empirically, as too long amplification can give excess of the product and therefore abrogate a difference between the samples. Once normalised, the same amount of cDNA was taken for analytical PCR with primers specific to *ken* (Ken-441-F and Ken-1366-R, see table 4.2). PCR reactions were performed with *Taq* DNA polymerase (Roche) according to the protocol described in the section 4.2.1.

4.2.6 RNA probe labelling for *in situ* hybridisation

For *in situ* hybridisation experiments, anti-sense RNA probes were prepared with using DIG-Labelling Kit (Roche). As a template either plasmids containing corresponding cDNA, or direct PCR products amplified from genomic DNA with T7-containing primers, were used (see table 4.3). The labelling was performed according to Roche Instruction Manual. The labelled probe was mixed with 10μl of 20mg/ml non-specific tRNA (Sigma) with the final volume adjusted up to 200μl with DEPC-treated water. RNA was precipitated by ethanol (salting agent 400mM LiCl) for at least 2h (or o/n) at -80°C. The recipitated RNA was centrifuged at maximal speed (Haeraus microfuge) for 15min, washed twice with 70% ethanol, vacuum-dried and dissolved in 100μl of DEPC-water for 30min at 37°C.

Table 4.3. Scheme of RNA probes preparation.

Probe	Plasmid	Restriction enzyme	Polymerase
ken	pCRII-ken	*Asp*718	T7
socs36A	pOT2A-socs36A	*EcoR*I	SP6

(table 4.3, continue)

Probe	Plasmid	Restriction enzyme	Polymerase
thr	pFLC-1-trh	*Xho*I	T3
vvl	pCRII-vvl	*Hind*III	T7
upd	pBS-KS(+)upd	*Bam*HI	T7
hb			
lacZ	pBS-KS-βgal	*Not*I	T3
mAbdB	Amplified from genomic DNA (see section 4.2.1.1)		T7
cAbdB			

The efficiency of labelling was tested on dot-blot. For that serial dilutions of the probes (1:10, 1:100, 1:1000) and control RNA (1ng/μl, 100pg/μl, 10pg/μl, 1pg/μl) were made. 1μl of the each – diluted controls, non-diluted and diluted probes – were spotted onto a piece of nylon membrane (Amersham). When fully dried, the nucleic acids were cross-linked to the membrane by UV-light for 2min. The membrane was washed in PBS 2x 5min, blocked with PBS supplemented with 10μg/ml BSA and 5% sheep serum for 30min, and hybridised with anti-DIG alkaline phosphatase (AP)-conjugated antibody (1:5000 dilution, Roche) for 30min at T_{room}. The membrane was washed 3x 10 min in PBS and 2x 10min in AP-buffer. Colour reaction was developed in NBT/BCIP solution (20μl of stock solution (Roche) per 1ml AP-buffer) in dark. The intensity of the experimental spots was compared with the control, and the approximate concentration of the labelled probe was estimated (suggested working concentration 1ng/ml).

Buffers:

PBS   130mM NaCl, 7mM Na_2HPO_4, 3mM NaH_2PO_4

AP-buffer   100mM NaCl, 100mM Tris-HCl pH 9.5, 0.1 Tween-20

Important, $MgCl_2$ included in AP-buffer for *in situ* hybridisation effects strong background on nylon membranes and should not be used for dot-blot.

For DEPC-treatment 1ml DEPC per 1l of water was constantly mixed for 1h at 37^oC or o/n at T_{room} and autoclaved.

4.2.7 DNA probe labelling and cold oligonucleotides synthesis for EMSA

For STAT92E probe, single-stranded top and bottom oligonucleotides were designed that contained STAT92E consensus (see table 4.4). For Ken probe synthesis, oligonucleotides contained two consensus sites, either wild type or with a single point mutation, oriented as a palindromic sequence imitating that of STAT92E (see table 4.4). 5pmole of each the top and bottom oligonucleotides were mixed in the final volume 100μl of Restriction Buffer 2 (New England Biolabs), denatured at 95°C for 10min and let cool down to T_{room} to anneal, which gave dsDNA fragments with 3'-overhangs. The calculated concentration of the resulting dsDNA was 5μM. The composition of the labelling reaction (50μl) was as follows:

> 1x Restriction buffer 2
>
> 0.5μM annealed oligonucleotides
>
> 0.4mM each dATP, dTTP and dGTPs
>
> 0.33μM ^{32}P-dCTP (Hartmann Analytik)
>
> 2U Klenow fragment (Boehringenn Mannheim)

The reaction was incubated for 20min at 37°C. As Klenow fragment exhibits 3'→5' exonuclease activity, unlabelled dNTPs were taken in excess, and the reaction allowed to progress no longer than 20min.

Synthesised probe was purified by the Nucleotide Removal Kit (Qiagen) according to the Qiagen Instruction Handbook. When eluted in 100μl, the calculated concentration of the probe was 250nM. Labelling efficiency was measured on Bioscan QC-4000 XER. Generally, 1μl of the probe gave 100000 –700000cpm (counts per minute), while 10000cpm is sufficient for one EMSA reaction.

Synthesis of the cold oligonucleotides was performed similarly, except that the reaction was carried in 100μl volume, the annealed oligonucleotides were added in 10x higher concentration, and ^{32}P-dCTP was replaced with dCTP with the final concentration of each dNTPs 0.5mM. When eluted in 100μl, the calculated concentration was 2.5μM.

Table 4.4. Sequence of oligonucleotides used for STAT92E and Ken probe labelling.

Name of oligonucleotide	Probe	Sequence
STAT-wt-top	*stat*	GGATTTTTCCCGGAAATG
STAT-wt-bottom		GACCATTTCCGGGAAAAA
ken-STAT-18-top	*wt*	GGACCTTTCCGTGAAAGG
ken-STAT-18-bottom		GACCCTTTCACGGAAAGG
ken-STAT-18-1m-top	*m1*	GGACCTTTCCTTGAAAGG
ken-STAT-18-1m-bottom		GACCCTTTCAAGGAAAGG
ken-STAT-18-3m-top	*m3*	GGACCTTTACGTTAAAGG
ken-STAT-18-3m-bottom		GACCCTTTAACGTAAAGG
ken-STAT-18-4m-top	*m4*	GGACCTTACCGTGTAAGG
ken-STAT-18-4m-bottom		GACCCTTACACGGTAAGG
ken-STAT-18-5m-top	*m5*	GGACCTATCCGTGATAGG
ken-STAT-18-5m-bottom		GACCCTATCACGGATAGG
ken-STAT-18-6m-top	*m6*	GGACCATTCCGTGAATGG
ken-STAT-18-6m-bottom		GACCCATTCACGGAATGG
ken-STAT-18-7m-top	*m7*	GGACATTTCCGTGAAATG
ken-STAT-18-7m-bottom		GACCATTTCACGGAAATG

4.3 *Drosophila* cell culture and transfection

4.3.1 Maintaining and storing cells

S2 (Schneider, 1972) and S2R$^+$ cells (Yanagawa *et al.*, 1998) were grown in 75cm^2 flasks (Falcon®) containing 10ml Schneider's *Drosophila* medium (Gibco) supplemented with 10% fetal calf serum (Sigma) and penicillin/streptavidin (0.1mg/ml) at 25°C.

For permanent storage in liquid nitrogen, 8x10^7 cells were centrifuged for 5min at 2000rpm (Kendro) and resuspended in freezing medium (Schneider's *Drosophila* medium, 10% DMSO) to achieve 2x10^7 cells/ml. 0.5ml aliquots in sterile cryovials were rolled in tissue papers and placed in a Dewar flask at T$_{room}$. The flask was tightly closed and placed at –80°C for at least two days to allow the cells to freeze down very slowly. The frozen vials were transferred to liquid nitrogen for long-term storage. For thawing the cells were brought to T$_{room}$ and immediately transferred into a flask with the medium.

4.3.2 Transfections

For EMSA experiments, 2x10^6 S2 or S2R$^+$cells were seeded in 100mm Petri dishes (Falcon®) a day before transfection. Transfections were performed using Effectene

Transfection Kit (Qiagen). For mock-transfections 0.4μg of pUC18-Act-GAL4, 0.6μg of empty pUAST vector and 1ng of pUAST-luc were diluted in an appropriate volume of transfection buffer (Qiagen). To express GFPKen the DNA composition was 0.4μg of pUC18-Act-GAL4, 0.2μg of pUAST-GFPken, 0.4μg of empty pUAST vector and 1ng of pUAST-luc. Transfections were carried out according to the Qiagen Handbook. Following 72h of growing, the cells were lysed as described in section 4.3.3.

To co-express STAT92E and STAT92E-GFP for subsequent co-immunoprecipitation assay, the cells were seeded as described above and transfected with 0.4μg of pUC18-Act-GAL4, 0.2μg of pUAST-stat92E, 0.2μg of pUAST-stat92E-GFP, 0.2μg of pUAST-hop^{Tuml} and 1ng of pUAST-luc.

For luciferase reporter assay, $1x10^4$ S2R+ cells were seeded in 96-well plates (Costar®) a day before transfection. For mock transfection DNA composition was 20ng of 2x*Draf*-STATwt-luc (or 2x*Draf*-STATmut-luc), 10ng of pUC18-Act-GAL4, 8ng of pUP-RL and 30ng of empty pUAST vector. To test the effect of STAT92E-GFP, Hop^{Tuml}, Ken, GFPKenΔZnF and KenΔPOZ (alone or in combinations), 10ng of pUAST in the described scheme was substituted for equal amount of each of the corresponding UAS-constructs.

4.3.3 Preparing crude cell lysates

For EMSA, cells were lysed by freezing/thawing procedure 72h after transfection. The cells were washed with 5ml rinse buffer, scraped in 1ml rinse buffer and centrifuged for 2min at 2000rpm (Haeraus microfuge). The cells were resuspended, washed in rinse buffer and centrifuged again. The pellet was then resuspended in 150μl resuspention buffer and subjected to three cycles of fast freezing in liquid nitrogen and thawing (preferably in hands). Cellular debris was removed by centrifugation at maximal speed for 15min at 4°C. The supernantant was transferred into a fresh tube, estimated for protein concentration and luciferase activity (see section 4.3.4), aliquoted when necessary and stored at −80°C. Protein concentration measurement was performed by modified Lowry method with using D$_c$ Protein Assay Kit (Bio-Rad). Generally, transfection in 100mm dishes yielded 5-10μg/μl of total protein.

For co-immunoprecipitation experiments, the crude lysates were obtained as described above except for the cell pellet derived from three 100mm dishes was resuspended in 400μl of RIPA buffer. After protein and luciferase activity measurement the lysates were immediately used in co-immunoprecipitation assay.

Alternatively, nuclear extracts were obtained. In this case the scraped, washed and centrifuged cells were rapidly resuspended in hypotonic buffer in a volume equal to 5 pellet volumes and immediately centrifuged for 5min at 3000rpm (Haeraus microfuge) at 4°C. The resulting pellet was resuspended in 3 volumes of hypotonic buffer and allowed to swell on ice for about 10min (cells should swell at least twice). This procedure should be monitored under a microscope. The nuclei were centrifuged for 15min at 4000rpm at 4°C, resuspended in 1 volume of RIPA buffer and lysed by freezing/thawing as described above.

For luciferase reporter assay, cells were lysed in the same 96-well plates where being grown. 50μl of passive lysis buffer (supplied by Promega) was added to each well and incubated for 15min. The resulting lysates were directly used for luciferase activity assay without protein concentration measurement.

Buffers:

Rinse buffer	150mM NaCl, 40mM Tris-HCl pH 7.4, 1mM EGTA
Resuspension buffer	40mM HEPES pH 7.9, 400mM KCl, 1mM DTT, 0.1mM PMSF, 2.5mM vanadate, 10% glycerol
RIPA buffer	50mM Tris-HCl pH 7.4, 50mM NaCl, 1mM DTT, 0.1mM PMSF, 2.5mM vanadate, 0.1% NP-40, 10% glycerol, protease inhibitors (Complete EDTA-free, Roche)
Hypotonic buffer	10mM HEPES pH 7.9, 1.5mM $MgCl_2$, 10mM KCl, 0.1mM PMSF, 1mM DTT, 2.5mM vanadate, protease inhibitors

4.3.4 Luciferase assay

Firefly and *Renilla* luciferase activity was measured by Dual-Luciferase® Reporter Assay (Promega) on Wallac Victor™ Light 1420 Luminescence counter (Perkin Elmer).

4.3.4.1 Firefly luciferase activity measurement

The relative tranfection efficiency of the cells prepared for EMSA or Co-IP analysis was estimated by firefly luciferase activity. The procedure was done according to the instructions suggested by Promega. Measurements were performed in non-transparent 96-well reading plates (Nunclon™ Δ Surface). 25μl of LAR-II (luciferase assay reagent, Promega) was injected into each well containing 5-10μl of the lysate and measured for 10sec, with the delay between injection and measurement lasting 2sec. Readouts of mock and experimental samples were compared.

4.3.4.2 Dual luciferase assay

Firefly luciferase activity reflecting 2x*Draf*-STATwt-luc reporter activation and *Renilla* activity indicating transfection efficiency were analysed as suggested by the Promega Technical Manual. 20μl of each sample was used for measuring. The scheme of the assay was as follows: 25μl of LAR II injected – 10sec delay – 10sec measurement – 25μl Stop&Glo® injected – 10sec delay – 10sec measurement. The relative reporter activity was estimated as ratio between the firefly luciferase readout to that of *Renilla* luciferase. Reporter activation values in experimental samples were normalised to mock transfected cells.

4.4 Protein biochemistry

4.4.1 GST-Ken purification

To tag with GST, Ken DBD was cloned into pGEX-4T-3 vector (see section 4.2.1). Expression in bacteria was induced with IPTG (see section 4.1.2).

All procedures were done on ice. Bacterial cell pellet was thawed and resuspended in buffer-1 (20ml of the buffer per 1l culture volume), with 0.1-1.0mg/ml lysozyme. The cells were rotated for 30min at 4^oC and then sonicated in a tip sonicator (Branson Sonifier 250) 2x 30sec with amplitude 15-25microns. The lysed cells were centrifuged at 15000rpm (Sorvall RC-5B, SS-34 rotor) for 30min at 4^oC. Meanwhile, Glutathione Sepharose 4B beads (Amersham) were washed twice in 20 bed-volumes of buffer-1 (500μl beads give about 250μl bed-volume and have a capacity to bind protein from 15ml of supernatant). The glutathione beads were added to the supernatant and rotated 1-2h at 4^oC to allow binding. The beads were centrifuged at

minimal speed for 2min, washed in buffer-1 5x 5min and then in buffer-2 5x 5min. GST-kenDBD was eluted in 2 bed-volumes of elution buffer by rotating for 30-24min at T_{room}. The beads were centrifuged, the eluted protein was aliquoted and stored at -80^oC.

After each step 5-10μl samples were kept and later analysed by SDS-PAGE (see section 4.4.5). The concentration of the eluted protein was measured by Lowry method using D_c Protein Assay Kit (Bio-Rad), when the elution fraction contained only the desired protein. When non-specific proteins were co-eluted, GST-KenDBD (5 and 10μl) was loaded onto a gel in which 10, 5, 1, 1 and 0.5μg samples of BSA were loaded. The proteins were run by 10% SDS-PAGE (see section 4.4.5) and images were captured with Fujifilm Luminescent Image Analyser LAS-1000 CH. GST-KenDBD concentration was estimated based on a graph showing dependence of BSA concentration on the bands intensity.

Buffers:

Buffer-1	HEMG (0.1% NP-40)
Buffer-2	HEMG (0.01% No-40);
Elution buffer	HEMG (0.01% NP-40), 15mM reduced glutathion
HEMG	25mM HEPES-KOH pH 7.6, 0.1mM EGTA, 12.5mM $MgCl_2$, 500mM NaCl, 0.1% NP-40, 10% glycerol, protease inhibitors (Complete EDTA-free, Roche)

4.4.2 His-Ken purification

The full-length Ken was cloned into pRSET-C vector to tag with oligo-His residues (see section 4.2.1). Expression in bacteria was induced with IPTG (see section 4.1.2).

All procedures were done on ice. Bacterial cell pellet was thawed and resuspended in 10ml lysis buffer per 1l culture volume, with lysozyme added in working concentration 0.1-1.0mg/ml. The cells were rotated for 30min at 4^oC and then sonicated in a tip sonicator (Branson Sonifier 250) 2x 30sec with amplitude 15-25microns. The lysed cells were centrifuged at 15000rpm (Sorvall RC-5B, SS-34 rotor) for 30min at 4^oC. Meanwhile, Ni-NTA-agarose beads (Qiagen) were washed once in distilled water and twice in lysis buffer in a volume equal 3 volumes of the

beads (1ml beads has a capacity to bind 5-10mg protein that corresponds to approximately 100ml of cell culture) and applied into a column. The column loaded with the supernatant was washed 4 times with 6 column volumes of lysis buffer and then with 6 column volumes of washing buffer till the A_{280} of the flow-through remained constant after continuing washing (<0.5). The His-Ken protein was eluted with 6 volumes of elution buffer. Two elution fractions were collected and concentrated, when necessary, in Vivaspin Concentrator (membrane selectivity 5000 MW, capacity 20ml) according to the manufactory instructions (VivaScience). Glycerol was added to the eluted protein to a final concentration 10%. The protein was aliquoted and stored at -80°C.

After each step 5-10μl samples were kept and later analysed by SDS-PAGE (see section 4.4.5). The concentration of the eluted protein was measured as described above.

Buffers:

Lysis buffer	50mM NaH_2PO_4, 300mM NaCl, 10mM imidazole, 0.1% Triton X-100, protease inhibitors (Complete EDTA-free, Roche)
Washing buffer	50mM NaH_2PO_4, 300mM NaCl, 20mM imidazole, 0.1% Triton X-100, protease inhibitors
Elution buffer	50mM NaH_2PO_4, 300mM NaCl, 110mM imidazole, 0.1% Triton X-100, protease inhibitors

Concentration of imidazol in elution buffer is critical and depends on a protein. Therefore it is suggested to titrate 50-250mM imidazole in a test experiment (elution efficiency can be monitored by A_{280} of elution fraction).

4.4.3 *In vitro* translation

Coupled *in vitro* transcription and translation with simultaneous radioactive labelling was performed in reticulocyte lysate using TNT® Quick System (Promega). The procedure was done according to the Promega Instruction Manual. 1μg of intact pcDNA3.1(+)ken plasmid was used in one reaction, containing protein inhibitors (Complete EDTA-free, Roche). TNT® PCR Enhancer (Promega) appeared to have facilitated *in vitro* translation. Labelling was achieved by incorporation of [^{35}S]-methionine (1000Ci/mmol, Amersham) into Ken molecule containing 11 methionine

residues. The reaction was incubated for 90min at 30°C. The results of translation were analysed by SGS-PAGE (see section 4.4.5) followed by radiography (see section 4.4.4). If not used immediately the product was stored at –80°C.

4.4.4 Co-immunoprecipitation

For STAT92E/STAT92E-GFP co-immunoprecipitation, the corresponding proteins were expressed in S2R$^+$ cells (see section 4.3.3). 400μl of the crude cell lysate or, alternatively, 50μl of the nuclear extract diluted with RIPA buffer up to 400μl, were mixed with 2μl of anti-GFP antibody (in concentration 10x higher than for Western-blotting) and rocked for 3h at 4°C. 50μl of 50% Protein-A agarose beads (Oncogene) were washed in RIPA buffer 3x 5 min at 4°C, added to the lysates and incubated on a rocker o/n at 4°C. The beads were washed in RIPA buffer 5x 20min, centrifuged, mixed with 15μl of 2x Laemmli buffer and boiled for 5min. The eluted proteins were resolved by SDS-PAGE and analysed by Western-blotting (see section 4.4.5).

For Ken/STAT92E-GFP co-immunoprecipitation, *in vitro* translated ^{35}S-labelled Ken (see section 4.4.3) and STAT92E-GFP expressed in cell culture (see section 4.3.3) were used. The reticulocyte lysate containing *in vitro* translated Ken was pre-incubated with Protein-A agarose beads (50μl of the lysate mixed with 50μl beads) for 1h at 4°C. Then 10μl of the pre-cleared lysate was mixed with 400μl of S2R$^+$ cell lysate and incubated for 3h at 4°C. Incubations with the antibody and the beads as well as washing steps were essentially the same as described above. After SDS-PAGE the gel was stained with Coumassi solution for 10min, washed in destaining solution and incubated with Amplify (Amersham) for 1h. The gel was transferred onto a 3mm filter paper, dried and covered by an X-ray film (X-OMAT™ AR, Kodak). The exposure was performed in a cassette o/n at –80°C.

Buffers:

RIPA buffer	50mM Tris-HCl pH 7.4, 50mM NaCl, 1mM DTT, 0.1mM PMSF, 2.5mM vanadate, 0.1% NP-40, 10% glycerol, protease inhibitors (Complete EDTA-free, Roche)

NaCl concentration may vary from 50-200mM (usually titrated) for different proteins or, alternatively, salt composition can be 60mM NaCl, 3mM MgCl$_2$ and 1mM CaCl$_2$. As a detergent NP-40, Triton X-100, Tween-20 or their combinations can be used. Also, after-precipitation washes can be done in higher salt RIPA buffer (up to 300mM) and RIPA buffer with increased detergent concentration (up to 0.4%).

4.4.5 SDS-PAGE (SDS-polyacrylamide gel-electrophoresis) and Western-blotting

SGS-PAG was composed of 10% polyacrylamide separating gel and 5% polyacrylamide stacking gel. Electrophoresis was run in 1x SDS-running buffer at 35mA (or 50mA when two gels running in same chamber) constant current. Pre-stained SDS-PAGE Standards (New England Biolabs or Bio-Rad) were used as molecular weight control. Following electrophoresis the gel was fixed and stained with Coumassi solution for 15min, clarified in destaining solution and photographed on Fujifilm Luminescent Image Analyser LAS-1000 CH.

For Western-blotting, unstained gel was rinsed with transfer buffer immediately after SDS-PAGE and put onto a piece of nitrocellulose membrane (Electrophoresis Grade, 0.2μm pore size, Sigma) moistened with transfer buffer. The protein transfer apparatus was assembled so that the membrane was oriented to the anode, while the gel faced the cathode. The transfer was carried out at 40V (10V/cm) for 2h at 4°C.

The membrane was rinsed twice in distilled water and blocked in PBT with 10mg/ml BSA for 20min at T_{room}. Incubation with anti-GFP antibody (Abcam) in 1:5000 dilution was done o/n at 4°C. Unbound antibody was removed by washing in PBT 5x 10min. The membrane was incubated with secondary horseradish peroxidase (HRP)-conjugated anti-rabbit antibody (1:10000 dilution, Sigma) in PBT with BSA for 1-2h at $T_{room.}$ Washing steps were the same as after primary antibody incubation. Enzymatic reaction was developed with using SuperSignal® West Pico Chemiluminescent Substrate (Pierce). The membrane was analysed on Fujifilm Luminescent Image Analyser LAS-1000 CH.

If to be blotted again with anti-STAT92E antibody (dilution 1:1000), the membrane was washed for 5min in 1M glycin (pH 2.0), which removed the antibody complexes. After several intensive washes the membrane was checked with using SuperSignal® West Pico Chemiluminescent Substrate (Pierce) for the presence of antibody traces. The clean membrane was used in the next round of blotting.

Solutions:

4x SDS-gel buffer   1.5M Tris-base, 0.4% SDS, pH 8.8

5x SDS-running buffer   0.125M Tris-base, 0.95M glycin, 0.5% SDS

Destaining solution	10% ethanol, 5% acetic acid
Transfer buffer	0.25M Tris, 0.2M glycin, 10% methanol
PBT	130mM NaCl, 7mM Na_2HPO_4, 3mM NaH_2PO_4, 0.1% Triton X-100

4.5 Protein/DNA interaction analysis

4.5.1 SELEX

For SELEX experiments (Tuerk & Gold, 1990), GST-KenDBD was purified from *E.coli* (see section 4.4.1). An oligonucleotide library (Sellib-F) was designed that contained a 20bp random sequence flanked by primers of known sequence (see table 4.2). To produce double-stranded library, Sellib-F was annealed with Sel-R primer and subjected to one cycle of PCR:

1x buffer with Mg^{2+} (supplied by manufactory)

5µM Sellib-F

5µM Sel-R

200µM dNTPs

5U *Taq* polymerase.

The cycling parameters were 1min at 94°C, 1min at 50°C, 1min at 72°C.

The double-stranded library was resolved on 4% agarose gel (MetaPhor® agarose BioWhittaker Molecular Applications), where also Sellib-F and Sel-R were loaded as a size control. The appropriate band was excised and purified with Gel Extraction Kit (Qiagen). The purified DNA was eluted in 50µl volume.

For binding reaction the protein is to be present in 10-fold excess of DNA. Therefore, 1nmole of Sellib was used for selection by 10nmole of GST-KenDBD.

The protein was allowed to bind to 10µl of Glutathion Sepharose beads in 50µl buffer A for 10min at T_{room}. The beads were washed in 300µl of buffer A 3x 1 min and then in 300µl of buffer B 3x 1min. 1nmole of Sellib was mixed with the beads in buffer B in a final volume 200µl and incubated on a rocker for 20min at T_{room}. The complexes

were washed in 300μl of buffer B 3x 1min and centrifuged at 2000rpm (Haeraus microfuge). 60μl of distilled water was added to the beads, and the bound DNA was recovered by boiling for 3min at 95°C. 10μl of the recovered DNA was used as a template in a PCR reaction described in the section 4.2.1.1.

The PCR product was run by electrophoresis and purified as described above. The DNA was eluted as concentrated as possible. One forth of the eluted fraction was used for the next round of selection as described above.

After 10th round of selection 100-200ng of the final PCR product was cloned into pCR®II-TOPO® vector. The transformed *E.coli* cells were plated onto X-Gal/IPTG LB-agar plates. Approximately 50 white colonies were selected. The extracted plasmids were digested with *Pvu*II and checked for the presence of the insertion. The positive plasmids were sequenced and analysed by using Gibbs Sampler software and manual techniques.

Buffers:

Buffer A	PBS, 1mg/ml BSA, 0.1% Triton X-100, 1mM PMSF, 2mM DTT, protease inhibitors (Complete EDTA-free, Roche)
Buffer B	20mM HEPES pH 7.9, 40mM KCl, 50μM ZnSO$_4$, 1.4mM MgCl$_2$, 0.1mM EGTA, 1mg/ml BSA, 2μg/ml poly(dI)-poly(dC) (Amersham), 0.5mM DTT, 1mM PMSF, 5% glycerol, protease inhibitors

To prepare X-Gal/IPTG LB-agar plate 40μl of 100mM IPTG and 40μl of 40mg/ml X-gal were spread on LB-agar plate and incubated at 37°C till dry.

4.5.2 Electroforetic Mobility Shift Assay (EMSA)

EMSA was performed either with using the bacteria-expressed GST-KenDBD (see section 4.4.1) or the full-length Ken derived from S2 cell lysates (see section 4.3.3).

Composition of binding reaction is shown in the table 4.5.

Table 4.5 Composition of binding reaction for EMSA.

Component	Concentration	Specified for GST-KenDBD	Specified for S2R+ crude cell lysates
HEPES, pH 7.9	20mM		
MgCl$_2$	1.4mM		
KCl	40mM		
EGTA	0.1mM		
poly(dI-dC)-poly(dI-dC)		5µg/ml	50µg/ml
DTT	0.5mM		
PMSF	1mM		
Glycerol	5%		
BSA		100µg/ml	-
protein		5-100nM	15µg total protein fraction
labelled DNA	8.3nM		
unlabelled DNA (when used)	83, 166 or		
anti-GFP antibody (when used)	830nM		1:3 000 dilution

Salt concentration is to be chosen empirically for each protein. When a purified protein used, BSA is required in the reaction. The protein/DNA ratio in EMSA may vary from 0.5 for strong interactions to 300 for weak those. Since it was not possible to precisely estimate the concentration of GFPKen in the S2R$^+$ cell lysates,15µg of total protein was taken for one reaction.

For cold oligo competition assays, unlabelled oligonucleotides were included in the binding mixture in a 10x, 50x or 100x excess (for concentrations see table 4.5). Super-shift was achieved by adding anti-GFP antibody (Abcam) directly to the binding reaction (for dilution see table 4.5).

All components were mixed in 30µl volume, and the binding reaction was carried out for 30 min at T_{room}. The DNA/protein complexes were separated from naked DNA by electrophoresis in non-denaturing 4% polyacrylamide gel in 0.5x TB buffer for approximately 45min at 20mA constant current (gel running was stopped when brom-phenol-blue loading dye reached about 2/3 of the gel). The gel was transferred onto a 3mm filter paper, dried and exposed to an X-ray film (X-OMAT™ AR, Kodak). The exposure was performed in a cassette at –80°C for 3-72h depending on the strength of the signal.

Buffers:

0.5x TB   44.5mM Tris-base, 44.5mM boric acid, pH 9.0

4.6 Fly work and genetics

4.6.1 Fly stocks

Fly stocks used were: wild type (Ore R), *GMR-updΔ3'* (Bach *et al.*, 2003), *Df(2R)Chi^{g320}* (Morcillo *et al.*, 1997)*, GMR-yan* (Rebay & Rubin, 1995), *GMR-rhoA* (Häcker & Perrimon, 1998), *ken^1* (Castrillon *et al.*, 1993)*, ken^{02970}* and *ken^{K11035}* (Lukacsovich *et al.*, 1999), and recombinant *(y,w);p[neoR, FRT]42D,ken^1/CyO*; *w;p[neoR,FRT]42D,ken^{K11035}/SM5a-TM6a, stat92E^{06342}* (Hou *et al.*, 1996), *stat92E^{HJ}* (Yan *et al.*, 1996a), *smr^{G0361}* (Peter *et al.*, 2002), *sgs3-GAL4* (Cherbas *et al.*, 2003), *daughterless-GAL4* (Wodarz *et al.*, 1995), *Mj21a-GAL4, domeless^{468}/FM7* and *domeless^{367}/ F M 7* (Brown *et al.*, 2001); the recombinant *y,w;p[w$^+$,Act>y$^+$>GAL4],p[w$^+$,UAS-EGFP],ff^{P1}* (Zeidler *et al.*, 1999a), *y,w;p[neoR,FRT]42D,p[w$^+$,Ubq-GFP]*, *y,w;p[w$^+$,UAS-GFP]* (M.Zeidler, unpublished) and *Df(1)os^{1A}* (Eberl *et al.*, 1992), *GMR-GAL4, nos-GAL4.NGT40* (Tracey *et al.*, 2000), *mat-α-tub-GAL4* (obtained from D. St Johnston).

4.6.2 Fly care and feeding

The care and feeding of *Drosophila melanogaster* was performed according to Ashburner (Ashburner, 1989). Unless otherwise specified, all flies, larvae and embryos were grown at 25°C.

4.6.3 Genetics

For genetic interaction assay experimental and control crosses were set up in parallel on the same batch of food. For *stat92E^{HJ}* interactions any deviation from a wild type venation pattern (both extra and missing tissue) was scored as phenotypic. For *dome^{367}* interactions in both control and experimental embryos weak and strong phenotype were distinguished.

4.6.4 Ectopic expression with using Gal4/UAS system

This system is based on using the yeast transcription factor Gal4 and its recognition site UAS (upstream activating sequence) (Brand & Perrimon, 1993). A driver line carries either a tissue specific or inducible enhancer sequence upstream of GAL4 gene, while an effector line is composed of an upstream UAS promoter and

downstream gene of interest. When crossed to the driver the target transgene is then expressed in the same tissue- and stage-specific pattern as the Gal4 driver. In this study the drivers *daughterless-GAL4, nos-GAL4.NGT40* and *mat-α-tub-GAL4* were used for embryonic expression and the *sgs-GAL4* driver for expression in the salivary gland. The drivers *GMR-GAL4* and *Mj21a-GAL4* induced expression in imaginal discs resulting in adult phenotypes.

4.6.5 Induction of LOF clones

This approach utilises yeast flipase recombinase FLP and its DNA recognition sites FRT (flipase recognition target). FRT sites are usually placed in the proximal to the centromere position. FLP is frequently cloned under the heat shock promoter, though tissue specific regulation can also be used. Combination of FLP and FRT sources within same cells results in interchromosomal exchange on the FRT sites between homological chromosomes thus producing homozygous mutant clones within the heterozygous surroundings. When heat shock-inducible FLP source is used, the stage of heat-shock is essential for the size of generated clones, while the duration (30min-2h) and the temperature (37-38°C) influence the clone frequency. In this study *y,w; p[w$^+$,hs-FLP]; p[neoR,FRT]42D, p[w$^+$,Ubq-EGFP]/CyO* flies were crossed to *y,w; p[neoR,FRT]42D, ken^1/CyO* and to *y,w; p[neoR,FRT]42D, ken^{K11035}/SM5a-TM6a*. Clones were induced at 48-72h of development by heat shock for 1h at 37°C. Adult eye clones were visualised by the absence of *w$^+$* marker.

4.6.6 Induction of GOF clones

This approach combines both Gal4/UAS and FLP/FRT cassette. In this system GAL4 gene and its promoter are separated by a marker gene flanked by FRT sites. Induced FLP excises the marker thus enabling Gal4 expression and allowing identification of clones by the absence of marker expression. In this study *w; p[Act>y$^+$>GAL4,w$^+$]; p[w$^+$,UAS-GFP],* line was crossed to *w; p[w$^+$,UAS-ken]* in the presence of *w; p[hs-FLP]*. First instar larvae (24-30hr) were heated for 1h at 38°C and grown up to third instar.

4.6.7 P-element mediated transgenosis

Transgenic flies were obtained by following the previously described protocol (Rubin & Spradling, 1982). DNA of each of the following constructs: pUAST-ken, pUAST-

kenGFP, pUAST-GFPken, pUAST-GFPkenΔZnF, pUAST-ken^{D34N,K49Q} mixed with the "helper" plasmid (for preparing DNA see section 4.2.2) were injected into approximately 300 w^- (white eyed) embryos at the appropriate pole cell stage. Each hatching fly was crossed to the original w^- strain. The transformants selected by coloured eyes (ranging from light yellow to dark red depending on the position of the insertion) were tested for carrying double instertions by additional crossing to w^- flies. Stable stocks were established by introducing balancer chromosomes. At least two, but preferably more, independent transgenic lines were established and analysed for each construct. The transgenic lines generated in this study are listed in the table 4.6.

Table 4.6. Transgenic lines generated.

Genotype	Phenotype
w; p[w$^+$, UAS-ken]1/TM3	strong
w; p[w$^+$, UAS-ken]2A/FM7	strong
w; p[w$^+$, UAS-kenGFP]1.1.2/CyO	strong
w; p[w$^+$, UAS-kenGFP]5.3.3/TM3	moderate
w; p[w$^+$, UAS-kenGFP]6.2.2/CyO	strong
w; p[w$^+$, UAS-kenGFP]7.1.3/TM3	moderate
w; p[w$^+$, UAS-GFPken]1D/TM3	weak
w; p[w$^+$, UAS-GFPken]2/FM7	strong
w; p[w$^+$, UAS-GFPkenΔZnF]16/TM3	no
w; p[w$^+$, UAS-GFPkenΔZnF]23.2/CyO	no
w; p[w$^+$, UAS-GFPkenΔZnF]30/FM7	no
w; p[w$^+$, UAS-ken^{D34N,K49Q}]2.0.1/CyO	no
w; p[w$^+$, UAS-ken^{D34N,K49Q}]2.1.1/CyO	no

4.7 Histology

4.7.1 Embryos manipulations

To collect embryos, flies were transferred to a cage closed by an apple juice agar plate spread with baker's yeast on it. The flies were allowed to lay eggs at 25°C, with a time window varying from 0-2h to 0-20h depending on experiment.

4.7.1.1 Fixing embryos

The embryos were brushed carefully from the apple juice agar plates with a paintbrush, washed to get rid of the yeast, transferred to a fine sieve and dechorionated in 50% bleach (Clorox) for 3min. The dechorionated embryos were rinsed several times with water, transferred into scintillation vials filled with 8ml fixative (4% ultra-pure formaldehyde in PBS) and 8ml heptane, and fixed for 20min with vigorous shaking. Afterwards, the fixative (lower phase) was removed and replaced with 8ml methanol. Intensive shaking in heptane/methanol for 60sec removes the vitelline membrane and the devitellinated embryos sink to the bottom, while the membranes and the embryos with the intact vitelline membrane stay in interphase. The devitellinated embryos were collected into Eppendorf tubes, washed twice with methanol and kept at –20°C for long-term storage.

Buffers:

PBS   130mM NaCl, 7mM Na_2HPO_4, 3mM NaH_2PO_4

4.7.1.2 Whole-mount antibody staining

Embryos stored in methanol (see section 4.7.1.1) were re-hydrated in methanol/PBS dilution series (4:1, 3:2, 2:3, 1:4). Unless otherwise specified, all procedures were performed at T_{room}. The fully re-hydrated embryos were washed in PBT 3x 10min, blocked in PBT with 5% sheep serum and, finally, incubated with primary antibody o/n at 4°C (for primary antibody see table 4.7). The embryos were washed in PBT 3x 5min, then in high-salt concentration PBT for 20min and in PBT again 3x 20min. Following incubation with preabsorbed biotin-conjugated secondary antibody (1:500 dilution, Vectastain® ABC Elite Kit) in PBT with 5% serum for 2h at T_{room} washing steps were the same as described for those after the primary antibody.

For detection the embryos were incubated with a complex of avidin/biotinylated horseradish peroxidase (HRP) (preformed for 30min) for 30-90min (Vectastain®). Then, the embryos were washed thoroughly 4x 20minutes at T_{room} or o/n at 4°C. For colour reaction 30µl DAB (10mg/ml stock) and 10µl H_2O_2 (0,37% stock) were added to the embryos in 0.5ml PBT. Colouring can be achieved very fast and should be monitored under a scope. To stop the reaction the embryos were washed several times in PBT. Finally, the embryos were dehydrated in ethanol dilution series (10%, 30%,

50%, 70%, 90%), washed twice in 100% ethanol, clarified in 0.5ml methyl salicilate and mounted in Canada balsam. Alternatively, mounting can be done in a mixture of methyl salicilate and Canada balsam (1:1). In this case the medium is not as viscous as the balsam, but slides may dry fast. Embryos were imaged with Zeiss Axioskop2 MOT microscope.

Buffers:

PBS	130mM NaCl, 7mM Na_2HPO_4, 3mM NaH_2PO_4
PBT	PBS with 0.1% Triton X-100 for nuclear proteins or 0.1% Tween-20 for cytoplasmic proteins
High-salt PBT	530mM NaCl in PBT

Table 4.7. Primary antibody used for staining embryos.

Antibody	Host animal	Dilution	Reference
Kr	rabbit, polyclonal	1:200	
Hb	polyclonal	1:5000	E.Entchev
Kni	rabbit, polyclonal	1:200	
Eve	mouse, monoclonal	1:50	
β-gal	rabbit, polyclonal	1: 5000	Cappel

4.7.1.3 Whole-mount *in situ* hybridisation

Embryos stored in methanol (see section 4.7.1.1) were re-hydrated as described in the section 4.7.1.2, washed in PBT 3x 5min and additionally fixed in 4% formaldehyde for 20min. After fixation washes were 3x 10min. Next, the embryos were treated with proteinase K (working concentration 50μg/ml in PBT) for 7min (suggested 4-10min). Digestion was stopped by 2mg/ml glycin 2x 30sec, followed by 2x 5min washes in PBT. The embryos were fixed once more for 7min (suggested 5-10min, longer fixation time may increase background), extensively washed in PBT 5x 10min, then 10min in a mixture PBT/hybridisation buffer (1:1) and 10min in hybridisation buffer. Afterwards, the embryos were pre-hybridised in a fresh aliquot of hybridisation buffer for 1-3h (suggested from 1h up to 5 days) at 62°C.

The embryos were hybridised with the probe in a minimal volume of hybridisation solution (around 50μl) o/n at 62°C. Suggested probe concentration is 1ng/ml. However, even at much lower concentrations it may give a very good signal.

Post-hybridisation washes were 20min in hybridisation solution and 20min in PBT/hybridisation solution (1:1) at 62°C. Afterwards, the embryos were washed 5x 20min at T_{room}. In order to prevent embryos from cracking the replacing solutions should be of the same temperature as the embryos.

The washed embryos were incubated with anti-DIG AP-conjugated antibody (1:2000 dilution, Roche) in PBT with 5% serum for 1h at T_{room}, washed in PBT 4x 20min and in AP-buffer 2x 10min. Colour reaction was developed in NBT/BCIP solution (20μl of stock solution (Roche) in 1ml AP-buffer) in dark. Colouring can take from 15min up to 24h. At 25°C the reaction proceeds faster than at 4°C.

The stained embryos were washed in PBT 3x 10min, dehydrated in ethanol dilution series 10%, 30%, 50% and 70%, washed in a fresh aliquot and left in 70% ethanol o/n. After extended incubation in 70% ethanol, which decreases colour fading during subsequent clarifying and mounting, the embryos were dehydrated in 90% and 100% ethanol, clarified in methyl salicilate and mounted in Canada balsam (or 1:1 mixture of methyl salicilate/Canada balsam). As methyl salicilate may wash out the coloured precipitates resulted from AP-induced chemical reaction, alternatively, dehydrated embryos can be dropped onto a slide, slightly dried and covered by a drop of the mixture benzyl benzoate/benzyl alcohol (2:1). This method does not change the product colour, but may make embryonic morphology hardly visible. The embryos were photographed with Zeiss Axioskop2 MOT microscope.

Buffers (all prepared on DEPC-treated water):

PBS   130mM NaCl, 7mM Na_2HPO_4, 3mM NaH_2PO_4

PBT   PBS with 0.1% Tween-20

Hybridisation buffer   50% deionised formamide

                                      5x SSC (2.5ml 20x stock in 10ml hybridisation buffer)

                                      100μg/ml tRNA

                                      50μg/ml heparin

100μg/ml salmon testis DNA

0.1% Tween-20

pH adjusted to 6.5-8 by 1 M citric acid

As pH can change signal/noise ratio, new probes are suggested to try at different pH.

AP-buffer   100mM NaCl, 50mM MgCl$_2$, 100mM Tris-HCl pH 9.5, 0.1% Tween-20

AP-buffer should be prepared freshly or at least contain no precipitate.

For DEPC-treatment 1ml DEPC per 1l water was stirred constantly for 1h at 37°C or o/n at T$_{room}$ and autoclaved.

4.7.1.4 X-gal staining

Embryos were dechorionated and fixed as described above (see section 4.7.1.1), but were not devitellinised. The fixative was removed and replaced with water to rinse the embryos. The water and, then, heptane were removed, so that the embryos stuck to the walls of the vial. The embryos were dehydrated in 10ml PBT for 5min, transferred into an Eppendorf tube and washed, first, in a fresh aliquot of PBT and, then, in X-gal staining solution. Finally, the embryos were stained with 0.2% X-gal at 37°C. The colour reaction takes from 15min to several hours. For devitellinisation the staining solution was replaced with heptane, followed by adding equal volume of methanol and vigorous shaking for 1min. The devitellinised embryos were collected, washed with methanol, mounted in Canada balsam and analysed under Zeiss Axioskop2 MOT microscope.

Solutions:

PBS   130mM NaCl, 7mM Na$_2$HPO$_4$, 3mM NaH$_2$PO$_4$

PBT   PBS with 0.1% Triton X-100

X-gal staining solution   10mM Na-phosphate buffer pH 7.2

                                 150mM NaCl

                                 1mM MgCl$_2$

                                 3mM K$_4$[FeII(CN)$_6$]

                                 3mM K$_3$[FeIII(CN)$_6$]

X-gal staining solution should be stored at T$_{room}$ in dark.

Na-phosphate buffer	0.1M Na-phosphate pH 7.2 (72 parts of 0.2M Na$_2$HPO$_4$, 28 parts 0.2M NaH$_2$PO$_4$, 100 parts of water)
X-gal stock	10% X-gal in DMSO, stored at -20°C

4.7.1.5 Embryonic cuticle preparation

Embryos were brushed carefully from the apple juice agar plates with a paintbrush, washed to get rid of the yeast, transferred to a fine sieve and dechorionated in 50% bleach (Clorox) for 3min. The dechorionated embryos were rinsed several times with water, transferred into scintillation vials filled with 8ml heptane and 8ml methanol. After intensive shaking in heptane/methanol during 60sec the embryos than sank to the bottom were collected into Eppendorf tubes and washed twice with methanol and twice with PBT. The embryos were transferred onto a slide with as little liquid as possible (extra liquid can be sucked off with a pipette), mounted in Hoyer's medium and incubated at 60°C o/n (at least 1h). The slides were analysed under Zeiss Axioskop2 MOT microscope.

When cuticles of hatched larvae were to be analysed, the larvae were collected, rinsed with PBT and directly mounted in Hoyer's medium.

Solutions:

PBS	130mM NaCl, 7mM Na$_2$HPO$_4$, 3mM NaH$_2$PO$_4$
PBT	PBS with 0.1% Ttiton X-100

To prepare Hoyer's medium 30g of gum arabic was dissolved in 50ml water on a magnetic stirrer o/n (heating to 60°C helps). 200g chloral hydrate was added in small batches. After the chloral hydrate dissolved, 20g glycerol was added. The liquid was centrifuged for 30min, and the supernatant was filtered through glass wood. Finally, the resulting medium was diluted with lactic acid (1:1) and stored at T$_{room}$.

4.7.2 Larvae manipulations

Third instar wandering larvae were partly dissected in PBS, leaving the imaginal discs complexes attached to a small piece of the body walls, so that they were not lost during subsequent procedures.

If necessary, only male or female larvae were taken for analysis. Genders can be distinguished by the presence of testes that are large and visible as clear spaces on each side of the abdomen, approximately one quarter of the way from the posterior end.

4.7.2.1 Whole-mount antibody staining of imaginal discs

The dissected disc complexes were fixed with 4% formaldehyde in PBS for 20min at T_{room}, washed in PBT 4x 10min, blocked in PBT with 5% serum for 20min and incubated with anti-β-galactosidase antibody o/n at 4°C (dilution 1:5000). Afterwards, the discs were washed in PBT 8x 10min and incubated with secondary Cy3-conjugated anti-rabbit antibody (dilution 1:200, Jackson Immunoresearch laboratories) for 1-2h at T_{room} in dark. The discs were washed 8x 10min, additionally fixed with 4% formaldehyde in PBS for 15min. Post-fixation washes were 2x 10min. Finally, the discs were dissected completely in glycerol (50% in PBT) and mounted on slides in 70% glycerol. Coverslips were sealed with a nail polish. The discs were imaged immediately or stored at 4°C for no longer than 2-3 days. Images were captured either with Zeiss Axioskop2 MOT fluorescent microscope or Leica TCS SP2 confocal microscope.

Buffers:

PBS	130mM NaCl, 7mM Na$_2$HPO$_4$, 3mM NaH$_2$PO$_4$
PBT	PBS with 0.1% or 0.2% Triton X-100 depending on penetrance for antibody

4.7.2.2 *In situ* hybridisation to imaginal discs

Partly dissected discs complexes were rocked in fixative1 for 30-45sec, then transferred into fixative2 and rocked for 20min at T_{room}. The fixed discs were washed in methanol 2x 5min (discs can be kept in methanol for long-term storage at –20°C) and then incubated in 0.6% H$_2$O$_2$ in methanol for 30min.

Pre-hybridisation treatment was 3x 5min in PBT, 10min in a mixture PBT/hybridisation buffer (1:1) and 10min in hybridisation buffer. The discs were pre-hybridised for 3-5h at 58°C and hybridised with the probe in a minimal volume o/n at 58°C.

Post-hybridisation treatment (all at 58°C) was 20min in a fresh aliquot of hybridisation solution and then 20min of each wash in hybridisation solution/PBT in a proportion 4:1, 3:2, 2:3 and 1:4. Next, the discs were washed in PBT 4x 10min, blocked in PBT with 5% serum and incubated with preabsorbed anti-DIG AP-conjugated antibody (1:2000, Roche) for 1h at T$_{room}$. Unbound antibody was removed by washings in PBT 4x 10min. The disc complexes were washed 2x 10min in AP-buffer and the colour reaction was developed in PBT/BCIP solution (20μl of the stock (Roche) in 1ml AP-buffer). Finally, the discs were washed in PBT 3x 5min, equilibrated in 70% glycerol (in PBT) for several hours at T$_{room}$ or o/n at 4°C, fully dissected and mounted on slides in 70% glycerol. Coverslips were sealed with a nail polish. Preparations can be stored at 4°C. The slides were analysed under Zeiss Axioskop2 MOT microscope.

Buffers (all prepared on DEPC-treated water):

PBS	130mM NaCl, 7mM Na$_2$HPO$_4$, 3mM NaH$_2$PO$_4$
PBT	PBS with 0.1% Tween-20)
Fixative1	325μl PBT, 75μl 16% formaldehyde and 500μl heptane
Fixative2	610μl PBT, 150μl 16% formaldehyde and 40μl DMSO
Hybridisation buffer	50% deionised formamide
	5x SSC (2.5ml 20x stock in 10ml hybridisation buffer)
	100μg/ml tRNA
	50μg/ml heparin
	100μg/ml salmon testis DNA
	0.1% Tween-20
	pH adjusted to 6.5-8 by 1 M citric acid

Since pH can change signal/noise ratio, new probes are suggested to try at different pH.

AP-buffer:	100mM NaCl, 50mM MgCl$_2$, 100mM Tris-HCl pH 9.5, 0.1% Tween-20.

AP-buffer should be prepared freshly or at least contain no precipitate.

For DEPC-treatment 1ml DEPC per 1l of water was constantly stirred for 1h at 37°C or o/n at T_{room} and autoclaved.

4.7.2.3 X-gal staining

Dissected disc complexes were fixed in 1% glutaraldehyde (in PBS) for 5min (up to 15min) at T_{room}, washed in PBT 3x 10min, rinsed once in X-gal staining solution and finally stained with X-gal in staining solution (working concentration 0.08%) at 37oC. The colour reaction may take from 15min to o/n. The stained discs were washed in PBT 2x 10min, fully dissected in 50% glycerol and mounted in 70% glycerol. Images were captured with Zeiss Axioskop2 MOT microscope.

Solutions:

PBS	130mM NaCl, 7mM Na_2HPO_4, 3mM NaH_2PO_4
PBT	PBS with 0.1% Triton X-100
X-gal staining solution	10mM Na-phosphate buffer pH 7.2
	150mM NaCl
	1mM MgCl2
	3mM $K_4[FeII(CN)_6]$
	3mM $K_3[FeIII(CN)_6]$, stored at T_{room} in dark
Na-phosphate buffer	0.1M Na-phosphate pH 7.2 (72 parts of 0.2M Na_2HPO_4, 28 parts 0.2M NaH_2PO_4, 100 parts of water)
X-gal stock	8% X-gal in DMSO, stored at -20°C

4.7.2.4 Salivary gland fixation and staining

Dissected disc complexes were fixed in 4% formaldehyde (in PBS) for 20min at T_{room}, washed in PBT 3x 10min and stained with TRITC-phalloidin (Sigma) and DRAQ5 (Biostatus). After staining the complexes were washed in PBT 3x 10min. The salivary glands were detached from the complexes and mounted in 70% glycerol

on slides. Coverslips were sealed with a nail polish. Images were captured with Leica TCS SP2 confocal microscope.

Buffers:

PBS   130mM NaCl, 7mM Na$_2$HPO$_4$, 3mM NaH$_2$PO$_4$

PBT   PBS with 0.1% Triton X-100

Chemicals abbreviated:

BCIP   5-bromo-4-chloro-3-indolyl phosphate-p-toluidine salt

BSA   bovine serum albumine

DAB   diamino-benzidine

DEPC   diethyl-pyrocarbonate

DIG   digoxigenin

DMSO   dimethyl-sulfoxid

dNTP   deoxy-ribonucleside-triphosphate

DTT   dithiothreitol

EDTA   ethylen-diamino-tetraacetic acid

EGTA   ethylene-glycol-tetraacetic acid

GST   glutathione S-transferase

HEPES   4-(2-hydroxy-ethyl)-1-piperazine-ethan-sulfonic acid

IPTG   isopropyl-beta-D-thiogalactopyranoside

MOPS   morpholin-propan-sulfonic acid

NBT   nitroblue tetrazolium

NP-40   nonidet P40 (also known as igepal)

PMSF   phenyl-methyl-sulphonyl-fluoride

SDS   sodium dodecyl sulfate (also known as sodium lauryl sulfate)

Tris   Toxics Release Inventory System

TRITC   tetramethyl-rhodamine isothiocyanate

X-gal   X-galactose (X = 4-chloro-3- bromo indole)

Solutions abbreviated:

HEMG   HEPES-EDTA-magnesium-glycerol

LB   Luria-Bertani medium

PBS   phosphate-saline-buffer

PBT   phosphate-saline-buffer with Triton X-100 or Tween 20

RIPA   Radioimmunoprecipitation

TBE   Tris-borate-EDTA

TB   Tris-borate

TE   Tris-EDTA

5 Summary

Signal transduction is a growing field in modern developmental biology as it sheds light on how adjacent cellular environment and distant interactions can specify cell fate. Cell-cell interactions during embryonic development are crucial in the co-ordination of growth, differentiation and maintenance of many different cell types. To achieve this co-ordination each cell must properly translate signals received from closely and distantly neighbouring cells, into spatially and temporally appropriate developmental responses. A surprisingly limited number of signal transduction pathways are responsible for the differentiation of enormous variety of cell types. As a result, pathways, including JAK/STAT, are frequently "reused" during development. Thus, in mammals the JAK/STAT pathway is required during pre-gastrulation stages of embryogenesis, for differentiation of the mammary gland epithelium, in hematopoiesis and, finally, plays a pivotal role in immune response.

The canonical model of the JAK/STAT signal transduction pathway is represented by a trans-membrane receptor associated with a <u>Ja</u>nus <u>k</u>inase (JAK), which upon stimulation by an extra-cellular ligand, phosphorylates itself, the receptor and, finally, the <u>s</u>ignal <u>t</u>ransducer and <u>a</u>ctivator of <u>t</u>ranscription (STAT) molecules. Phosphorylated STATs dimerise and are translocated to the nucleus where they activate transcription of target genes.

The JAK/STAT pathway has been conserved throughout evolution, and all known components are present in the genome of the fruit fly *Drosophila melanogaster*. Haematopoietic and immunity functions of the vertebrate pathway have also been shown in flies. The pathway is also required during fly development for processes including embryonic segmentation, tracheal morphogenesis, posterior spiracle formation, hindgut elongation and imaginal disc development. Given the importance of the JAK/STAT pathway, it is not surprising that proper response is based on synergy between precise action of positive and negative regulators. Three major families of moderators have been identified and characterised on the basis of their negative regulation of the JAK/STAT pathway, with each appearing to function at different steps of the signalling cascade.

This study describes the *Drosophila* protein Ken&Barbie (Ken) as a selective negative regulator of JAK/STAT signal transduction. *ken* mutations were identified in a screen for modulators of an eye overgrowth phenotype, caused by over-expression of the pathway ligand *unpaired,* and interact genetically with the pathway receptor *domeless* (*dome*) and the transcription factor *stat92E* during development. Over-expression of Ken can phenocopy developmental defects in the head skeleton and the posterior spiracles known to be caused by the loss of JAK/STAT signalling. These genetic interactions suggest that Ken may function as a negative regulator of the JAK/STAT pathway. Ken molecule possesses C-terminal Zn-finger domain, presumably for DNA binding, and N-terminal BTB/POZ domain, often found in transcriptional repressors. Taken together with the nuclear accumulation of Ken observed when using EGFP-fused construct expressed *in vivo*, it is proposed that Ken may act as a suppresser of STAT92E pathway target genes. In order to identify whether Ken can bind DNA, an *in vitro* assay has been undertaken that has determined that Ken specifically binds to a DNA sequence, with the essential for DNA recognition core overlapping that of STAT92E. This interesting observation suggests that not all sites recognised by STAT92E may also allow Ken binding, and it is likely that among a variety of sequences that can be successfully bound by STAT92E only a subset is also suitable for Ken. Strikingly, when effects of ectopically expressed Ken on the expression of putative JAK/STAT pathway target genes was examined, only a subset of the genes tested, namely *ventral vein lacking* (*vvl*), *tracheless* and *knirps* were down-regulated by Ken, whereas some others, such as *even-skipped* and *four-jointed,* appeared to be unresponsive. According to the proposed selective site hypothesis, this discriminating regulation may depend on the precise sequence of the STAT92E binding sites present within the promoters of the examined targets.

Further analysis of *vvl*, one of the genes susceptible to ectopic Ken, was undertaken. In the developing hindgut, expression of *vvl* is highly dependent of the JAK/STAT pathway, but remains repressed in the posterior spiracles, despite the stimulation of STAT92E by Upd in their primordia. Importantly, *ken* is also expressed in the developing posterior spiracles. Strikingly, up-regulation of *vvl* is observed in these tissues in the mutant embryos lacking a large proportion of Ken. These imply that while ectopic Ken is sufficient to repress the expression of *vvl* in the hindgut,

endogenous Ken is also necessary to prevent its activation in the posterior spiracles. It is therefore conceivable that ectopic *vvl* expression in the posterior spiracles of the *ken* mutants may be the result of de-repression of endogenous STAT92E activity. Another consequence of these observations is a fine balance that must exist between STAT92E and Ken activities. Apparently, endogenous level of Ken is sufficient to repress *vvl*, but not other, as yet unidentified, JAK/STAT pathway targets, whose presumable activation by STAT92E is required for posterior spiracle development as the embryos mutant for *dome*, the receptor of the pathway, show severe spiracle defects. These defects are also observed in the embryos mis-expressing Ken. Though it is possible that the posterior spiracle phenotype caused by higher levels of Ken results from a JAK/STAT pathway independent activity, it seems to be more likely that Ken acts in a dosage dependent manner, and extra Ken is able to further antagonise JAK/STAT pathway target genes.

While STAT92E binding sites required for target gene expression have been poorly characterised, the existence of genome data allows the prediction of candidate STAT92E sites present in target genes promoters to be attempted. When a 6kb region containing the putative regulatory domains flanking the *vvl* locus are examined, only a single potential STAT92E binding site located 825bp upstream of the translational start can be detected. Strikingly, this site also includes a perfect Ken binding sequence. Such an *in silico* observation, though consistent with both Ken DNA binding assay *in vitro* and regulation of STAT92E target genes *in vivo*, however, requires further analysis. Investigations of this potential mechanism of Ken regulation represents an important future direction for research into the functions of Ken.

The JAK/STAT pathway is implicated in a variety of processes during embryonic and larval development as well as in imago. In each case, stimulation of the same transcription factor results in different developmental outcomes. While many potential mechanisms have been proposed and demonstrated to explain such pleiotropy, the present study indicates that Ken may represent another mechanism, with which signal transduction pathways are controlled. Ken selectively down-regulates a subset of potential target genes and so modifies the transcriptional profile generated by activated STAT92E – a mechanism, which may be partially responsible for differences in the morphogenetic processes elicited by JAK/STAT signalling during development.

Additionally, while we have shown that Ken is involved in the regulation of JAK/STAT signal transduction, it may function in other developmental processes. This is indicated both by its broad embryonic expression pattern, and the genital defects present in hypomorphic *ken* mutants. Indeed, given the relatively short DNA recognition sequence of Ken, it is feasible that it may regulate a wide range of developmentally important genes. Investigations into JAK/STAT pathway independent functions of Ken represent a task for future research.

6 Zusammenfassung

Die Forschung an zellulärer Signalübertragung ist ein Bereich wachsender Bedeutung in der modernen Entwicklungsbiologie, der darüber Aufschluss gibt, wie die unmittelbare zelluläre Umgebung und weit entfernte Wechselwirkungen zwischen Zellen die Entwicklung eines Organismus bestimmen. Wechselwirkungen zwischen Zellen während der embryonalen Entwicklung sind von großer Bedeutung für die Koordination von Wachstum, Differenzierung und Erhaltung vieler verschiedener Zelltypen. Für diese Koordination muss jede Zelle sowohl die Signale von benachbarten als auch von weit entfernten Zellen in räumlich und zeitlich adäquate Entwicklungsvorgänge übersetzen. Einer enormen Zahl von Differenzierungsvorgängen unterschiedlicher Zelltypen steht dabei eine vergleichbar geringe Anzahl verschiedener Signaltransduktionswege gegenüber. Deshalb werden solche Signalwege, wie der JAK/STAT-Signalübertragungsweg, mehrfach für unterschiedliche Entwicklungsprozesse gebraucht. Bei Säugetieren z.B. spielt der JAK/STAT-Signalweg für die Prä-Gastrulations-Stadien der Embryogenese, für die Differenzierung des Brustdrüsen–Epithels, für die Hämatopoese und auch für das Immunsystem eine bedeutende Rolle.

Im kanonischen Modell der JAK/STAT-Signalübertragung ist ein Transmembran-Rezeptor mit der Janus Kinase (JAK) assoziiert, die nach Stimulation durch einen extrazellulären Liganden zuerst sich selbst und dann auch den Rezeptor und schließlich STAT-Moleküle (Signal Transducer and Activator of Transcription) phosphoryliert. Phosphorylierte STAT-Moleküle dimerisieren, werden in den Kern transportiert und aktivieren dort die Transkription von Ziel-Genen.

Der JAK/STAT-Signalweg ist evolutionär konserviert. Auch das Genom der Fruchtfliege *Drosophila melanogaster* enthält alle bekannten Komponenten des Signalwegs, deren Aktivität während der Hämotopoese und bei der Immunantwort eine Rolle spielt und für Entwicklungsprozesse wie embryonale Segmentierung, Morphogenese des Trachealsystems, Bildung des posterioren Atemlochs, Ausdehnung des Hinterdarms sowie die Imaginalscheiben-Entwicklung essentiell ist. Drei Hauptgruppen von Signalwegs-Modulatoren wurden bisher als negative

Regulatoren des JAK/STAT-Signalwegs charakterisiert, wobei jede Gruppe jeweils verschiedene Stationen der Signalkaskade kontrolliert.

In dieser Arbeit wird Ken&Barbie (Ken) als negativer Regulator der JAK/STAT-Signalübertragung bei *Drosophila melanogaster* beschreiben. Mutationen im *ken* Lokus wurden in einer systematischen Suche nach Modulatoren identifiziert. *ken* interagiert genetisch mit dem Signalwegs-Liganden *unpaired*, dem Rezeptor *domeless* (*dome*) und dem Transkriptionfaktor *stat92E*. Über-Expression von Ken resultiert in Entwicklungsstörungen des Kopf-Skeletts und des posterioren Atemlochs, Phänotypen, die auch durch den Verlust von JAK/STAT-Signal-Aktivität verursacht werden. Die genetischen Interaktionen deuten auf eine negativ-regulatorische Funktion von Ken im JAK/STAT-Signalweg hin.

Ken enthält eine C-terminale Zn-Finger-Domäne, die vermutlich der DNA-Bindung dient, und eine N-terminale BTB/POZ Domäne, die häufig in transkriptionellen Repressoren auftritt. Zusammen mit der Beobachtung, dass ein Ken-EGFP-Reporter-Protein im Nukleus akkumuliert, deuten diese Ergebnisse auf eine mögliche Funktion von Ken als Suppressor von STAT92E Ziel-Genen hin. Zur Klärung der DNA-Bindungs-Aktivität von Ken wurde ein *in vitro* Testverfahren angewandt. Ken bindet spezifisch an DNA. Die Zielsequenz überlappt mit der von STAT92E. Diese Beobachtung lässt vermuten, dass nicht alle STAT92E Zielsequenzen die Bindung von Ken erlauben. Es ist daher wahrscheinlich, dass unter den DNA-Sequenzen, an die STAT92E binden kann, nur wenige auch die Bindung von Ken ermöglichen. Diese Hypothese wird durch Experimente untermauert, in denen der Effekt von ektopisch exprimiertem Ken auf die Expression von Ziel-Genen des JAK/STAT-Signalwegs untersucht wurde. Nur einige dieser Gene, nämlich *ventral veins lacking* (*vvl*), *trachealess* and *knirps*, wurden von Ken supprimiert. Die Expression anderer JAK/STAT Ziel-Gene wie *even-skipped* and *four-jointed* waren von ektopischer Ken-Aktivität nicht betroffen. Unter Berücksichtigung der oben vorgeschlagenen Hypothese hängt die spezifische Suppression durch Ken von der Sequenz der STAT92E-Bindestellen in den untersuchten Zielgen-Promotoren ab.

Zur genaueren Klärung wurden weitergehende Studien mit dem gemeinsamen Ziel-Gen *vvl* durchgeführt. Im sich entwickelnden Hinterdarm hängt die Expression von *vvl* von JAK/STAT-Aktivität ab. Trotz Stimulation von STAT92E durch Upd wird *vvl*-Expression in den Bereichen, aus denen sich das posteriore Atemloch bildet und

wo auch *ken* exprimiert wird, nicht aktiviert. Interessanterweise, wird *vvl* vermehrt in den genannten Geweben exprimiert, wenn Ken-Aktivität durch eine Mutation gestört wird. Diese Ergebnisse deuten darauf hin, dass ektopisch exprimiertes Ken ausreicht, die Expression von *vvl* im Hinterdarm zu reprimieren, und endogenes Ken notwendig ist, um *vvl*-Aktivierung im posterioren Atemloch zu verhindern. Es scheint daher, dass ektopische Expression von *vvl* im Gewebe, aus dem das posteriore Atemloch hervorgeht, das Ergebnis von De-Reprimierung endogener STAT92E-Aktivität ist. Eine weitere Konsequenz dieser Beobachtungen sollte ein sensibles Gleichgewicht sein, das zwischen den Aktivitäten von STAT92E und Ken herrschen muss. Offensichtlich reichen endogene Mengen von Ken aus, um *vvl* aber nicht bisher unidentifizierte JAK/STAT-Zielgene zu reprimieren, deren Aktivierung durch STAT92E für die Entwicklung des posterioren Atemlochs notwendig ist, da Mutanten des Rezeptors *dome* schwere Defekte in dem posterioren Atemloch aufweisen. Obwohl die Möglichkeit besteht, dass der durch ektopisch exprimiertes Ken verursachte Phänotyp des posterioren Atemlochs von einer JAK/STAT-unabhängigen Aktivität herrührt, scheint es aber eher wahrscheinlich, dass Ken in einer Dosis-abhängigen Weise agiert und erhöhte Ken-Aktivität in der Lage ist, Ziel-Gene des JAK/STAT-Signalwegs weiter zu suprimieren.

STAT92E-Bindestellen, die für die Expression von Ziel-Genen notwendig sind, wurden bisher kaum charakterisiert. Die verfügbaren Daten des Genom-Projekts ermöglichen allerdings die Vorhersage von möglichen STAT92E-Bindestellen in Promotoren von potenziellen Ziel-Genen. So befindet sich in einer durch Sequenz-Analyse vorhergesagten 6kb großen regulatorischen Region, die den *vvl* locus flankiert, eine einzige mögliche STAT92E Bindestelle (825bp vor dem Translationstart). Diese Bindestelle überlappt mit eine *in-vitro*-Ken-Bindesequenz.

In der vorliegenden Arbeit wird Ken als Teil eines neuartigen Mechanismus vorgestellt, mit dem Signaltransduktionswege kontrolliert werden können. Ken suprimiert eine Teilmenge möglicher Ziel-Gene, die der JAK/STAT-Signalweg aktiviert, und verändert dadurch das STAT92E-abhängige Expressionsprofil. Dieser Mechanismus könnte für die unterschiedlichen Auswirkungen des JAK/STAT-Signalwegs in den morphogenetischen Prozessen während der Entwicklung verantwortlich sein.

Ken ist außer der hier beschriebenen Funktion als Suppressor der JAK/STAT-Signalübertragung an anderen Entwicklungsvorgängen beteiligt. Diese Folgerung ergibt sich aus seinem weitgefächerten Expressionsmuster während der Embryogenese und Genital-Defekten in hypomorphen *ken* Mutanten, die nicht im Zusammenhang mit JAK/STAT-Aktivität stehen. Die vergleichsweise kurze DNA-Erkennungssequenz von Ken deutet außerdem darauf hin, dass Ken eine große Bandbreite von wichtigen Entwicklungsgenen regulieren könnte. Untersuchungen der JAK/STAT-unabhängigen Funktionen von Ken stellen einen Bereich möglicher zukünftiger Forschungs-Anstrengungen dar.

7 References

Aaronson DS & Horvath CM (2002) A road map for those who don't know JAK-STAT. *Science,* **296**, 1653-5.

Affolter M, Marty T, Vigano MA & Jazwinska A (2001) Nuclear interpretation of Dpp signaling in *Drosophila. Embo J,* **20**, 3298-305.

Agaisse H & Perrimon N (2004) The roles of JAK/STAT signaling in *Drosophila* immune responses. *Immun Rev,* **198**, 72-82.

Agaisse H, Petersen UM, Boutros M, Mathey-Prevot B & Perrimon N (2003) Signaling role of hemocytes in *Drosophila* JAK/STAT-dependent response to septic injury. *Dev Cell,* **5**, 441-50.

Ahmad KF, Melnick A, Lax S, Bouchard D, Liu J, Kiang C, Mayer S, Takahashi S, Licht JD & Privé GG (2003) Mechanism of SMRT corepressor recruitment by the BCL6 BTB domain. *Mol Cell,* **12**, 1551-64.

Akira S (2000) Roles of STAT3 defined by tissue-specific gene targeting. *Oncogene,* **19**, 2607-11.

Al-Lazikani B, Sheinerman FB & Honig B (2001) Combining multiple structure and sequence alignments to improve sequence detection and alignment: application to the SH2 domains of Janus kinases. *Proc Natl Acad Sci U S A,* **98**, 14796-801.

Albagli O, Dhordain P, Deweindt C, Lecocq G & Leprince D (1995) The BTB/POZ domain: a new protein-protein interaction motif common to DNA- and actin-binding proteins. *Cell Growth Differ.,* **6**, 1193-8.

Ali S, Nouhi Z, Chughtai N & Ali S (2003) SHP-2 regulates SOCS-1-mediated Janus kinase-2 ubiquitination/degradation downstream of the prolactin receptor. *J Biol Chem,* **278**, 52021-31.

Alonso CR (2002) Hox proteins: sculpting body parts by activating localized cell death. *Curr Biol,* **12**, R776-R8.

Aoki N & Matsuda T (2000) A cytosolic protein-tyrosine phosphatase PTP1B specifically dephosphorylates and deactivates prolactin-activated STAT5a and STAT5b. *J Biol Chem,* **275**, 39718-26.

Ashburner M (1989) *Drosophila: a laboratory handbook and manual.* Cold Spring Harbor Laboratory Press, Cold Spring Harbor.

Bach EA & Perrimon N (2003) Prime time for the *Drosophila* JAK/STAT pathway. In / Sehgal PB, Levy DE & Hirano T / *Signal Transducers and Activators of Transcription (STATs); Activation and Biology.* / Kluwer Academic Press, Dordrecht/Boston/London.

Bach EA, Vincent S, Zeidler MP & Perrimon N (2003) A sensitized genetic screen to identify novel regulators and components of the *Drosophila* JAK/STAT pathway. *Genetics,* **165**, 1149-66.

Baksa K, Parke T, Dobens LL & Dearolf CR (2002) The *Drosophila* STAT protein, STAT92E, regulates follicle cell differentiation during oogenesis. *Dev Biol,* **243**, 166-75.

Bardwell VJ & Treisman R (1994) The POZ domain: a conserved protein-protein interaction motif. *Genes Dev,* **8**, 1664-77.

Baron BW, Nucifora G, McCabe N, Espinosa R, Le Beau MM & McKeithan TW (1993) Identification of the gene associated with the recurring chromosomal translocations *t(3;14)(q27;q32)* and *t(3;22)(q27;q11)* in B-cell lymphomas. *Proc Natl Acad Sci U S A,* **90**, 5262-6.

Baron BW, Stanger RR, Hume E, Sadhu A, Mick R, Kerckaert JP, Deweindt C, Bastard C, Nucifora G, Zeleznik-Le N & McKeithan TW (1995) BCL6 encodes a sequence-specific DNA-binding protein. *Genes Chromosomes Cancer,* **13**, 221-4.

Bartoe JL & Nathanson NM (2002) Independent roles of SOCS-3 and SHP-2 in the regulation of neuronal gene expression by leukemia inhibitory factor. *Mol Brain Res,* **107**, 108-19.

Bartunek P, Koritschoner NP, Brett D & Zenke M (1999) Molecular cloning, expression and evolutionary analysis of the avian tyrosine kinase JAK1. *Gene,* **230**, 129-36.

Bauer R, Lehmann C, Fuss B, Eckardt F & Hoch M (2002) The *Drosophila* gap junction channel gene *innexin 2* controls foregut development in response to Wingless signalling. *J Cell Sci,* **115**, 1859-67.

Beccari S, Teixeira L & Rorth P (2002) The JAK/STAT pathway is required for border cell migration during *Drosophila* oogenesis. *Mech Dev,* **111**, 115-23.

Bereshchenko OR, Gu W & Dalla-Favera R (2002) Acetylation inactivates the transcriptional repressor BCL6. *Nat Genet,* **32**, 606-13.

Betz A, Lampen N, Martinek S, Young MW & Darnell JE, Jr. (2001) A *Drosophila* PIAS homologue negatively regulates STAT92E. *Proc Natl Acad Sci U S A,* **98**, 9563-8.

Binari R & Perrimon N (1994) Stripe-specific regulation of pair-rule genes by *hopscotch*, a putative Jak family tyrosine kinase in Drosophila. *Genes Dev,* **8**, 300-12.

Boehm U, Klamp T, Groot M & Howard JC (1997) Cellular responses to interferon-gamma. *Annu Rev Immunol,* **15**, 749-95.

Boube M, Llimargas M & Casanova J (2000) Cross-regulatory interactions among tracheal genes support a co-operative model for the induction of tracheal fates in the *Drosophila* embryo. *Mech Dev,* **91**, 271-8.

Boulay JL, O'Shea JJ & Paul WE (2003) Molecular phylogeny within type I cytokines and their cognate receptors. *Immunity,* **19**, 159-63.

Boulet AM, Lloyd A & Sakonju S (1991) Molecular definition of the morphogenetic and regulatory functions and the cis-regulatory elements of the *Drosophila* Abd-B homeotic gene. *Development,* **111**, 393-405.

Brand AH & Perrimon N (1993) Targeted gene expression as a means of altering cell fates and generating dominant phenotypes. *Development,* **118**, 401-15.

Braunstein J, Brutsaert S, Olson R & Schindler C (2003) STATs dimerize in the absence of phosphorylation. *J Biol Chem,* **278**, 34133-40.

Brown S, Hu N & Castelli-Gair Hombria J (2001) Identification of the first invertebrate interleukin JAK/STAT receptor, the *Drosophila* gene *domeless*. *Curr Biol,* **11**, 1700-5.

Brown S, Hu N & Castelli-Gair Hombria J (2003) Novel level of signalling control in the JAK/STAT pathway revealed by *in situ* visualisation of protein-protein interaction during *Drosophila* development. *Development,* **130**, 3077-84.

Bull AL (1966) *Bicaudal*, a genetic factor which affects the polarity of the embryo in *Drosophila melanogaster*. *J Exp Zool,* **161**, 221-42.

Bullock SL & Ish-Horowicz D (2001) Conserved signals and machinery for RNA transport in *Drosophila* oogenesis and embryogenesis. *Nature,* **414**, 611-6.

Burke LJ & Baniahmad A (2000) Co-repressors 2000. *FASEB J,* **14**, 1876-88.

Callus BA & Mathey-Prevot B (2002) SOCS36E, a novel *Drosophila* SOCS protein, suppresses JAK/STAT and EGF-R signalling in the imaginal wing disc. *Oncogene,* **21**, 4812-21.

Calò V, Migliavacca M, Bazan V, Macaluso M, Buscemi M, Gebbia N & Russo A (2003) STAT proteins: From normal control of cellular events to tumorigenesis. *J. Cell. Physiol.,* **197**, 157-68.

Campos-Ortega JA & Hartenstein V (1997) *The Embryonic Development of Drosophila melanogaster.* Springer,

Casares F & Sanchez-Herrero E (1995) Regulation of the infraabdominal regions of the *bithorax* complex of *Drosophila* by gap genes. *Development,* **121**, 1855-66.

Castelli-Gair Hombria J & Brown S (2002) The fertile field of *Drosophila* Jak/STAT signalling. *Curr Biol,* **12**, R569-75.

Castrillon DH, Gönczy P, Alexander S, Rawson R, Eberhart CG, Viswanathan S, Di Nardo S & Wasserman SA (1993) Towards a molecular genetic analysis of spermatogenesis in *Drosophila melanogaster*: characterization of male-sterile mutants generated by single P element mutagenesis. *Genetics,* **135**, 489-505.

Celniker SE, Keelan DJ & Lewis EB (1989) The molecular genetics of the *bithorax* complex of *Drosophila*: characterization of the products of the Abdominal-B domain. *Genes Dev,* **3**, 1424-36.

Chagnovich D & Lehmann R (2001) Poly(A)-independent regulation of maternal *hunchbac*k translation in the *Drosophila* embryo. *Proc Natl Acad Sci U S A,* **98**, 11359-64.

Chang CC, Ye BH, Chaganti RS & Dalla-Favera R (1996) BCL-6, a POZ/zinc-finger protein, is a sequence-specific transcriptional repressor. *Proc Natl Acad Sci U S A,* **93**, 6947-52.

Chen HW, Chen X, Oh SW, Marinissen MJ, Gutkind JS & Hou SX (2002) *mom* identifies a receptor for the *Drosophila* JAK/STAT signal transduction pathway and encodes a protein distantly related to the mammalian cytokine receptor family. *Genes Dev,* **16**, 388-98.

Chen X, Vinkemeier U, Zhao Y, Jeruzalmi D, Darnell Jr. JE & Kuriyan J (1998) Crystal structure of a tyrosine phosphorylated STAT-1 dimer bound to DNA. *Cell,* **93**, 827-39.

Cherbas L, Hu X, Zhimulev I, Belyaeva E & Cherbas P (2003) EcR isoforms in *Drosophila*: testing tissue-specific requirements by targeted blockade and rescue. *Development,* **130**, 271-84.

Collins T, Stone JR & Williams AJ (2001) All in the family: the BTB/POZ, KRAB, and SCAN domains. *Mol Cell Biol,* **21**, 3609-15.

Constantinescu SN & Moucadel V (2003) STAT signalling by erythropoietin. In / Sehgal PB, Levy DE & Hirano T / *Signal Transducers and Activators of Transcription (STATs); Activation and Biology.* / Kluwer Academic Press, Dordrecht/Boston/London.

Conti P, Kempuraj D, Frydas S, Kandere K, Boucher W, Letourneau R, Madhappan B, Sagimoto K, Christodoulou S & Theoharides TC (2003) IL-10 subfamily members: IL-19, IL-20, IL-22, IL-24 and IL-26. *Immun Lett,* **88**, 171-4.

Darnell JE, Jr. (1997) STATs and gene regulation. *Science,* **277**, 1630-5.

Davey HW, Wilkins RJ & Waxman DJ (1999) STAT5 signaling in sexually dimorphic gene expression and growth patterns. *Am J Hum Genet,* **65**, 959-65.

De Souza D, Fabri LJ, Nash A, Hilton DJ, Nicola NA & Baca M (2002) SH2 domains from suppressor of cytokine signaling-3 and protein tyrosine phosphatase SHP-2 have similar binding specificities. *Biochemistry,* **41**, 9229-36.

Dearden P & Akam M (1999) Developmental evolution: Axial patterning in insects. *Curr Biol,* **9**, R591-4.

Decker T & Kovarik P (1999) Transcription factor activity of STAT proteins: structural requirements and regulation by phosphorylation and interacting proteins. *Cell Mol Life Sci,* **55**, 1535-46.

Delorenzi M & Bienz M (1990) Expression of Abdominal-B homeoproteins in *Drosophila* embryos. *Development,* **108**, 323-9.

Denef N & Schüpbach T (2003) Patterning: JAK-STAT signalling in the *Drosophila* follicular epithelium. *Curr Biol,* **13**, R388-R90.

Dent AL, Shaffer AL, Yu X, Allman D & Staudt LM (1997) Control of inflammation, cytokine expression, and germinal center formation by BCL-6. *Science,* **276**, 589-92.

Dhordain P, Albagli O, Lin RJ, Ansieau S, Quief S, Leutz A, Kerckaert JP, Evans RM & Leprince D (1997) Corepressor SMRT binds the BTB/POZ repressing domain of the LAZ3/BCL6 oncoprotein. *Proc Natl Acad Sci U S A,* **94**, 10762-7.

Dhordain P, Lin RJ, Quief S, Lantoine D, Kerckaert JP, Evans RM & Albagli O (1998) The LAZ3(BCL-6) oncoprotein recruits a SMRT/mSIN3A/histone deacetylase containing complex to mediate transcriptional repression. *Nucleic Acids Res.,* **26**, 4645-51.

Driever W & Nüsslein-Volhard C (1989) The Bicoid protein is a positive regulator of *hunchback* transcription in the early *Drosophila* embryo. *Nature,* **337**, 138-43.

Eberl DF, Perkins LA, Engelstein M, Hilliker AJ & Perrimon N (1992) Genetic and developmental analysis of polytene section 17 of the X chromosome of *Drosophila melanogaster. Genetics,* **130**, 569-83.

Eggenschwiler JT, Espinoza E & Anderson KV (2001) Rab23 is an essential negative regulator of the mouse Sonic hedgehog signalling pathway. *Nature,* **412**, 194-8.

Endo TA, Masuhara M, Yokouchi M, Suzuki R, Sakamoto H, Mitsui K, Matsumoto A, Tanimura S, Ohtsubo M, Misawa H, Miyazaki T, Leonor N, Taniguchi T, Fujita T, Kanakura Y, Komiya S & Yoshimura A (1997) A new protein containing an SH2 domain that inhibits JAK kinases. *Nature,* **387**, 921-4.

Ephrussi A & St Johnston D (2004) Seeing is believing: the Bicoid morphogen gradient matures. *Cell,* **116**, 143-52.

Estrada B & Sánchez-Herrero E (2001) The Hox gene Abdominal-B antagonizes appendage development in the genital disc of *Drosophila. Development,* **128**,

Fagerlund R, Melen K, Kinnunen L & Julkunen I (2002) Arginine/Lysine-rich nuclear localization signals mediate interactions between dimeric STATs and importin. *J Biol Chem,* **277**, 30072-8.

Foe VE, Odell GM & Edgar BA (1993) Mitosis and morphogenesis in the *Drosophila* embryo: point and counterpoint. In / Bate M & Martinez Arias A / *The development of Drosophila melanogaster.* / Cold Spring Harbor Laboratory Press, Cold Spring Harbor.

Frank SJ (2002) Receptor dimerization in GH and erythropoietin action - it takes two to tango, but how? *Endocrinology,* **143**, 2-10.

Frasch M & Levine M (1987) Complementary patterns of *even-skipped* and *fushi tarazu* expression involve their differential regulation by a common set of segmentation genes in *Drosophila. Genes Dev,* **1**, 981-95.

Freeland DE & Kuhn DT (1996) Expression patterns of developmental genes reveal segment and parasegment organization of *D. melanogaster* genital discs. *Mech Dev,* **56**, 61-72.

Frohnhöfer HG, Lehmann R & Nüsslein-Volhard C (1986) Manipulating the anteroposterior pattern of the *Drosophila* embryo. *J Embryol Exp Morphol,* **97 Suppl**, 169-79.

Fu XY, Schindler C, Improta T, Aebersold R & Darnell JE, Jr. (1992) The proteins of ISGF-3, the interferon alpha-induced transcriptional activator, define a gene family involved in signal transduction. *Proc Natl Acad Sci U S A,* **89**, 7840-78-43.

Fukuzawa M, Araki T, Adrian I & Williams JG (2001) Tyrosine phosphorylation-independent nuclear translocation of a *Dictyostelium* STAT in response to DIF signaling. *Mol Cell,* **7**, 779-88.

Fuller MT (1998) Genetic control of cell proliferation and differentiation in *Drosophila* spermatogenesis. *Semin Cell Dev Biol,* **9**, 433-44.

Gao B, Shen X, Kunos G, Meng K, Goldberg ID, Rosen EM & Fan S (2001) Constitutive activation of JAK-STAT3 signaling by BRCA1 in human prostate cancer cells. *FEBS Letters,* **488**, 179-84.

Gao Q & Finkelstein R (1998) Targeting gene expression to the head: the *Drosophila* orthodenticle gene is a direct target of the Bicoid morphogen. *Development,* **125**, 4185-93.

Gaul U & Jäckle H (1990) Role of gap genes in early *Drosophila* development. *Adv Genet,* **27**, 239-75.

Geyer R, Wee S, Anderson S, Yates J & Wolf DA (2003) BTB/POZ domain proteins are putative substrate adaptors for cullin 3 ubiquitin ligases. *Mol Cell,* **12**, 783-90.

Gibson MC & Schubiger G (2001) *Drosophila* peripodial cells, more than meets the eye? *Bioessays,* **23**, 691-7.

Girault J-A, Labesse G, Mornon J-P & Callebaut I (1999) The N-termini of FAK and JAKs contain difergent band 4.1 domains. *TIBS,* **24**, 54-7.

Goenka S, Marlar C, Schindler U & Boothby M (2003) Differential roles of C-terminal activation motifs in the establishment of Stat6 transcriptional specificity. *J Biol Chem,* **278**, 50362-70.

Goto T, Macdonald P & Maniatis T (1989) Early and late periodic patterns of *even skipped* expression are controlled by distinct regulatory elements that respond to different spatial cues. *Cell,* **57**, 413-22.

Gross M, Yang R, Top I, Gasper C & Shuai K (2004) PIASy-mediated repression of the androgen receptor is independent of sumoylation. *Oncogene,* **23**, 3059-66.

Häcker U & Perrimon N (1998) DRhoGEF2 encodes a member of the *dbl* family of oncogenes and controls cell shape changes during gastrulation in *Drosophila*. *Genes Dev.,* **12**, 274-84.

Hanlon AM, Jang S & Salgame P (2002) Signaling from cytokine receptors that affect Th1 responses. *Front Biosci,* **7**, d2147-d1254.

Hanratty WP & Dearolf CR (1993) The *Drosophila* Tumorous-lethal hematopoietic oncogene is a dominant mutation in the *hopscotch* locus. *Mol Gen Genet,* **238**, 33-7.

Harding K & Levine M (1988) Gap genes define the limits of *antennapedia* and *bithorax* gene expression during early development in *Drosophila*. *Embo J,* **7**, 205-14.

Hari KL, Cook KR & Karpen GH (2001) The *Drosophila Su(var)2-10* locus regulates chromosome structure and function and encodes a member of the PIAS protein family. *Genes Dev,* **15**, 1334-48.

Harris MB, Chang CC, Berton MT, Danial NN, Zhang J, Kuehner D, Ye BH, Kvatyuk M, Pandolfi PP, Cattoretti G, Dalla-Favera R & Rothman PB (1999) Transcriptional repression of Stat6-dependent interleukin-4-induced genes by BCL-6: specific regulation of transcription and immunoglobulin E switching. *Mol Cell Biol,* **19**, 7264-75.

Harrison DA, Binari R, Nahreini TS, Gilman M & Perrimon N (1995) Activation of a *Drosophila* Janus kinase (JAK) causes hematopoietic neoplasia and developmental defects. *Embo J,* **14**, 2857-65.

Harrison DA, McCoon PE, Binari R, Gilman M & Perrimon N (1998) *Drosophila unpaired* encodes a secreted protein that activates the JAK signaling pathway. *Genes Dev,* **12**, 3252-63.

Hartatik T, Okada S, Okabe S, Arima M, Hatano M & Tokuhisa T (2001) Binding of BAZF and Bcl6 to STAT6-binding DNA sequences. *Biochem Biophys Res Commun.,* **284**, 26-32.

Haspel RL & Darnell Jr. JE (1999) A nuclear protein tyrosine phosphatase is required for the inactivation of Stat1. *Proc Natl Acad Sci U S A,* **96**, 10188-93.

Hay BA, Maile R & Rubin GM (1997) P element insertion-dependent gene activation in the *Drosophila* eye. *Proc. Natl. Acad. Sci. USA,* **94**, 5195-200.

Heinrich PC, Behrmann I, Haan S, Hermanns HM, Muller-Newen G & Schaper F (2003) Principles of interleukin (IL)-6-type cytokine signalling and its regulation. *Biochem J.,* **374**, 1-20.

Hemmati-Brivanlou A & Melton DA (1994) Inhibition of activin receptor signaling promotes neuralization in *Xenopus. Cell,* **77**, 273-81.

Hemmati-Brivanlou A & Melton DA (1997) Vertebrate embryonic cells will become nerve cells unless told otherwise. *Cell,* **88**, 13-7.

Henriksen MA, Betz A, Fuccillo MV & Darnell JE, Jr. (2002) Negative regulation of STAT92E by an N-terminally truncated STAT protein derived from an alternative promoter site. *Genes Dev,* **16**, 2379-89.

Hoeve J, Ibarra-Sanchez MJ, Fu Y, Zhu W, Tremblay M, David M & Shuai K (2002) Identification of a Nuclear Stat1 Protein Tyrosine Phosphatase. *Mol Cell Biol,* **22**, 5662-8.

Hoey T & Schindler U (1998) STAT structure and function in signaling. *Curr Opin Genet Dev,* **8**, 582-7.

Hoey T, Zhang S, Schmidt N, Yu Q, Ramchandani S, Xu X, Naeger LK, Sun Y-L & Kaplan MH (2003) Distinct requirements for the naturally occurring splice forms Stat4a and Stat4b in IL-12 responses. *Embo J,* **22**, 4237-48.

Horvath CM (2000) STAT proteins and transcriptional responses to extracellular signals. *Trends Biochem Sci.,* **25**, 496-502.

Horvath CM & Darnell JE, Jr. (1997) The state of the STATs: recent developments in the study of signal transduction to the nucleus. *Curr Opin Cell Biol.,* **9**, 233-9.

Hou XS, Melnick MB & Perrimon N (1996) *marelle* acts downstream of the *Drosophila* HOP/JAK kinase and encodes a protein similar to the mammalian STATs. *Cell,* **84**, 411-9.

Hu N & Castelli-Gair J (1999) Study of the posterior spiracles of *Drosophila* as a model to understand the genetic and cellular mechanisms controlling morphogenesis. *Dev Biol,* **214**, 197-210.

Huang LJ, Constantinescu SN & Lodish HF (2001) The N-terminal domain of Janus kinase 2 is required for Golgi processing and cell surface expression of erythropoietin receptor. *Mol Cell,* **8**, 1327-38.

Hülskamp M, Pfeifle C & Tautz D (1990) A morphogenetic gradient of Hunchback protein organizes the expression of the gap genes Krüppel and Knirps in the early *Drosophila* embryo. *Nature,* **346**, 577-80.

Huynh KD & Bardwell VJ (1998) The BCL-6 POZ domain and other POZ domains interact with the co-repressors N-CoR and SMRT. *Oncogene,* **17**, 2473-84.

Ihle JN, Witthuhn BA, Quelle FW, Yamamoto K & Silvennoinen O (1995) Signaling through the hematopoietic cytokine receptors. *Annu Rev Immunol,* **13**, 369-98.

Imada K & Leonard WJ (2000) The Jak-STAT pathway. *Mol Immunol,* **37**, 1-11.

Ito K, Awano W, Suzuki K, Hiromi Y & Yamamoto D (1997) The *Drosophila* mushroom body is a quadruple structure of clonal units each of which contains a virtually identical set of neurones and glial cells. *Development,* **124**, 761-71.

Iuchi S (2001) Three classes of C2H2 zinc finger proteins. *Cell Mol Life Sci.,* **58**, 625-35.

Jackson PK (2001) A new RING for SUMO: wrestling transcriptional responses into nuclear bodies with PIAS family E3 SUMO ligases. *Genes Dev,* **15**, 3053-8.

Jinks TM, Polydorides AD, Calhoun G & Schedl P (2000) The JAK/STAT signaling pathway is required for the initial choice of sexual identity in *Drosophila melanogaster. Mol Cell,* **5**, 581-7.

Johansen KA, Iwaki DD & Lengyel JA (2003) Localized JAK/STAT signaling is required for oriented cell rearrangement in a tubular epithelium. *Development,* **130**, 135-45.

John S, Vinkemeier U, Soldaini E, Darnell Jr. JE & Leonard WJ (1999) The significance of tetramerization in promoter recruitment by Stat5. *Mol Cell Biol,* **19**, 1910-8.

Johnson LR, McCormack SA, Yang CH, Pfeffer SR & Pfeffer LM (1999) EGF induces nuclear translocation of STAT2 without tyrosine phosphorylation in intestinal epithelial cells. *Am J Physiol,* **276**, C419-C25.

Josten F, Fuss B, Feix M, Meissner T & Hoch M (2004) Cooperation of JAK/STAT and Notch signaling in the *Drosophila* foregut. *Dev Biol,* **257**, 181-9.

Jürgens G & Hartenstein V (1993) The terminal regions of the body pattern. In / Bate M & Martinez Arias A / *The development of Drosophila melanogaster.* / Cold Spring Harbor Laboratory Press, Cold Spring Harbor.

Karsten P, Häder S & Zeidler M (2002) Cloning and expression of *Drosophila* SOCS36E and its potential regulation by the JAK/STAT pathway. *Mech Dev,* **117**, 343.

Kawamata N, Miki T, Ohashi K, Suzuki K, Fukuda T, Hirosawa S & Aoki N (1994) Recognition DNA sequence of a novel putative transcription factor, BCL6. *Biochem Biophys Res Commun.,* **204**, 366-74.

Kiger AA, Jones DL, Schulz C, Rogers MB & Fuller MT (2001) Stem cell self-renewal specified by JAK-STAT activation in response to a support cell cue. *Science,* **294**, 2542-5.

Kile BT, Schulman BA, Alexander WS, Nicola NA, Martin HME & Hilton DJ (2002) The SOCS box: a tale of destruction and degradation. *Trends Biochem Sci.,* **27**, 235-41.

Kopp A, Duncan I, Godt D & Carroll SB (2000) Genetic control and evolution of sexually dimorphic characters in *Drosophila. Nature,* **408**, 553-9.

Kotaja N, Karvonen U, Janne OA & Palvimo JJ (2002) PIAS proteins modulate transcription factors by functioning as SUMO-1 ligases. *Mol Cell Biol.,* **22**, 5222-34.

Kühnlein RP, Chen CK & Schuh R (1998) A transcription unit at the *ken and barbie* gene locus encodes a novel *Drosophila* zinc finger protein. *Mech Dev,* **79**, 161-4.

Kwon EJ, Park HS, Kim YS, Oh EJ, Nishida Y, Matsukage A, Yoo MA & Yamaguchi M (2000) Transcriptional regulation of the *Drosophila raf* proto-oncogene by *Drosophila* STAT during development and in immune response. *J Biol Chem,* **275**, 19824-30.

Lagueux M, Perrodou E, Levashina EA, Capovilla M & Hoffmann JA (2000) Constitutive expression of a complement-like protein in *toll* and JAK gain-of-function mutants of *Drosophila. Proc Natl Acad Sci U S A,* **97**, 11427-32.

Laity JH, Lee BM & Wright PE (2001) Zinc finger proteins: new insights into structural and functional diversity. *Curr Opin Struct Biol,* **11**, 39-46.

Lalli E, Ohe K, Latorre E, Bianchi ME & Sassone-Corsi P (2003) Sexy splicing: regulatory interplays governing sex determination from *Drosophila* to mammals. *J Cell Sci,* **116**, 441-5.

Langer JA, Cutrone EC & Kotenko S (2004) The Class II cytokine receptor (CRF2) family: overview and patterns of receptor-ligand interactions. *Cytokine Growth Factor Rev,*

Larsen L & Ropke C (2002) Suppressors of cytokine signalling: SOCS. *APMIS,* **110**, 833-44.

Leaman DW, Leung S, Li X & Stark GR (1996) Regulation of STAT-dependent pathways by growth factors and cytokines. *FASEB J,* **10**, 1578-88.

Lehmann R & Nüsslein-Volhard C (1986) Abdominal segmentation, pole cell formation, and embryonic polarity require the localized activity of *oskar*, a maternal gene in *Drosophila. Cell,* **47**,

Leonard WJ & O'Shea JJ (1998) Jaks and STATs: biological implications. *Annu Rev Immunol,* **16**, 293-322.

Leu JH, Yan SJ, Lee TF, Chou CM, Chen ST, Hwang PP, Chou CK & Huang CJ (2000) Complete genomic organization and promoter analysis of the round-spotted pufferfish JAK1, JAK2, JAK3, and TYK2 genes. *DNA Cell Biol,* **19**, 431-46.

Levy DE (1999) Physiological significance of STAT proteins: investigations through gene disruption *in vivo. Cell Mol Life Sci,* **55**, 1559-67.

Levy DE & Darnell JE, Jr. (2002) Stats: transcriptional control and biological impact. *Nat Rev Mol Cell Biol,* **3**, 651-62.

Lewis RS & Ward AC (2004) Conservation, duplication and divergence of the zebrafish *stat5* genes. *Gene,* **338**, 65-74.

Li J, Li W, Calhoun HC, Xia F, Gao FB & Li WX (2003) Patterns and functions of STAT activation during *Drosophila* embryogenesis. *Mech Dev,* **120**, 1455-68.

Li X, Leung S, Kerr IM & Stark GR (1997) Functional subdomains of STAT2 required for preassociation with the alpha-interferon receptor and for signalling. *Mol Cell Biol,* **17**, 2048-56.

Lickert H, Kutsch S, Kanzler B, Tamai Y, Taketo MM & Kemler R (2002) Formation of multiple hearts in mice following deletion of beta-catenin in the embryonic endoderm. *Dev Cell,* **3**, 171-81.

Lipshitz HD (1991) Axis specification in the *Drosophila* embryo. *Curr Opin Cell Biol.,* **3**, 966-75.

Liu B & Shuai K (2003) The PIAS protein family and TC-PTP. In / Sehgal PB, Levy DE & Hirano T / *Signal Transducers and Activators of Transcription (STATs); Activation and biology.* / Kluwer Academic Press, Dordrecht/Boston/London.

Liu X, Quinn AM, Chin YE & Fu XY (1999) STAT genes found in *C. elegans. Science,* **285**, 167a.

Lukacsovich T, Asztalos Z, Juni N, Awano W & Yamamoto D (1999) The *Drosophila melanogaster* 60A chromosomal division is extremely dense with functional genes: their sequences, genomic organization, and expression. *Genomics,* **57**, 43-56.

Lukacsovich T, Yuge K, Awano W, Asztalos Z, Kondo S, Juni N & Yamamoto D (2003) The *ken and barbie* gene encoding a putative transcription factor with a BTB domain and three zinc finger motifs functions in terminalia development of *Drosophila. Arch Insect Biochem Physiol.,* **54**, 77-94.

Luo H, Asha H, Kockel L, Parke T, Mlodzik M & Dearolf CR (1999) The *Drosophila* Jak kinase *hopscotch* is required for multiple developmental processes in the eye. *Dev Biol,* **213**, 432-41.

Luo H, Rose P, Barber D, Hanratty WP, Lee S, Roberts TM, D'Andrea AD & Dearolf CR (1997) Mutation in the Jak kinase JH2 domain hyperactivates *Drosophila* and mammalian Jak-Stat pathways. *Mol Cell Biol,* **17**, 1562-71.

Margolis JS, Borowsky ML, Steingrimsson E, Shim CW, Lengyel JA & Posakony JW (1995) Posterior stripe expression of *hunchback* is driven from two promoters by a common enhancer element. *Development,* **121**, 3067-77.

Mascle X, Albagli O & Lemercier C (2003) Point mutations in BCL6 DNA-binding domain reveal distinct roles for the six zinc fingers. *Biochem Biophys Res Commun,* **300**, 391-6.

Matozaki T & Kasuga M (1996) Roles of protein-tyrosine phosphatases in growth factor signalling. *Cell Signal,* **8**, 13-9.

McBride KM, Banninger G, McDonald C & Reich NC (2002) Regulated nuclear import of the STAT1 transcription factor by direct binding of importin-alpha. *Embo J,* **21**, 1754-63.

McGregor JR & Harrison DA (2002) JAK signaling is somatically required for follicle cell differentiation in *Drosophila. Development,* **129**, 705-17.

Meister M & Lagueux M (2003) *Drosophila* blood cells. *Cell Microbiol,* **5**, 573-80.

Melnick A, Ahmad KF, Arai S, Polinger A, Ball H, Borden KL, Carlile GW, Prive GG & Licht JD (2000) In-depth mutational analysis of the promyelocytic leukemia zinc finger BTB/POZ domain reveals motifs and residues required for biological and transcriptional functions. *Mol Cell Biol,* **20**, 6550-67.

Melnick A, Carlile G, Ahmad KF, Kiang CL, Corcoran C, Bardwell V, Prive GG & Licht JD (2002) Critical residues within the BTB domain of PLZF and Bcl-6 modulate interaction with corepressors. *Mol Cell Biol,* **22**, 1804-18.

Meyer T, Hendry L, Begitt A, John S & Vinkemeier U (2004) A single residue modulates tyrosine dephosphorylation, oligomerization, and nuclear accumulation of Stat transcription factors. *J Biol Chem,* **279**, 18998-9007.

Mikita T, Daniel C, Wu P & Schindler U (1998) Mutational analysis of the STAT6 SH2 domain. *J Biol Chem,* **273**, 17634-42.

Morcillo P, Rosen C, Baylies MK & Dorsett D (1997) Chip, a widely expressed chromosomal protein required for segmentation and activity of a remote wing margin enhancer in *Drosophila. Genes Dev,* **11**, 2729-40.

Morgan MM & Mahowald AP (1996) Multiple signaling pathways establish both the individuation and the polarity of the oocyte follicle in *Drosophila. Arch Insect Biochem Physiol.,* **33**, 211-30.

Myrick KV & Dearolf CR (2000) Hyperactivation of the *Drosophila* Hop Jak kinase causes the preferential overexpression of *eIF1A* transcripts in larval blood cells. *Gene,* **244**, 119-25.

Naka T, Narazaki M, Hirata M, Matsumoto T, Minamoto S, Aono A, Nishimoto N, Kajita T, Taga T, Yoshizaki K, Akira S & Kishimoto T (1997) Structure and function of a new STAT-induced STAT inhibitor. *Nature,* **387**, 924-9.

Nilson LA & Schüpbach T (1999) EGF receptor signaling in *Drosophila* oogenesis. *Curr Top Dev Biol,* **44**, 203-43.

Nishinakamura R, Matsumoto Y, Matsuda T, Ariizumi T, Heike T, Asashima M & Yokota T (1999) Activation of Stat3 by cytokine receptor gp130 ventralizes *Xenopus* embryos independent of BMP-4. *Dev Biol,* **216**, 481-90.

Niu H (2002) The proto-oncogene BCL-6 in normal and malignant B cell development. *Hematol Oncol,* **20**, 155-66.

Oates AC, Brownlie A, Pratt SJ, Irvine DV, Liao EC, Paw BH, Dorian KJ, Johnson SL, Postlethwait JH, Zon LI & Wilks AF (1999a) Gene duplication of zebrafish JAK2 homologs is accompanied by divergent embryonic expression patterns: only *jak2a* is expressed during erythropoiesis. *Blood,* **94**, 2622-36.

Oates AC, Wollberg P, Pratt SJ, Paw BH, Johnson SL, R.K. H, J.H. P, Zon LI & Wilks LF (1999b) Zebrafish *stat3* is expressed in restricted tissues during embryogenesis and *stat1* rescues cytokine signaling in a

STAT1-deficient human cell line. *Dev Dyn,* **215**, 352-70.

Parmar H & Platanias LC (2003) Interferons: mechanisms of action and clinical applications. *Curr Opin Oncol,* **15**, 431-9.

Pascal A, Riou J-F, Carron C, Boucaut J-C & Umbhauer M (2001) Cloning and developmental expression of STAT5 in *Xenopus laevis. Mech Dev,* **106**, 171-4.

Paulson M, Pisharody S, Pan L, Guadagno S, Mui AL & Levy DE (1999) Stat protein transactivation domains recruit p300/CBP through widely divergent sequences. *J Biol Chem,* **274**, 25343-9.

Penalva LO & Sanchez L (2003) RNA binding protein *sex-lethal (Sxl)* and control of *Drosophila* sex determination and dosage compensation. *Microbiol Mol Biol Rev,* **67**, 343-59.

Perkins LA, Larsen I & Perrimon N (1992) *corkscrew* encodes a putative protein tyrosine phosphatase that functions to transduce the terminal signal from the receptor tyrosine kinase *torso*. *Cell,* **70**, 225-36.

Perrimon N & Mahowald AP (1986) *l(1)hopscotch*, A larval-pupal zygotic lethal with a specific maternal effect on segmentation in *Drosophila*. *Dev Biol,* **118**, 28-41.

Peter A, Schottler P, Werner M, Beinert N, Dowe G, Burkert P, Mourkioti F, Dentzer L, He Y, Deak P, Benos PV, Gatt MK, Murphy L, Harris D, Barrell B, Ferraz C, Vidal S, Brun C, Demaille J, Cadieu E, Dreano S, Gloux S, Lelaure V, Mottier S, Galibert F, Borkova D, Minana B, Kafatos FC, Bolshakov S, Siden-Kiamos I, Papagiannakis G, Spanos L, Louis C, Madueno E, de Pablos B, Modolell J, Bucheton A, Callister D, Campbell L, Henderson NS, McMillan PJ, Salles C, Tait E, Valenti P, Saunders RD, Billaud A, Pachter L, Klapper R, Janning W, Glover DM, Ashburner M, Bellen HJ, Jäckle H & Schäfer U (2002) Mapping and identification of essential gene functions on the X chromosome of *Drosophila*. *EMBO Rep,* **3**, 34-8.

Pignoni F & Zipursky SL (1997) Induction of *Drosophila* eye development by *decapentaplegic*. *Development,* **124**, 271-8.

Ramirez-Weber FA & Kornberg TB (2000) Signaling reaches to new dimensions in *Drosophila* imaginal discs. *Cell,* **103**, 189-92.

Rebay I & Rubin GM (1995) Yan functions as a general inhibitor of differentiation and is negatively regulated by activation of the Ras1/MAPK pathway. *cell,* **81**, 857-66.

Rorth P, Szabo K, Bailey A, Laverty T, Rehm J, Rubin GM, Weigmann K, Milan M, Benes V, Ansorge W & Cohen SM (1998) Systematic gain-of-function genetics in *Drosophila*. *Development,* **125**, 1049-57.

Roth S (2001) *Drosophila* oogenesis: coordinating germ line and soma. *Curr Biol,* **11**, R779-R81.

Rubin GM & Spradling AC (1982) Genetic transformation of *Drosophila* with transposable element vectors. *Science,* **218**, 348-53.

Saharinen P & Silvennoinen O (2002) The pseudokinase domain is required for suppression of basal activity of Jak2 and Jak3 tyrosine kinases and for cytokine-inducible activation of signal transduction. *J Biol Chem,* **277**, 47954-63.

Saharinen P, Takalouma K & Silvennoinen O (2000) Regulation of the Jak2 tyrosine kinase by its pseudokinase domain. *Mol Cell Biol,* **20**, 3387-95.

Saharinen P, Vihinen M & Silvennoinen O (2003) Autoinhibition of Jak2 tyrosine kinase is dependent on specific regions in its pseudokinase domain. *Mol Biol Cell,* **14**, 1448-59.

Sanchez L & Guerrero I (2001) The development of the *Drosophila* genital disc. *Bioessays,* **23**, 698-707.

Sanchez L & Thieffry D (2001) A logical analysis of the *Drosophila* gap-gene system. *J Theor Biol,* **211**, 115-41.

Sanson B (2001) Generating patterns from fields of cells. Examples from *Drosophila* segmentation. *Embo J, 2*, 1083-8.

Schaeffer TS, Sanders LK, Park OK & Nathans D (1997) Functional differences between Stat3a and Stat3b. *Mol Biol Cell, 17*, 5307-16.

Schindler C & Darnell JE, Jr. (1995) Transcriptional responses to polypeptide ligands: the JAK-STAT pathway. *Annu Rev Biochem, 64*, 621-51.

Schindler C, Fu XY, Improta T, Aebersold R & Darnell JE, Jr. (1992) Proteins of transcription factor ISGF-3: one gene encodes the 91-and 84-kDa ISGF-3 proteins that are activated by interferon alpha. *Proc Natl Acad Sci U S A, 89*, 7836-9.

Schindler CW (2002) JAK-STAT signaling in human disease. *J Clin Invest., 109*, 1133-7.

Schlessinger J & Lemmon MA (2003) SH2 and PTB domains in tyrosine kinase signaling. *Sci STKE, 191*, 1-12.

Schmidt D & Müller S (2002) Members of the PIAS family act as SUMO ligases for c-Jun and p53 and repress p53 activity. *Proc Natl Acad Sci U S A, 99*, 2872-7.

Schneider I (1972) Cell lines derived from late embryonic stages of *Drosophila melanogaster*. *J Embryol Exp Morphol, 27*, 353-65.

Sefton L, Timmer JR, Zhang Y, Beranger F & Cline TW (2000) An extracellular activator of the *Drosophila* JAK/STAT pathway is a sex-determination signal element. *Nature, 405*, 970-3.

Skaer H (1993) The alimentary canal. In / Bate M & Martinez Arias A / *The development of Drosophila melanogaster.* / Cold Spring Harbor Laboratory Press, Cold Spring Harbor.

Small S, Blair A & Levine M (1996) Regulation of two pair-rule stripes by a single enhancer in the *Drosophila* embryo. *Dev Biol, 175*, 314-24.

Sofer L, Kampa D & Burnside J (1998) Molecular cloning of a chicken JAK homolog from activated T cells. *Gene, 215*, 29-36.

Soriano SF, Serrano A, Hernanz-Falcon P, Martin de Ana A, Monterrubio M, Martinez C, Rodriguez-Frade JM & Mellado M (2003) Chemokines integrate JAK/STAT and G-protein pathways during chemotaxis and calcium flux responses. *Eur J Immunol, 33*, 1328-33.

Sorrentino RP, Melk JP & Govind S (2004) Genetic analysis of contributions of dorsal group and JAK-Stat92E pathway genes to larval hemocyte concentration and the egg encapsulation response in *Drosophila*. *Genetics, 166*, 1343-56.

Spemann H & Mangold H (1924) Über Induktion von Embryoanlagen durch Implantation artfremder Organisatoren. *W Roux Arch Entw Organ, 100*, 588-638.

Spradling AC, Stern D, Beaton A, Rhem EJ, Laverty T, Mozden N, Misra S & Rubin GM (1999) The Berkeley Drosophila genome project gene disruption project. Single P-element insertions mutating 25% of vital *Drosophila* genes. *Genetics, 153*, 135-77.

St Johnston D (1993) Pole plasm and posterior group genes. In / Bate M & Martinez Arias A / *The development of Drosophila melanogaster.* / Cold Spring Harbor Laboratory Press, Cold Spring Harbor.

St Johnston D & Nüsslein-Volhard C (1992) The origin of pattern and polarity in the *Drosophila* embryo. *Cell,* **68**, 201-19.

Stanojevic D, Hoey T & Levine M (1989) Sequence-specific DNA-binding activities of the gap gene proteins encoded by *hunchback* and *krüppel* in *Drosophila. Nature Biol,* **341**, 331-5.

Starr R, Willson TA, Viney EM, Murray LJ, Rayner JR, Jenkins BJ, Gonda TJ, Alexander WS, Metcalf D, Nicola NA & Hilton DJ (1997) A family of cytokine-inducible inhibitors of signalling. *Nature,* **387**, 917-21.

Stein D & Stevens LM (2001) The torso ligand, unmasked? *Sci STKE,* **98**, 1-3.

Steward R & Govind S (1993) Dorsal-ventral polarity in the Drosophila embryo. *Curr Opin Genet Dev,* **3**, 556-61.

Streuli M (1996) Protein tyrosine phosphatases in signaling. *Curr Opin Cell Biol.,* **8**, 182-8.

Sweitzer SM, Calvo S, Kraus MH, Finbloom DS & Larner AC (1995) Characterization of a Stat-like DNA binding activity in *Drosophila melanogaster. J Biol Chem,* **270**, 16510-3.

Symes A, Stahl N, Reeves SA, Farruggella T, Servidei T, Gearan T, Yancopoulos G & Fink JS (1997) The protein tyrosine phosphatase SHP-2 negatively regulates ciliary neurotrophic factor induction of gene expression. *Curr Biol,* **7**, 697-700.

Tracey WD, Jr., Ning X, Klingler M, Kramer SG & Gergen JP (2000) Quantitative analysis of gene function in the *Drosophila* embryo. *Genetics,* **154**, 273-84.

Trinchieri G (2003) Interleukin-12 and the regulation of innate resistance and adaptive immunity. *Nat Rev Immunol,* **3**, 133-46.

Tsai CC, Kao HY, Yao TP, McKeown M & Evans RM (1999) SMRTER, a *Drosophila* nuclear receptor coregulator, reveals that EcR-mediated repression is critical for development. *Molec. Cell,* **4**, 175-86.

Tsai YC & Sun YH (2004) Long-range effect of Upd, a ligand for Jak/STAT pathway, on cell cycle in *Drosophila* eye development. *Genesis,* **39**, 141-53.

Tuerk C & Gold L (1990) Systematic evolution of ligands by exponential enrichment: RNA ligands to bacteriophage T4 DNA polymerase. *Science,* **249**, 505-10.

Tulina N & Matunis E (2001) Control of stem cell self-renewal in *Drosophila* spermatogenesis by JAK- STAT signaling. *Science,* **294**, 2546-9.

Tzou P, De Gregorio E & Lemaitre B (2002) How *Drosophila* combats microbial infection: a model to study innate immunity and host–pathogen interactions. *Curr Opin Microbiol,* **5**, 102-10.

Usacheva A, Kotenko S, Witte MM & Colamonici OR (2002) Two distinct domains within the N-terminal region of Janus kinase 1 interact with cytokine receptors. *J Immunol,* **169**, 1302-8.

van den Heuvel S (2003) Protein degradation: CUL-3 and BTB--partners in proteolysis. *Curr Biol,* **14**, R59-R61.

Vidal M, Gigoux V & Garbay C (2001) SH2 and SH3 domains as targets for anti-proliferative agents. *Crit Rev Oncol Hematol,* **40**, 175-86.

Vihinen M, Villa A, Mella P, Schumacher RF, Savoldi G, O'Shea JJ, Candotti F & Notarangelo LD (2000) Molecular modeling of the Jak3 kinase domains and structural basis for severe combined immunodeficiency. *Clin Immunol,* **96**, 108-18.

Vinkemeier U, Moarefi I, Darnell JE, Jr. & Kuriyan J (1998) Structure of the amino-terminal protein interaction domain of STAT-4. *Science,* **279**, 1048-52.

Voas MG & Rebay I (2004) Signal integration during development: insights from the *Drosophila* eye. *Dev Dyn,* **229**, 162-75.

Watford WT, Moriguchi M, Morinobu A & O'Shea JJ (2003) The biology of IL-12: coordinating innate and adaptive immune responses. *Cytokine Growth Factor Rev,* **14**, 361-8.

Wharton RP & Struhl G (1989) Structure of the *Drosophila* BicaudalD protein and its role in localizing the the posterior determinant *nanos. Cell,* **59**, 881-92.

Wharton RP & Struhl G (1991) RNA regulatory elements mediate control of *Drosophila* body pattern by the posterior morphogen *nanos. Cell,* **67**, 955-67.

Whittle JR, Tiong SY & Sunkel CE (1986) The effect of lethal mutations and deletions within the *bithorax* complex upon the identity of caudal metameres in the *Drosophila* embryo. *J Embryol Exp Morphol,* **93**, 153-66.

Wodarz A, Hinz U, Engelbert M & Knust E (1995) Expression of *crumbs* confers apical character on plasma membrane domains of ectodermal epithelia of *Drosophila. Cell,* **82**, 67-76.

Wong CW & Privalsky ML (1998) Components of the SMRT corepressor complex exhibit distinctive interactions with the POZ domain oncoproteins PLZF, PLZF-RARalpha, and BCL-6. *J Biol Chem,* **273**, 27695-702.

Xi R, McGregor JR & Harrison DA (2003) A gradient of JAK pathway activity patterns the anterior-posterior axis of the follicular epithelium. *Dev Cell,* **4**, 167-77.

Yamamoto K, Yamaguchi M, Miyasaka N & Miura O (2003) SOCS-3 inhibits IL-12-induced STAT4 activation by binding through its SH2 domain to the STAT4 docking site in the IL-12 receptor b2 subunit. *Biochem Biophys Res Commun,* **310**, 1188-93.

Yamamoto T, Sekine Y, Kashima K, Kubota A, Sato N, Aoki N & Matsudaa T (2002) The nuclear isoform of protein-tyrosine phosphatase TC-PTP regulates interleukin-6-mediated signaling pathway through STAT3 dephosphorylation. *Biochem Biophys Res Commun,* **297**, 811-7.

Yan R, Luo H, Darnell JE, Jr. & Dearolf CR (1996a) A JAK-STAT pathway regulates wing vein formation in *Drosophila. Proc Natl Acad Sci U S A,* **93**, 5842-7.

Yan R, Small S, Desplan C, Dearolf CR & Darnell JE, Jr. (1996b) Identification of a *stat* gene that functions in *Drosophila* development. *Cell,* **84**, 421-30.

Yanagawa S, Lee JS & Ishimoto A (1998) Identification and characterization of a novel line of *Drosophila* Schneider S2 cells that respond to Wingless signaling. *J Biol Chem,* **273**, 32353-9.

Yasukawa H, Misawa H, Sakamoto H, Masuhara M, Sasaki A, Wakioka T, Ohtsuka S, Imaizumi T, Matsuda T, Ihle JN & Yoshimura A (1999) The JAK-binding protein JAB inhibits Janus tyrosine kinase activity through binding in the activation loop. *Embo J,* **18**, 1309-20.

Ye BH, Cattoretti G, Shen Q, Zhang J, Hawe N, de Waard R, Leung C, Nouri-Shirazi M, Orazi A, Chaganti RS, Rothman P, Stall AM, Pandolfi PP & Dalla-Favera R (1997) The BCL-6 proto-oncogene controls germinal-centre formation and Th2-type inflammation. *Nat Genet,* **16**, 161-70.

Yeh TC & Pellegrini S (1999) The Janus kinase family of protein tyrosine kinases and their role in signaling. *Cell Mol Life Sci,* **55**, 1523-34.

Zeidler M & Perrimon N (2000) Sex determination: co-opted signals determine gender. *Curr Biol,* **10**, R682-4.

Zeidler MP, Perrimon N & Strutt DI (1999a) The *four-jointed* gene is required in the *Drosophila* eye for ommatidial polarity specification. *Curr Biol,* **9**, 1363-72.

Zeidler MP, Perrimon N & Strutt DI (1999b) Polarity determination in the *Drosophila* eye: a novel role for *unpaired* and JAK/STAT signaling. *Genes Dev,* **13**, 1342-53.

Zeidler MP, Perrimon N & Strutt DI (2000) Multiple roles for *four-jointed* in planar polarity and limb patterning. *Dev Biol,* **228**, 181-96.

Zhao C, Dave V, Yang F, Scarborough T. & Ma J (2000) Target selectivity of Bicoid is dependent on nonconsensus site recognition and protein-protein interaction. *Mol Cell Biol,* **20**, 8112-23.

Zhao GQ & Garbers DL (2002) Male germ cell specification and differentiation. *Dev Biol,* **2**, 537-47.

Hiermit versichere ich, dass ich die vorliegende Dissertation selbständig und ohne unerlaubte Hilfe angefertigt und andere als die in der Dissertation angegebenen Hilfsmittel nicht benutzt habe. Alle Stellen, die wörtlich oder sinngemäß aus veröffentlichten oder unveröffentlichten Schriften entnommen sind, habe ich als solche kenntlich gemacht. Kein Teil dieser Arbeit ist in einem anderen Promotions- oder Habilitationsverfahren verwendet worden.

Göttingen, _____

_____

Natalia I. Arbouzova

Acknowledgements

This PhD thesis was done in the laboratory of Dr. Martin Zeidler in the department of Prof. Dr. Herbert Jäckle at the Max Planck Institut for Biophysical Chemistry in Göttingen.

First, I would like to thank Herbert Jäckle for giving me the opportunity to do this PhD thesis, as it was his kind decision to admit in the department a foreigner who dared to come to Germany without being able to speak German. I am frequently asked how I manage not to speak fluent German having been surrounded by native speakers for three years. This became possible because the native speakers around me spoke wonderful English and never forced me to learn German. Therefore, after all these years my German is only good enough to explain to a doctor "*was tut mir weh*", while my English improved so much that I was able to give a scientific talk at an international meeting.

I would like to give my largest thanks to Martin Zeidler for his support, advice and guidance. I am ever grateful for his patience, understanding and, no less important, the very warm atmosphere in his laboratory. I wish I could have a chief like Martin in the future. Speaking about the friendly environment I also want to thank Sabine Häder, who is not only a technical assistant of the lab 6, but also its right hand and soul. I will never forget our fascinating trips to canoe on the Diemel river, to climb down to the cold Gosslar mines, playing bowling, drinking beer and many others. She made our work comfortable and organised our leisure in the warmest way. For the good time we shared in the lab and beyond it, I also thank all the members of my lab: Peter Karsten, Tina Mukherjee, Iris Plischke and Patrick Müller. The frequency of jokes and cakes made our colleagues wonder whether the members of the lab 6 ever worked. We did work, though I must admit that in my 28 years I have never experienced work as something that I had to do without enjoying it.

I am sincerely grateful to Prof. Dr. Mireille A. Schäfer and her colleagues at the University in Kassel for the great opportunity to defend my PhD thesis there. I

appreciate very much their help, supervision and the time they have spent on my thesis and me, as these days time is something that we never have in excess.

I thank Alex Matyash for his professional assistance especially in the biochemical part of my project and for bringing a little Russian into my work abroad.

I appreciate Ralf Pflanz and his willingness to share chemicals, protocols and his personal scientific experience. Ralf and also Alexander Prell helped me a great deal with computer stuff, which sometimes saved not only my time, but my good mood as well.

I acknowledge Ursula Jahns-Meyer and Iris Plischke for injecting *Drosophila* embryos, and Gordon Dowe and Nicole Beinert for all the sequencing. Especial thanks to Gordon for his English usage guidance and everyday cheering up.

I would also like to give thanks to Ulrich Nauber and Else Vetter for organising things that sometimes we do not notice merely because people like Ulrich and Else are doing them for us and saving our time. Especially important was their help, as well as support by Dima Ossipov, a former member of the department, during my first days in Germany.

And finally many thanks to every person in the department for help, assistance, support, jokes, friendliness and concern.

Appendix

Figure A.1 Lab 6

(A, E, G & H) Canoeing down the Diemel river, 2003. (B) Trip to the Gosslar mines, 2004. (C) BBQ in Martin's garden, 2004. (D) Visiting „Biothechnika 2003" exhibition in Hannover, 2003. (F) Seminarraum, Abt 170. Trying out Peter's birthday gift, 2003. Martin Zeidler (MZ), Sabine Häder (SH), Peter Karsten (PK), Tina Mukherjee (TM), Iris Plischke (IP), Patrick Müller (PM) and Natalia Arbouzova (NA) are distinguished. Susan Smith (SS) and Marta Vuchkovic (MV) are also present.

Figure A.2 Abt 170

(A, B, D, F & G) Trip to the Harz mountains, 2003. (C & E) Ringberg retreat, 2003. Notice Alexei Matyash (AM), Else Vetter (EV) and Ulrich Nauber (UN) mentioned in the "Acknowledgements" section. Red arrow points out Prof. Herbert Jäckle.

Curriculum Vitae

Date/Place of birth   1.05.1976, Saint-Petersburg, Russia

Parents   Igor Anatolievich Arbouzov

Galina Vladimirovna Arbouzova

Nationality   Russian

Education   1984-1993 Secondary School, Saint-Petersburg, Russia

1994-2000 The Saint-Petersburg State University

Degrees   22.06.1998 BSc, Department of Embryology

The Saint-Petersburg State University, Russia

15.12.2000 MSc, Department of Embryology

The Saint-Petersbur State University, Russia

Research Training   1995-1996: Institute of Cytology, Saint-Petersburg, Russia

A 1 year student work

Studying neurosecretory system formation of the burbot *Lota lota.*

1996-1998: Institute of Cytology, Saint-Petersburg, Russia

A 2 year BSc degree research

Studying *in vitro* development of pre-implantation mouse embryos and the phenomenon of "2-cell block *in vitro*".

1998-2000: Institute for Experimental Medicine, Saint-Petersburg, Russia

A 2,5 year MSc research

Generating "transmitochondrial" mice carrying human mitochondrial DNA as an attempt to design an animal model of human diseases.

2001-present: Max-Planck Institute for Biophysical Chemistry, Göttingen, Germany

Postgraduate research

Characterisation of the *Drosophila ken&barbie* gene and its function in JAK/STAT pathway signalling.

Publications   Vassilyev V.B., Sokolova V.A., Sorokin A.V., Bass M.G., Arbuzova N.I., Patkin E.L., Golubkov V.I., Dyban A.P., Gaitskhoki V.S. Persistence of human mitochondrial DNA throughout the development to the blastocyst of mouse zygotes microinjected with human mitochondria. *Zygote*, 1999, V.7, pp. 279-283.

Sokolova V.A., Kustova M.E., Arbuzova N.I., Sorokin A.V., Moskaliova O.S., Bass M.G., Vasiliev V.B. Obtaining mice that carry human mitochondrial DNA transmitted to the progeny. *Mol Reprod Dev*, 2004, 68:299-307.

Arbouzova N.I., Bach E.A., Zeidler M.P. *Drosophila* Ken&Barbie represents a novel class of JAK/STAT pathway regulating proteins (in preparation).

Presentations   Arbouzova N., Häder S., Bach E., Zeidler M. (2003). Characterisation of the role of Ken&Barbie in JAK/STAT

signalling. 44th Annual Drosophila Research Conference. Chicago, Illinois, USA (oral presentation)

Arbouzova N., Häder S., Bach E., Zeidler M. (2003) Characterisation of *ken&barbie* in JAK/STAT signalling. European Drosophila Research Conference. Goettingen, Germany (oral presentation)

Arbouzova N., Bach E., Zeidler M. (2004) *Drosophila* Ken&Barbie represents a novel class of JAK/STAT pathway regulating proteins European Life Science Organisation Meeting. Nice, France (oral presentation)